FBXL5 IS REQUIRED FOR THE MANTAINANCE OF CELLULAR AND SYSTEMIC IRON HOMEOSTASIS

APPROVED BY SUPERVISORY COMMITTEE

_____

Richard K. Bruick, PH.D.

_____

Joseph Garcia, MD, Ph.D.

_____

Benjamin Tu, Ph.D.

_____

Shawn Burgess, Ph.D.

DEDICATION

To God for giving me wisdom and guidance throughout my life.

To my parents Julio and Marisa, whose sacrifice and encouragement have allowed me to complete my dissertation.

To my wife Marcela, and my sons Juan Pablo, Agustin and Tomas whose love and joy have brought happiness to my life.

To my brothers Juan and Mariano, and good friends whom I love and miss daily.

FBXL5 IS REQUIRED FOR THE MANTAINANCE OF CELLULAR AND SYSTEMIC IRON HOMEOSTASIS

by

Julio Cesar Francisco Ruiz

DISSERTATION

Presented to the Faculty of the Graduate School of Biomedical Sciences

The University of Texas Southwestern Medical Center at Dallas

In Partial Fulfillment of the Requirements

For the Degree of

DOCTOR OF PHILOSOPHY

The University of Texas Southwestern Medical Center at Dallas

Dallas, Texas

October, 2012

ACKNOWLEDGEMENT

First, I would like to thank my mentor Dr. Richard Bruick for his support, encouragement, patience and guidance throughout my dissertation research. Rick has taught me to ask the right scientific question and to design and perform the best experiments to answer such question. I am also indebted to the members of my thesis committee Drs. Joseph Garcia (Chair), Benjamin Tu and Shawn Burgess for their helpful suggestions.

I would like to thank Joel Thompson and Ameen Salahudeen with whom I had the opportunity to share research projects as well as memorable days in the lab. I am very grateful to Scott Walker and Kyle Mecham for their help taking care of the animal colony. I am also obliged to current and past members of the Bruick lab Cameron Shokri, Srinivas Chollangi, Donald Rozario, Hanzhi Wang and Victor Pashkov for their continuous help.

I am thankful to Sarah Straud and Vural Tagal for their helpful suggestions during the preparation of my qualifying exam as well as during the completion of my dissertation research.

I would like to thank Dr. Robert Hammer and the Transgenic Technology Center for making the FBXL5 knockout mice. I would also like to thank Dr. James Richardson, John Shelton and the pathology core for assistance with histology slides preparation and analysis. I thank Sandi Jo Estill, the McKnight lab and Dr. Joyce Repa for teaching me how to work with mice.

I also would like to thank Drs. Richard Eisenstein and Sheila Anderson at the University of Wisconsin-Madison for their assistance and help making the *Irp1*$^{-/-}$*; Fbxl5*$^{GT/GT}$ and *Irp2*$^{-/-}$*; Fbxl5*$^{GT/GT}$ mice.

I am deeply grateful to Drs. Pablo Murcia, Gustavo Delhon, Julio Turrens and Lewis Pannell for introducing me to the fascinating world of research.

Lastly, I gratefully acknowledge support from the Sara and Frank McKnight graduate student fellowship

FBXL5 IS REQUIRED FOR THE MANTAINANCE OF CELLULAR AND SYSTEMIC IRON HOMEOSTASIS

JULIO CESAR FRANCISCO RUIZ, 2012

RICHARD KEITH BRUICK, Ph.D.

Iron is an essential element for most living organisms. Due to its chemical properties, iron plays an important role in many vital biochemical processes. Both iron excess and deficiency have detrimental effects in human health. Therefore, iron metabolism must be tight regulated. Maintenance of cellular iron homeostasis requires coordinate posttranscriptional regulation of iron metabolism genes by Iron Regulatory Proteins 1 and 2 (IRP1 and IRP2). IRP2 is targeted for proteasomal degradation in iron replete cells by the E3 ubiquitin ligase complex

containing F-box and Leucine-rich Repeat Protein 5 (FBXL5). Depletion of FBXL5 leads to aberrant accumulation of IRP2 and misregulation of IRP2 under high iron conditions, underscoring FBXL5 importance in regulation of iron metabolism. Interestingly, FBXL5 is regulated in an inverse fashion to IRP2 as it is stabilized under iron-replete conditions and preferentially degraded when iron or oxygen becomes limiting. However, FBXL5's iron- and oxygen-dependent regulation and its role in the maintenance of systemic iron homeostasis are poorly understood. Biochemical and molecular biology assays revealed that FBXL5 features a hemerythrin-like domain that serves as a direct sensor of cellular iron as well as oxygen availability and subsequently governs FBXL5's own stability. Importantly, *in vivo* deletion of the ubiquitously-expressed murine *Fbxl5* gene results in a failure to sense increased cellular iron availability, accompanied by constitutive IRP2 accumulation and misexpression of IRP2 target genes. FBXL5-null mice die during embryogenesis, though viability is restored by simultaneous deletion of the IRP2, but not IRP1, gene. *Fbxl5* heterozygous mice behave like their wild type littermates when fed an iron-sufficient diet. However, unlike wild type mice that manifest decreased hematocrit and hemoglobin levels when fed a low-iron diet, *Fbxl5* heterozygotes maintain normal hematologic values due to increased iron absorption. IRP2's responsiveness to low iron is specifically enhanced in the duodena of the heterozygotes and is accompanied by increased expression of the Divalent Metal

Transporter-1. These results confirm FBXL5's role in the *in vivo* maintenance of cellular and systemic iron homeostasis and reveal a privileged role for the intestine in their regulation by virtue of its unique FBXL5 iron sensitivity.

TABLE OF CONTENTS

PRIOR PUBLICATIONS

- McGee DJ, Kumar S, Viator RJ, Bolland JR, **Ruiz JC**, Spadafora D, Testerman TL, Kelly DJ, Pannell LK, Windle HJ. Helicobacter Pylori Thioredoxin is an Arginase Chaperone and Guardian against Oxidative and Nitrosative Stresses. J Biol Chem. 2006 Feb 10;281(6):3290-6.

- Salahudeen AA, Thompson JW, **Ruiz JC**, Ma HW, Kinch LN, Li Q, Grishin NV, Bruick RK. An E3 Ligase Possessing an Iron Responsive Hemerythrin Domain Is a Regulator of Iron Homeostasis. Science. 2009 Sep 17.

- Nandal A, **Ruiz JC**, Subramanian P, Ghimire-Rijal S, Sinnamon RA, Stemmler TL, Bruick RK, Philpott CC. Activation of the HIF prolyl hydroxylase by the iron chaperones PCBP1 and PCBP2. Cell Metab 2011 Nov 2;14(5):647-57.

- Thompson JW, Salahudeen AA, Chollangi S, **Ruiz JC**, Brautigam CA, Makris TM, Lipscomb JD, Tomchick DR, Bruick RK. Structural and molecular characterization of the iron-sensing hemerythrin-like domain within F-box and leucine-rich repeat protein 5 (FBXL5). J Biol Chem. 2012 Jan 17.

- Chollangi S, Thompson JW, **Ruiz JC**, Gardner KH, Bruick RK. The hemerythrin-like domain within F-box and leucine-rich repeat protein 5

communicates cellular iron and oxygen availability by distinct mechanisms. J Biol Chem. 2012 May 30.

LIST OF FIGURES

LIST OF TABLES

LIST OF DEFINITIONS

ATP - Adenosine Triphosphate
CBC – Complete Blood Counts
DFO - Deferoxamine Mesylate
DMT1 – Divalent Metal Transporter 1
DNA - Deoxyribonucleic Acid
DTT - Dithiothreitol
E1 - Ubiquitin Activating Enzyme
E2 - Ubiquitin Conjugating Enzyme
E3 - Ubiquitin Ligase
FAC - Ferric Ammonium Citrate
FBXL5 – F-Box and Leucine rich repeat Protein 5
FTH1 – Ferritin Heavy Chain 1
GT – Gene Trapping
HEK 293 - Human Embryonic Kidney Cell Line
HEPES - 4-(2-hydroxyethyl)-1-piperazineethanesulfonic acid
HOIL-1 - Haem-Oxidized IRP2 Ubiquitin Ligase-1
Hr – Hemerythrin
ICP-MS – Inductively Coupled Plasma Mass Spectrometry
IRE - Iron Responsive Element
IRP - Iron Regulatory Protein
MEC – Mouse Embryonic Cells
MG132 - Proteasome Inhibitor Z-Leu-Leu-CHO
PAGE - Polyacrylamide Gel Electrophoresis
PBS - Phosphate Buffered Saline
PCR - Polymerase Chain Reaction
qRT-PCR - Quantitative Real Time PCR
RNA - Ribonucleic Acid
RNAi - RNA interference
SDS - Sodium Dodecyl Sulfate
SCF - Skp1, Cul1, F-box containing E3 ubiquitin ligase complex
siRNA - small interfering RNA
shRNA - short hairpin RNA
TIBC – Total Iron Binding Capacity
TfR1 – Transferrin Receptor 1
Tris - Tris(hydroxymethyl)methylglycine
UTR - Untranslated Region

Chapter 1: Principles of Iron Metabolism

Introduction

Iron is the second most abundant metal in the Earth's crust (90), and it was present in the prebiotic times (31). The chemoautotrophic theory suggests that iron sulfide may have been one of the most important catalysts for the formation of complex organic compounds over a billion years ago (41, 161). Iron's unique electrochemical properties arising from its flexible coordination chemistry and redox reactivity make iron an ideal cofactor for many biological processes (3, 31, 90, 115). Specifically, iron-utilizing proteins participate in many vital oxidation and transport reactions. Heme-containing proteins constitute the majority of iron-using proteins (141). Heme is a prosthetic group that binds iron in the center of a heterocyclic ring called protoporphyrin (28, 141). Living organisms use a variety of heme-containing proteins to carry out redox reactions (109, 125) and electron transport processes (109, 126, 174). For example, hemoglobin and myoglobin utilize heme molecules to transport or store oxygen in red blood cells and muscle cells, respectively (117, 125). Together with heme-containing proteins, iron-sulfur cluster assembling proteins participate in the process of electron transport during oxidative phosphorylation, the major source of energy for the cell (14, 128). Iron is also required in many other essential biochemical

processes such as oxygen sensing (13) and DNA synthesis (176). Therefore, iron has become an indispensable nutrient in most living organisms.

Iron's property of easily gaining and losing electrons also makes it potentially harmful. Iron can donate electrons to oxygen and hydrogen peroxide resulting in the formation of damaging reactive oxygen species (3, 50, 51, 165). Disruption of iron homeostasis has detrimental effects on human health. Hemochromatosis, an iron overload disorder, is characterized by the progressive accumulation of iron in the liver, pancreas and heart leading to hepatic cirrhosis, diabetes and cardiomyopathy (58, 119). On the other hand, iron's poor solubility under physiological conditions make its acquisition problematic (63). Iron deficiency in humans results in developmental and cognitive defects as well as insufficient hemoglobinization of red blood cells also known as anemia (86, 99). Currently, iron deficiency anemia is the most common nutritional disorder in the world (43, 113). Thus, organisms must tightly regulate iron homeostasis since its excess or deficiency is deleterious.

Accordingly, organisms have developed sophisticated molecular mechanisms that allow them to regulate iron metabolism both at the systemic and the cellular levels.

Systemic Iron Homeostasis

Most of the iron in the body is found bound to hemoglobin in erythrocytes. Recycling of iron from senescent red blood cells provides the majority of iron required by the body (8, 86). However, humans lose a small, but steady, amount of iron by sweating, menstruation and physiologic exfoliation of cells from epithelial surfaces including the skin, genitourinary track and gastrointestinal track (7). This means that humans must continue to absorb iron to balance the loss. Importantly, the lack of a regulated iron excretory system in mammals (7) obligates iron absorption to be tightly regulated.

Intestinal Non-Heme Iron Absorption

Dietary iron absorption takes place in the duodenum (Fig. 1-1). A typical Western diet contains 15-20 mg of iron, most of which exists in a highly insoluble ferric (Fe^{3+}) form, which must be reduced to Fe^{2+} before it can be internalized (76, 112).

Duodenal cytochrome B (DcytB), a ferric reductase that uses ascorbate as a coenzyme, catalyzes the reduction of Fe^{3+} to Fe^{2+} (104, 105). DcytB is highly expressed in the apical surface of the duodenal epithelium and its expression is induced by iron deficiency and hypoxia suggesting it plays a role in iron uptake

(104, 105). However, when *DcytB*$^{-/-}$ mice are fed a low iron diet or exposed to hypoxia, though iron uptake is diminished, they do not develop iron deficiency (48, 104). This implies that another mechanism of iron reduction must exist. While DcytB may not be required, iron reduction is necessary as the iron importer, Divalent Metal transporter 1 (DMT1), is selective for ferrous iron.

DMT1, a proton symporter, carries Fe^{2+} across the duodenal membrane (8). In addition to Fe^{2+}, DMT1 also transport other divalent metals including Zn^{2+}, Mn^{2+}, Co^{2+} and Cu^{2+}(66). Although DMT1 is found in late endosomes and lysosomes in all cell types (19), it is mainly expressed in the apical membrane of duodenal enterocytes especially in response to iron deficiency (18, 157). Mice and rats having a missense mutation (G185R) display defects in iron absorption resulting in microcytic anemia (46, 47, 150). Furthermore, *Dmt1*$^{-/-}$ mice are born without abnormalities, but succumb to anemia in the first week of life (65). Similar results were observed when DMT1 was selectively inactivated in the intestine (48). These observations confirmed that DMT1 plays a major role in iron absorption and erythroid iron utilization.

Once internalized, cytosolic iron can be exported to the circulation to be distributed to all tissues. Ferroportin (FPN), a multipass transmembrane protein located in the basolateral surface of duodenal enterocytes (38, 106, 166), is the only known iron exporter in mammals (1, 37, 106). Ferroportin's iron exporting capabilities were demonstrated by expressing it in Xenopus oocytes. Addition of

iron to media resulted in increased cytosolic iron and subsequent increase in ferritin levels. When iron was removed from the media, FPN expressing oocytes exported iron resulting in decreased cytosolic iron and ferritin levels (103). Experiments in mice revealed that ferroportin is essential for life. *Fpn*$^{-/-}$ mice die early *in utero* due to defective iron transfer from the mother (38). During embryonic development, prior placenta formation, the extraembryonic visceral endoderm (exVE) transport nutrients to the embryo. Immunohistochemistry showed that FPN is highly expressed in the exVE. If FPN is deleted in every tissue but the exVE, pups are born, but they die due to severe anemia by day 10 as iron stores are depleted and intestinal absorption is the only source of iron (38). Postnatal deletion of FPN in the intestine results in severe anemia that can be reversed by parenteral administration of iron (38). These findings indicate that FPN is a major iron exporter in the exVE and the intestine.

Fe^{2+} must be oxidized before it can bind to its carrier transferrin in the blood. Hephaestin (Heph), a membrane bound multicopper ferroxidase located in the basolateral membrane of the duodenal mucosa, catalyzes the oxidation of Fe^{2+} to Fe^{3+} (8, 22, 76). Heph's role in iron absorption was discovered by studying the sex-linked anemia (sla) mice. In these mice, the *Heph* gene has an in-frame deletion of 582 bases. Affected homozygous mice develop microcytic, hypochromic anemia. Iron uptake is normal, but iron accumulates inside the enterocytes as iron export is impaired (160). This suggests that Heph is required

for iron release from the duodenum and that the functions of both FPN and Heph are coupled for iron transport (23). Another multicopper ferroxidase, Ceruloplasmin (Cp), is found in the plasma (73). It is believed Cp facilitates iron export from the reticuloendothelial system and parenchymal cells, as it is not expressed in the duodenum (24). Like Heph, Cp also plays an important role in iron homeostasis as humans suffering from aceruloplasminemia, also known as Wilson's disease develop iron accumulation in brain, liver and other tissues (74).

Serum Fe^{3+} binds rapidly to Transferrin (TF), an abundant iron-binding plasma glycoprotein (138). Each TF molecule binds 2 iron atoms (139) with high affinity (Kd = 10^{-25} M) at physiological pH (4). TF is synthesized in liver in response to changes in iron, estrogen and nutritional status (30). During iron overload, serum TF levels decrease whereas iron deficiency increases serum TF concentration (175). In addition to facilitating iron delivery to tissues, TF also helps to solubilize and decrease iron's reactivity. Iron-laden TF is recognized by Transferrin Receptor 1 (TfR1), which is ubiquitously expressed (59). The complex is then internalized via receptor-mediated endocytosis. Once in the endosome, the acidic environment maintained by ATPase proton pumps promote the dissociation of iron from TF. Freed Fe^{3+} is reduced to Fe^{2+} by STEAP3, an endosomal ferrireductase, and transported to the cytosol by DMT1 (Fig. 1-2) (7). Experiments in mice have demonstrated that TfR1 is essential for early development, as *Tfr1*$^{-/-}$ mice die *in utero* (48). On the other hand, mice (*Trf*$^{hpx/hpx}$)

and humans suffering from hypotransferrinemia develop growth retardation and severe anemia (9, 156). Interestingly, hypotransferrinemic humans and mice also develop massive iron overload in liver and heart suggesting that a TF-independent iron uptake mechanism must exist. It has been shown that calcium channels promote iron uptake in neurons and cardiomyocytes (21, 77, 114). Furthermore, several groups have demonstrated that lipocalin 24p3 can bind iron and deliver it to or remove it from cells (36, 62, 172). However, the severe anemia observed in hypotransferrimic patients indicates that TF-dependent iron uptake is the main mechanism used by the erythroid system to acquire iron. Once in the cytosol, iron can be stored, used by iron-containing proteins or exported by ferroportin (Fig. 1-2).

Iron Storage

As free iron can react with oxygen and water to generate damaging reactive oxygen species, excess cytosolic iron is tightly regulated and compartmentalized by nature to diminish these effects (78). Ferritins form spherical "iron nanocages" consisting of 24 protein subunits of ferritin heavy chain and ferritin light chain that store iron in a soluble and non-toxic form (78, 101). Up to 4500 iron atoms bound to oxygen can be kept within ferritin (43). The ferritin heavy chain has ferroxidase activity that allows iron to be stored in a less

reactive ferric form (101). Ferritin is also found in the serum (155). Measurement of serum ferritin levels is a common clinical test used to determine body iron stores. The function of circulating ferritin is still not well understood. It has been suggested that it may play a role in immunity and iron delivery (112). The importance of ferritin in iron homeostasis is reflected in the fact that mutations in a ferritin gene are associated with many human diseases (32, 61) and, that ferritin gene deletion is embryonic lethal in mice (44).

Iron Recycling

Macrophages play a critical role in maintaining plasma iron at adequate levels (92). Since only 10% of the requisite iron is covered by intestinal absorption of dietary iron, most of the iron required by the body is recycled from old or damaged red blood cells through the action of macrophages (143). Once phagocytated, iron is extracted from heme by hemoxygenase, an enzyme that catalyzes the degradation of heme (167). Freed iron is then transported to the cytosol through NRAMP1, an enzyme located in the phagolysosomal membrane that is homologous to DMT1 (148). Finally, iron is exported to the plasma by ferroportin. Due to the important role played by ferroportin in various aspects of iron homeostasis, its expression is regulated at multiple levels. Transcription of ferroportin is induced by erythrocyte phagocytosis and the presence of heme iron.

Post-transcriptionally, ferroportin translation is inhibited by the iron regulatory proteins (IRPs) (see cellular iron homeostasis), and its protein stability is regulated by hepcidin (see regulation of systemic iron homeostasis).

Iron Utilization

Cells utilize internalized iron in several ways. Iron is incorporated into iron-sulfur containing proteins that play a major role in electron transport during mitochondrial oxidative phosphorylation (14). Ribonucleotide reductase uses iron as a cofactor to catalyze the formation of deoxyribonucleotides from ribonucleotides, which are later used for DNA synthesis (176). Iron is also needed for oxygen sensing by the HIF-prolyl hydroxylases (13). However, most of the recycled iron is dedicated to hemoglobin synthesis (76). In the erythroid system, iron uptake is carried out mainly by the TF-TfR1 axis (7). Hypotransferrinemic mice and humans undergo iron overload in the liver and other tissues but they develop severe iron deficiency anemia (156); thus, emphasizing the importance of the TF-TfR1 system in iron uptake by the erythrocyte progenitor cells. Imported iron is immediately delivered to mitochondria by an inner membrane protein mitoferrin1 (126). When the demand for red blood cells is high, iron is thought to bypass the cytosol and moved directly into the mitochondria through a “kiss-and-run” mechanism that requires the fusion of the endosome with mitochondria

(140). Once in the mitochondria, iron is utilized for the production of heme. The synthesis of the organic heterocyclic ring, protoporphyrin IX is coordinated to iron availability by the IRPs. When bioavailable iron is limiting, IRP1 inhibits the synthesis of the rate-limiting enzyme, d-aminolevulinic acid synthase 2 (ALAS2) (168). Genetic defects that lead to constitutively active IRP1 result in anemia due to ALAS2 down-regulation (16, 168).

Intestinal Absorption of Heme

Dietary iron can also be absorbed as heme, an important iron-containing molecule. Unlike non-heme inorganic iron that is highly insoluble under physiological conditions, heme is easily and more effectively absorbed (8). Dietary heme is derived from animal sources in the form of hemoglobin and myoglobin. The iron released as result of heme degradation constitutes 2/3 of the iron stores in the body (131). Although heme is an important source of iron, its absorption mechanism is poorly understood.

One major obstacle to study heme transport is that mammals are capable of synthesizing heme de novo in an iron-dependent manner (6). In contrast, *Caenorhabditis elegan*s turned out to be an ideal model organism for studying heme transport. These helminthes are heme auxotroph and must uptake heme from the environment to survive (124). Performing genome-wide microarrays in

C. elegans, the Hamza lab identified the first heme transporter the Heme Responsive Gene 1 (HRG1). Knockdown of the HGR1 homolog in zebrafish resulted in severe anemia, which can be rescued by adding worm HRG1 (123). Homologs of HRG1 have been found in human that, like worm HRG1, bind and transport heme suggesting an evolutionary conserved function for the HRG1.

Heme Carrier Protein 1 (HCP1) is a putative heme transporter localized in the intestinal mucosa (142). Although initially described as a heme transporter, HCP1 function has been challenged. HCP1 binds folic acid with higher affinity than heme (93), and humans carrying a loss-of-function mutation in HCP1 develop folate malabsorption, but no problems in erythropoiesis (170). However, *Hcp1*$^{-/-}$ mice develop severe anemia (135). Therefore, the role of HCP1 in heme absorption is yet to be clarified.

The mechanism by which heme iron gets to the circulation is not well understood, but it is believed that it follows a common pathway to non-heme iron.

Regulation of Systemic Iron Homeostasis

The main regulator of systemic iron homeostasis is Hepcidin (HAMP), a 25 amino acids peptide hormone produced in the liver. Hepcidin regulates iron transport across the mucosal as well as the release of recycled iron from macrophages (56). Hepcidin synthesis is regulated by iron and inflammation (33).

When iron is abundant, hepcidin production is increased, while under iron deficient conditions, hepatocytes produce less hepcidin. Circulating Fe-TF levels are sensed by the transferrin receptors 1 and 2 (TfR1 and TfR2, respectively) together with HFE, which are found in the hepatocyte membranes. HFE, a membrane protein similar to MHC class I proteins, regulates the interaction of TfR1 with iron-bound transferrin (holotransferrin). The most accepted mechanism proposes that as iron levels increase, HFE is displaced from TfR1 as its binding site overlaps with holotransferrin. Free HFE interacts with TfR2, which also gets stabilized by holotranferrin. The FeTF/TfR2/HFE complex initiates a signal transduction cascade that together with the binding of bone morphogenetic protein (BMP) ligands to its receptor in the cell surface promotes hepcidin transcription. However, the interaction between BMPs and its receptor is weak resulting in an ineffective production of hepcidin. A more robust transcription of hepcidin is achieved by the presence of BMP co-receptor hemojuvelin (HJV), which significantly increase the affinity of BMP receptor for its ligand (57) (Fig. 1-3).

Genetic mutations resulting in hepcidin deficit cause iron overload. Mutations have been found in most factors involved in the regulation of hepcidin transcription (35). However, mutations in hepcidin and HJV cause more severe forms of iron overload. Interestingly, misregulation of HJV protein levels can also lead to anemia. HJV levels are regulated by a cell surface protease known as TMPRSS6, which under iron deficient conditions cleaves HJV resulting in

reduced hepcidin synthesis (40, 145). During Iron Resistant Iron Deficiency Anemia (IRIDA), mutations in TMPRSS6 results in uncontrolled production of hepcidin and, thus, reduced recycled iron release and iron absorption (86).

In order for absorbed, recycled or stored iron to reach the circulation, it must cross the plasma membrane via the iron exporter ferroportin. Therefore, inhibition of ferroportin prevents iron from reaching the plasma. In conditions where iron is abundant, hepcidin is synthesized and released from the liver. Hepcidin binds to ferroportin, promoting its internalization and degradation (34). In pathologic situations where FPN cannot be internalized but can bind hepcidin, iron export still takes place, suggesting that hepcidin does not control FPN activity but its stability (166). Hepcidin binding to FPN results in the recruitment of the tyrosine kinase JAK2, which, after undergoing autophosphorylation, phosphorylates FPN. Phosphorylated FPN is internalized by clathrin-coated pits. Internalized FPN gets ubiquitinated in a critical lysine residue (K253), which is required for endosome and lysosome fusion where it gets degraded (33). Mutations in ferroportin also result in iron overload. Expression of a hepcidin-resistant ferroportin due to a mutation in the hepcidin-binding site results in dysregulated iron absorption. Likewise, impeded phosphorylation of FPN following hepcidin binding results in the same outcome (86). Therefore, hepcidin-mediated FPN internalization and degradation regulates the levels of bioavailable iron in the plasma.

Cellular Iron Homeostasis

Iron homeostasis must be tightly regulated as failure to maintain iron concentration within appropriate levels may result in disease. Iron Regulatory Proteins (IRPs) regulate the post-transcriptional expression of genes involved in iron uptake, storage, utilization and export upon binding to Iron Responsive Elements (IREs) within the 5' and 3' Untranslated Region (UTR) of their mRNAs.

Iron Responsive Elements

The study of two iron regulated proteins involved in iron storage and uptake, ferritin and TfR1 respectively, provided the initial step in the elucidation of the iron-dependent post-transcriptional regulation of iron metabolism genes.

Initially, the fact that iron administration to cultured cells resulted in recruitment of ferritin mRNA to polysomes and increased ferritin translation (10), led researchers to elucidate the structural features of these mRNAs. Fusion of the 5' untranslated region (UTR) of the rat ferritin light chain mRNA to the bacterial chloramphenicol acetyl-transferase (CAT) mRNA resulted in increased CAT activity upon iron addition. However, this iron dependent response was lost when the 5' UTR lacking a few key residues was fused to CAT (11). Bioinformatics analysis of the 5' UTR of ferritin revealed that 30 nucleotides conserved in

human, rat, chicken and frog adopt a stem-loop structure. These 30 nucleotides were necessary and sufficient for ferritin mRNA to be post-transcriptionally regulated by changes in intracellular iron. Biophysical and structural studies revealed that these stem loop structures consist of 9-10 base pairs with a terminal conserved loop containing the sequence CAGUGU/C. Five base pairs 5' of the loop; there is a bulge nucleotide region that varies in size depending in the mRNA analyzed. This bulge region contains an unpaired cytosine that is critical for IRE function (Fig. 1-4) (11, 42). This motif was named Iron Responsive Element (IRE).

Shortly after the discovery of an IRE in ferritin mRNA, it was determined that the region conferring iron-dependent regulation to Tranferrin Receptor 1 (TfR1) is localized in the 3' UTR of the mRNA. This region contains 5 stem loop structures resembling the description of IREs found in ferritin (20, 91). However, the iron-dependent regulation of TfR1 is different from ferritin. While TfR1 synthesis is increased under iron deplete conditions, ferritin levels drop (69). This observation suggested that the location of cis-acting IREs within the UTR has opposite effects on the iron-dependent regulation of the gene. Furthermore, IREs located in the 5' UTR are involved in translation initiation whereas IREs found in the 3' UTR control mRNA stability. Currently, in addition to both ferritins, Light and Heavy chain, 5 more genes have been found to have IREs in their 5' UTR including ferroportin (FPN), mitochondrial aconitase (m-acon), erythroid amino

levulinate synthase 2 (eALAS2), succinate dehydroxygenase (SDH) and hypoxia inducible factor 2 α (HIF-2α). Genes containing IREs in their 3' UTRs, besides TfR1, include divalent metal transporter 1 (DMT1) and CDC14A (133).

Iron Regulatory Proteins

During the discovery of ferritin's IRE, it was observed that deletion of this cys-regulatory motif rendered ferritin unresponsive to changes in iron concentration. This suggested that an iron-sensitive factor(s) in the cytoplasm might bind this sequence and regulate ferritin mRNA accessibility for translation (97). Using a combination of affinity chromatography and RNA gel retardation assays, where ferritin light chain IRE was used as bait, two independent groups identified and purified an IRE-binding protein (IRE-BP) (97, 130). The interaction of the IRE/IRE-BP was iron dependent. Iron deprivation induced complex formation whereas high iron promoted complex dissociation (97, 130). This IRE binding protein was later named Iron Regulatory Protein 1 (IRP1).

While cloning IRP1, a cDNA closely related to IRP1's cDNA was also cloned. Characterization of this protein revealed that it shared 70% homology to IRP1 except for a unique stretch of 73 amino acids (136). Like IRP1, it also recognized and bound to IREs in an iron-dependent manner. This second IRE binding protein was named Iron Regulatory Protein 2 (IRP2).

In iron deficient cells, both IRPs bind IRE with high affinity (Kd = 0.02 – 0.1 nM) (42). Binding to an IRE located in the 5' UTR of ferritin mRNA prevents its translation whereas binding to IREs in the 3' UTR of TfR1 transcript protects it from endonuclease degradation (76, 96). Consequently, under low iron conditions, cells promote iron uptake via TfR1. At the same time, iron storage is inhibited; thus, making iron readily available for its utilization. On the other hand, when iron is plentiful, IRPs do not bind IREs, and ferritin and other transcripts containing IREs in their 5' UTR are translated while TfR1 mRNA get degraded by endonucleases (76, 96). Hence, in the presence of abundant iron, cells inhibit iron uptake while promoting its storage, thus, preventing accumulation of excess iron in the cytosol.

Regulation of Iron Regulatory Proteins

Despite sharing >70% identity, the mechanisms by which the IRE-binding activity of IRP1 and IRP2 are inactivated in iron-replete cells largely differ (98). IRP1 is a bifunctional cytosolic protein that belongs to the family of Fe-S isomerases. When iron is abundant, IRP1 assembles an 4Fe-4S cluster (holo-IRP1) and acquires aconitase activity (70, 88). Like other aconitases (i.e. mitochondrial aconitase), holo-IRP1 catalyzes the interconversion of citrate and isocitrate. However, the physiological significance of IRP1 aconitase activity is

poorly understood. Importantly, 4Fe-4S-loaded IRP1 lacks of IRE binding activity. Biophysical studies have shown that the Fe-S cluster binding site in IRP1 overlaps with the IRE binding site (162). Thus, IRP1 functions are mutually exclusive (Fig. 1-5).

In addition to iron concentration, IRP1 RNA binding activity is regulated by nitric oxide (NO), reactive oxygen species (ROS) and hypoxia (71, 75, 116). Treatment of cells with ROS promotes IRP1's IRE binding activity (116). Although poorly understood, it is believed that ROS promote the disassembly of Fe-S cluster from IRP1. On the other hand, hypoxia negatively regulates IRP1 binding to IRE (71). This observation created a regulatory link between iron metabolism, oxygen availability and response to oxidative stress.

Evidence suggests that an Fe-S cluster-independent regulatory mechanism controlling IRP1 IRE binding activity must exist. This alternative regulatory mechanism could control IRP1 IRE binding when assembly of Fe-S clusters is perturbed. Clarke et al. used IRP1 mutants that destabilize or block the assembly of Fe-S cluster to mimic IRP1 response to disruption of Fe-S metabolism. In these mutants, IRP1 protein levels dropped when iron was sufficient. Similar results were observed in mice lacking enzymes involved in neutralizing oxidative stress (29, 164). Therefore, iron-dependent degradation of IRP1 is an alternative mechanism controlling IRP1 IRE binding activity.

IRP2 differs from IRP1 in two aspects. First, although it is also a member of the aconitase gene family, it lacks aconitase activity (68). Second, unlike IRP1, whose protein levels remain practically unchanged as a function of iron bioavailability, iron-replete conditions induce IRP2 protein degradation and, therefore, decrease IRE binding. When iron is plentiful, IRP2 synthesis and mRNA remain unchanged. Instead, iron promotes IRP2 polyubiquitination follow by degradation at the proteasome (67).

Like IRP1, IRP2 is also regulated in an oxygen-dependent manner. However, in contrast to IRP1, low oxygen conditions induce IRP2 RNA binding activity by preventing its polyubiquitination and degradation. Therefore, both iron and oxygen bioavailability control IRP2's activity.

Identification of the iron regulatory proteins and elucidation of their regulatory mechanisms facilitate our understanding the iron-dependent regulation of IRE-containing genes. Under iron deplete conditions, both IRPs interact with IREs. Binding of IRPs to the ferritin 5' UTR IRE inhibits its translation by preventing ribosome binding. Conversely, IRP binding to TfR1's multiple IREs in the 3' UTR protects the transcript from endonucleolytic degradation, thus, increasing its stability and expression. When iron is plentiful, IRP1 assembles a [4Fe-4S] cluster and acquires cytosolic aconitase activity. Concurrently, IRP2 is polyubiquitinated and degraded by the proteasome. Under these conditions, IRE

binding activity is drastically reduced resulting in increased translation of ferritin and TfR1 mRNA endonucleolytic degradation (Figs. 1-5 and 1-6).

Physiological Role of Iron Regulatory Proteins

In mammals, the IRP/IRE system is responsible for the coordinated regulation of iron metabolism genes and the maintenance of cellular iron homeostasis. Generation of mice in which the expression of either or both IRPs was ablated gave a great insight to the physiological role of the IRPs *in vivo*.

Initial studies showed that both iron regulatory proteins are simultaneously expressed in most tissues and cells (111) and that IRE containing genes can be bound by either IRP, suggesting IRPs are functionally redundant (89). However, IRP1 seemed to be more abundant than IRP2 in cells. Therefore, it was believed that IRP1 would play a major role in the post-transcriptional regulation of iron metabolism genes.

Surprisingly, when *Irp1*$^{-/-}$ mice were generated, they did not display an overt phenotype (107). On the other hand, *Irp2*$^{-/-}$ mice developed microcytic anemia, high serum ferritin and adult onset neurodegeneration characterized by ataxia, tremor and postural abnormalities. However, the neurodegeneration phenotype is not observed in all *Irp2*$^{-/-}$ mice as its penetrance is limited (52). In

addition, *Irp2*$^{-/-}$ mice also exhibited iron accumulation in the cerebellum, liver and small intestine (54, 94).

The temporal and spatial expression pattern of both IRPs helped to rationalize the phenotypes observed. While both IRPs are ubiquitously expressed, IRP2 expression is highly increased in the forebrain, cerebellum, spinal cord and retina. On the contrary, IRP1 levels were only elevated in the brown fat of newborn pups and kidneys (52, 107).

Expression of the IRPs target genes, ferritin and TfR1, was altered in most tissues of *Irp2*$^{-/-}$ mice. Ferritin levels were elevated in several tissues, consistent with ferritin translation derepression. Meanwhile, TfR1 was decreased in the cerebellum, forebrain and other tissues, which can explain anemia. On the other hand, ferritin levels were aberrantly increased only in brown fat and kidneys of *Irp1*$^{-/-}$ mice (107). This suggested that in the absence of IRP2, IRP1 was unable to maintain normal levels of iron metabolisms genes in most tissues and, therefore, IRP2 ostensibly plays a more dominating role regulating iron homeostasis in mice.

The secondary role played by IRP1 in maintaining iron homeostasis *in vivo* can be explained by the fact that under normal physiological conditions, only 4-18% of IPR1 is found in an IRE-binding state (107). Furthermore, *Irp2*$^{-/-}$*; Irp1*$^{+/-}$ mice develop a more severe form of anemia and neurodegenerative disease (146). This observation confirms that IRP1 contributes to the regulation of iron

metabolism, but since only a small fraction is in a RNA binding state, it is unable to rescue the *Irp2*$^{-/-}$ phenotype.

Emphasizing the physiological importance of both IRPs is the early embryonic lethality observed in *Irp1*$^{-/-}$*; Irp2*$^{-/-}$ mice (147). *Irp1*$^{-/-}$*; Irp2*$^{-/-}$ blastocysts showed abnormal morphology and brown discoloration due to accumulation of ferric iron bound to ferritin. Thus, IRPs are essential for embryonic development and viability.

A deeper insight about the physiological role of IRPs was achieved by the generation of tissue-specific IRP knockout mice (53). Selective ablation of IRP2 in the intestinal mucosa (*Irp2*^{VilCre}) resulted in iron accumulation associated with ferritin up-regulation (45). Unlike global *Irp2*$^{-/-}$ mice, *Irp2*^{VilCre} did not develop either microcytic anemia or neurodegeneration suggesting that these could be cell-autonomous phenotypes explained by impaired iron acquisition in erythroid cells due to TfR1 down-regulation, and ferritin up-regulation in the brain (45). Interestingly, deletion of both IRPs in duodenum results in an even higher increase in ferritin expression associated with DMT1 down-regulation and increased ferroportin expression. Although hematologic and serum iron values are normal, *Irp1*$^{-/-}$*; Irp2*$^{-/-}$ mice die before weaning due to severe growth retardation and dehydration (55). Overall these data suggest that ferritin derepression in the intestines is partially limited by IRP1 in *Irp2*^{VilCre} mice explaining the more drastic increase in ferritin levels in duodenum specific *Irp1*$^{-/-}$*; Irp2*$^{-/-}$ mice. These

data also suggested that the opposite effects in DMT1 and ferroportin in *Irp2*$^{-/-}$; *Irp1*$^{-/-}$ mice balance each other to maintain normal serum iron levels.

Specific deletion of IRP2 in the hepatocytes (*Irp2*$^{\Delta lfp}$) resulted in iron accumulation in the liver. Iron loading may be secondary to hepatic ferritin up-regulation because TfR1 mRNA levels remain normal. As such, increased ferritin iron might not be sensed as iron overload; thus, explaining the normal systemic iron homeostasis (45).

In conclusion, mouse studies using single or double IRP ablation have delineated a specific role for each IRP. While IRP1 may be predominantly functioning as an aconitase, IRP2 is responsible for responding to changes in iron bioavailability by regulating IRE containing mRNAs and, therefore, plays a more important role in maintaining iron homeostasis. Importantly, the IRE/IRP system exerts its affect in a cell-autonomous manner.

Role of FBXL5 in Cellular Iron Homeostasis

The Ubiquitin-Proteasome System (UPS) plays an important role in maintaining protein homeostasis by clearing abnormal and damaged proteins as well as those proteins undergoing regulated degradation (84). Proteins are targeted for degradation at the proteasome by covalent modification of a lysine residue with ubiquitin. Ubiquitination is carried out by the coordinated action of

three enzymes. In the first step, the ubiquitin-activating enzyme (E1) hydrolyzes ATP and adenylates an ubiquitin molecule. This adenylated ubiquitin is then transferred to an E1 active site cysteine through a high-energy thioester bond. In the next step, ubiquitin is transferred to a cysteine in the active site of a second enzyme, the ubiquitin-conjugating enzyme (E2) (84, 100). Finally, an ubiquitin ligase (E3) recognizes the specific protein to be ubiquitinated and catalyzes the transfer of ubiquitin from E2 to this target protein in the case of the majority of E3's including the RING family. Therefore, the E3 enzyme gives specificity to the system (25). Target proteins containing at least 4 ubiquitin subunits held together by isopeptide bonds are degraded at the proteasome. After a protein has been ubiquitinated, they are recognized by the proteasome, a multiprotein cylindrical complex, unfolded and then translocated into the proteasome where they undergo proteolysis (132).

IRP2 is regulated in an iron-dependent manner. The protein accumulates under iron and oxygen deficient conditions but is polyubiquitinated and degraded by the proteasome when iron is plentiful (67). However, the mechanism underlying IRP2 iron-dependent degradation has been difficult and controversial to delineate.

Because IRP1 and IRP2 amino acid composition differ by the presence of a unique 73 amino acids stretch in IRP2, initial studies to understand IRP2 iron-dependent regulation were focused on this unique domain. Deletion of this

domain from IRP2 rendered the protein unresponsive to changes in iron levels, and IRP2 aberrantly accumulated under iron-replete conditions. In addition, insertion of this domain to IRP1 resulted in iron-dependent degradation of the protein (83). These observations suggested that this unique 73 amino acid stretch, termed Iron-Dependent Degradation (IDD) domain, conferred iron-dependent regulation to IRP2.

Later, it was shown that, in the presence of oxygen and iron, cysteines located in the IDD were oxidized. *In vitro* ubiquitination assays revealed that oxidized IRP2 was better ubiquitinated than unmodified IRP2 (82). Subsequent studies using recombinant IRP2 treated with iron and DTT in the presence of oxygen revealed that cysteine 178 located in the IDD domain underwent oxidation as determined by mass spectrometry (85). As a result, it was proposed that iron promoted the oxidation of cysteine 178, which allowed IRP2 to be recognized by an unidentified E3 ubiquitin ligase followed by its degradation by the proteasome.

A putative E3 ubiquitin ligase that ubiquitinated IRP2 was identified performing a yeast two-hybrid screen. Heme-oxidized IRP2 ubiquitin Ligase 1 (HOIL-1) interacted with IRP2's IDD domain under aerobic conditions, but the interaction was blocked under anaerobic conditions. In mammalian cells, IRP2 and HOIL-1 interaction was demonstrated by co-immunoprecipitation assay. Furthermore, HOIL-1 ubiquitinated IRP2 *in vitro* when both proteins were

recombinantly expressed (171). Interestingly, it was also shown that IRP2's IDD domain binds heme and, heme-loaded IRP2 was a better substrate for HOIL-1 dependent polyubiquitination than oxidized IRP2 (81). Overall, these data suggested a model where heme binding to IRP2's IDD domain induced cysteine 178 oxidation. Oxidized IRP2 is then recognized by HOIL-1, which promotes IRP2 polyubiquitination targeting for degradation by the proteasome.

Shortly after this model of IRP2 regulation was proposed, several lines of evidence were published challenging its veracity. Initially, it was shown that IRP2 constructs lacking the IDD domain underwent normal iron-dependent degradation when expressed in HEK 293 cells (72, 163). Subsequently, it was demonstrated that neither HOIL-1 overexpression nor HOIL-1 depletion altered IRP2 degradation. Finally, it was proven that HOIL-1 and IRP2 interact, but this interaction is not iron-dependent (179). Furthermore, *Hoil-1*$^{-/-}$ mice did not show IRP2 misregulation nor altered iron homeostasis (154). These observations suggested that in most cells IRP2 stability is regulated in a HOIL-1 independent manner.

Recently, our laboratory reported that an E3 ubiquitin ligase complex containing the F-box and Leucine-rich repeat protein 5 (FBXL5) regulates IRP2 stability (134). Identification of FBXL5 was achieved performing a high throughput siRNA screening using a HEK 293 cell line stably transfected with a plasmid expressing N-terminal hemagglutinin (HA)-tagged and C-terminal

FLAG-tagged IRP2. When iron was depleted upon treatment with the chelator deferoxamine mesylate (DFO), these cells accumulated IRP2. On the other hand when cells were treated with ferric ammonium citrate (FAC), IRP2 levels were significantly reduced as measured by immunobloting or luminescent proximity assay (AlphaScreen).

Depletion of FBXL5 by siRNA resulted in aberrant accumulation of IRP2 under iron-replete conditions. Consistent with the inappropriate increase in IRP2 levels, TfR1 mRNA, an IRP2 target, was abnormally increased as well. Co-immunoprecipitation assays revealed that FBXL5 and IRP2 physically interact in an iron- dependent manner. Moreover, recombinant SCF^{FBXL5} polyubiquitinates IRP2 *in vitro*. Similarly, depletion of FBXL5 by siRNA in cells expressing an IRP1 mutant form unable to assemble an 4Fe-4S clusters aberrantly accumulated this IRP1 variant when iron is abundant (134). Together, these data suggest that FBXL5 can recognize and regulate IRP2 and IRP1 stability in an iron-dependent manner.

Remarkably, immunoblot analysis of lysates prepared from cells treated with DFO or FAC revealed that FBXL5 is regulated in a reciprocal manner to IRP2. The protein is stabilized under iron-replete conditions and degraded when iron and oxygen are limiting. Since FBXL5 mRNA levels remained constant regardless of the iron levels, it was determined that FBXL5 protein levels change as a function of iron availability. Domain mapping studies showed that the first

161 residues of the N-terminus are responsible for FBXL5 iron-dependent regulation. Deletion of this domain rendered FBXL5 unresponsive to iron. Moreover, expression of FBXL5 residues 1 to 161 was sufficient to recapitulate iron-dependent regulation. Bioinformatic analysis predicted that FBXL5 residues 1-161 adopt a hemerythrin (Hr)-like structure (134). Hemerythrin domains are found in a few marine invertebrates and bacteria and are involved in oxygen transport, storage and chemotaxis. Previously reported Hr domains are composed of a bundle of α-helices surrounding a di-iron center capable of oxygen binding. Biophysical and structural studies of FBXL5 Hr domain determined that it consist of an extended bundle of 5 α-helices held together by a di-iron center (134, 152). Therefore, FBXL5's iron dependent regulation and iron-binding property suggest that FBXL5 may serve as an intracellular iron sensor.

Specific Aims of Dissertation Research

In cell culture systems, disruption of FBXL5 expression promotes IRP2 accumulation and misregulation of its target genes, thus, underscoring FBXL5 importance in maintaining cellular iron homeostasis. Proper regulation of IRP2 requires cells to be able to sense and respond to changes in bioavailable iron and oxygen. FBXL5 has emerged as a potential intracellular iron and oxygen sensor. However, the mechanism governing FBXL5's iron and oxygen-dependent

regulation remains poorly understood. Additionally, given FBXL5's important role in the maintenance of cellular iron homeostasis, it is likely that it may also play a vital role in the regulation of systemic iron homeostasis, a function that has not been studied yet. Therefore, I began my dissertation research asking two central questions:

1. **What are the molecular mechanisms governing FBXL5's iron- and oxygen-dependent regulation?**

2. **What is FBXL5's role in the *in vivo* maintenance of systemic and cellular iron homeostasis?**

Understanding FBXL5 iron- and oxygen-dependent regulation might allow elucidating how cells linked iron and oxygen availability to IRP2 stability and, consequently, to the maintenance of cellular iron homeostasis. Furthermore, determining FBXL5's physiological role may provide a new insight in the relationship between cellular and systemic iron homeostasis, which may result in the development of new therapies for the treatment of human diseases such as hemochromatosis and iron deficiency.

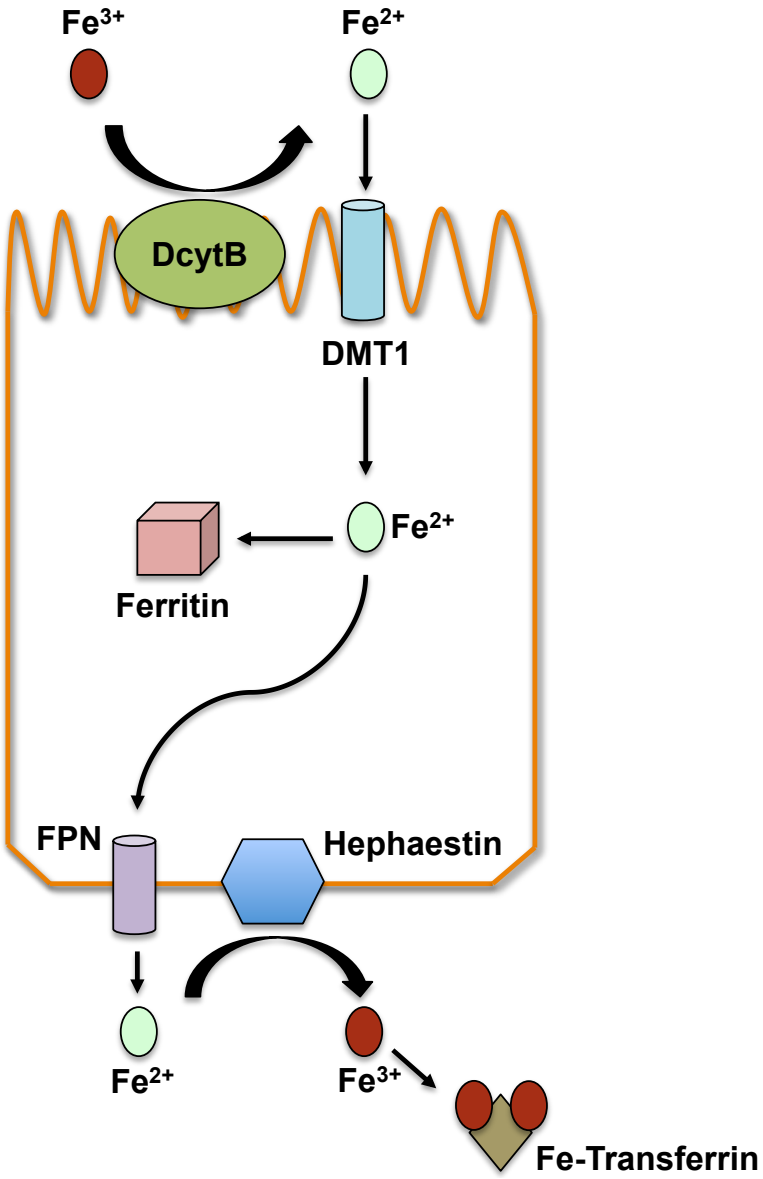

Figure 1-1. Dietary iron absorption at the duodenal enterocytes. Duodenal cytochrome B (DcytB) reduces Fe^{3+} to Fe^{2+}, which is subsequently internalized by Divalent Metal Transporter 1 (DMT1). Cytosolic iron is stored bound to ferritin or exported to the circulation via ferroportin. Hephaestin oxidizes Fe^{2+} to Fe^{3+}, which binds transferrin to be delivered to the tissues. Adapted from Biol. Res. 2006, 39: 113-124.

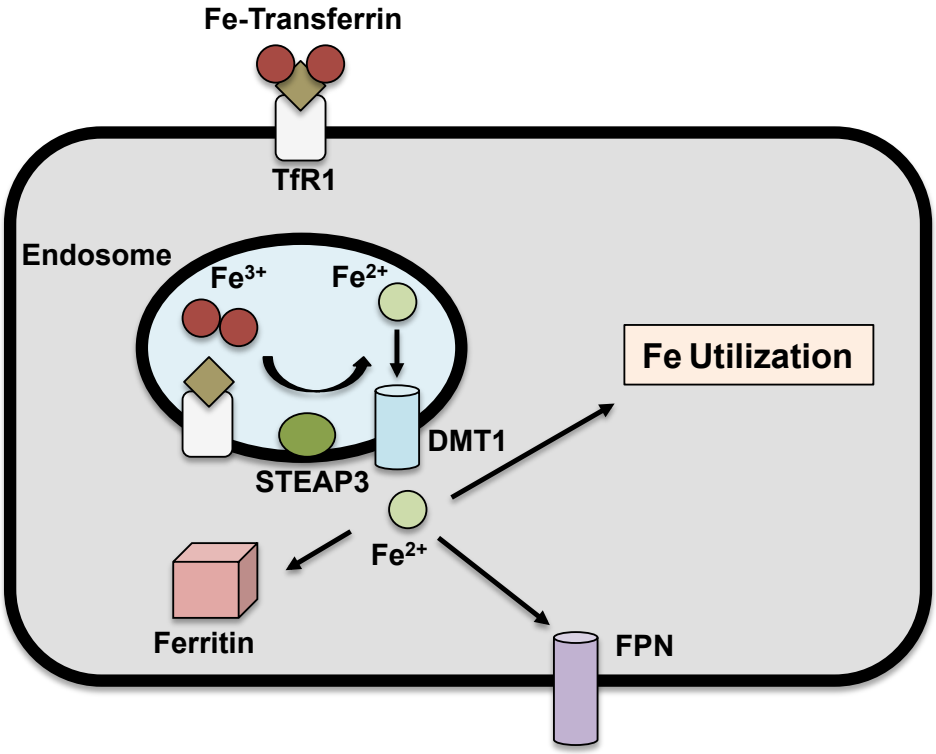

Figure 1-2. Cellular iron uptake. Iron-laden transferrin (Fe-Transferrin) binds to the tranferrin receptor 1 (TfR1). The Fe-transferrin-TfR1 complex is internalized by receptor mediated endocytosis. A reduction in endosomal pH induces iron release, which is later oxidized by the ferric oxidase STEAP3. Ferrous iron is transported to the cytosol by DMT1. Once in the cytosol, iron can be stored bound to transferrin, utilized by iron-dependent biochemical processes or exported via ferroportin (FPN). Adapted from Cell 117:285-297, 2004.

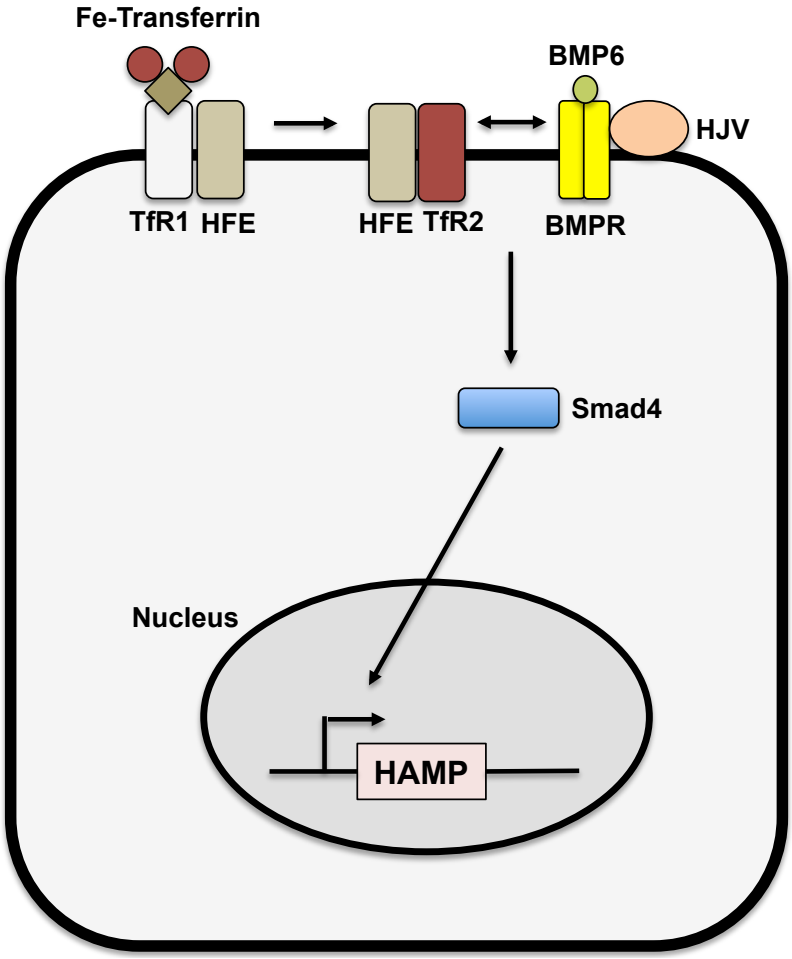

Figure 1-3. Regulation of Hepcidin expression by hepatocytes. Binding of iron-laden transferrin to transferrin receptor 1 releases HFE. Freed HFE interacts with transferrin receptor 2 (TfR2), which together with ligand-bound bone morphogenetic protein receptor (BMPR) in the presence of hemojuvelin (HJV) initiates a signal transduction cascade involving Smad4 that results in hepcidin transcription. Adapted from Blood. 2011, 117:4425-33.

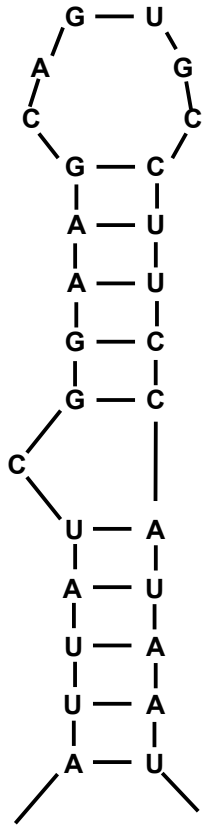

Figure 1-4. Structure of Transferrin Receptor 1 Iron Responsive Element (IRE). TfR1 IREs consist of 10 base pairs with a terminal conserved loop containing the sequence CAGUGC. Five base pairs 5' of the the loop; there is a bulge nucleotide that contains an unpaired cytosine that is critical for IRE function. Adapted from RNA. 2007, 13: 952-966.

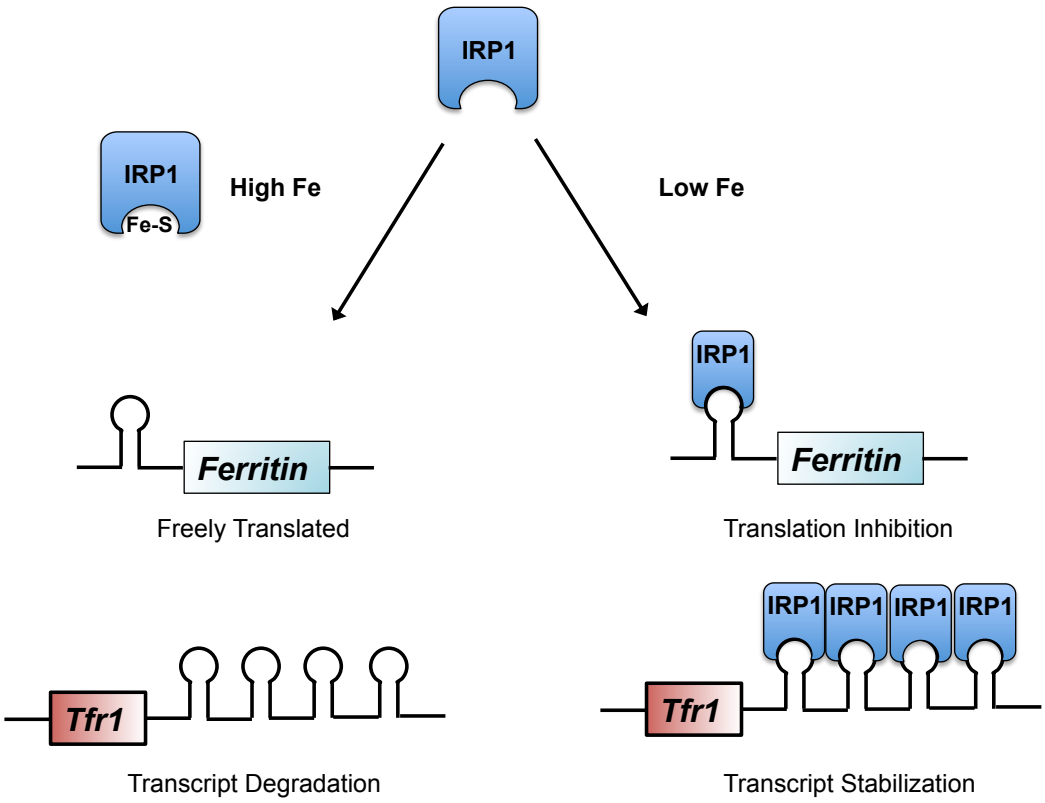

Figure 1-5. IRP1 mediated regulation of iron metabolism genes. Under iron-deplete conditions, IRP1 binds to IREs located in ferritin 5' UTR and in transferrin receptor 1 (TfR1) 3' UTR inhibiting ferritin translation and promoting TfR1 transcript stabilization. When iron is plentiful, IRP1 assembles an Fe-S cluster, acquires aconitase activity and loses its IRE-binding properties. Under these conditions, ferritin is freely translated and TfR1 mRNA is degraded. Adapted from Cell. 2004, 117:285-97.

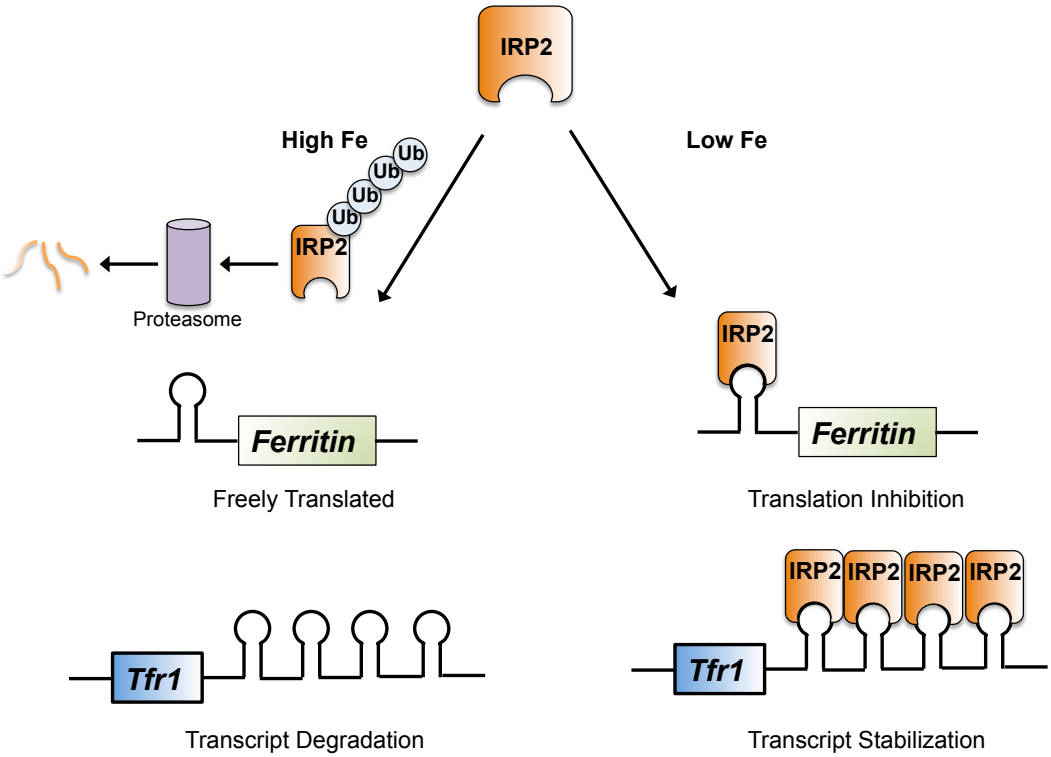

Figure 1-6. Cellular iron homeostasis regulation by IRP2. Under iron-deplete conditions, IRP2 binds to IREs in ferritin 5' UTR and TfR1 3' UTR inhibiting iron storage and promoting iron uptake. When iron is plentiful, IRP2 gets polyubiquitinated and degraded by the proteasome resulting in increased iron storage and diminished iron uptake. Adapted from Cell. 2004, 117:285-97.

Chapter 2: Iron- and Oxygen-Dependent Regulation of FBXL5

Introduction

As both iron excess and iron deficiency have detrimental effects, cells must tightly regulate iron metabolism to maintain iron concentration within normal levels. Cellular iron homeostasis is regulated by the Iron Regulatory Proteins 1 and 2 (IRP1 and 2) that post-transcriptionally regulate the coordinate expression of genes involved in iron metabolism (76). These RNA-binding proteins interact with cis-regulatory stem loop structures called Iron Responsive Elements (IREs) found in the 5' and 3' untranslated regions (UTRs) of target mRNA (41, 42). Under iron deplete conditions, IRPs bind IREs with high affinity inhibiting iron storage and promoting iron uptake. Binding of IRPs to a single IRE in the 5' UTR of ferritin mRNA prevents its translation while binding to multiple IREs in TfR1 mRNA 3' UTR protects the transcript from endonuclease degradation, thus, inducing its synthesis (79, 126, 175). When iron is plentiful, IRPs lose their IRE binding activity, ferritin mRNA is freely translated and TfR1 mRNA is degraded.

In vivo studies revealed that IRP2 has a more prominent role in maintaining iron homeostasis tha IRP1 (107). IRP2 stability is regulated in an iron-dependent manner. When iron and oxygen are limiting, IRP2 accumulates and binds IRE-containing mRNAs while in conditions where iron and oxygen are abundant, IRP2 gets degraded by the proteasome (67). IRP2 stability is regulated by a Skp1/Cullin1/F-box (SCF) E3 ubiquitin complex containing the F-box and Leucine-rich repeat protein 5 (FBXL5) (134, 159). Interestingly, FBXL5 is regulated in a reciprocal manner to IRP2. Under iron-replete conditions, FBXL5 recruits IRP2 to the SCF complex where it gets polyubiquitinated targeting it for degradation by the proteasome. When iron is limiting, FBXL5 is degraded and IRP2 becomes stabilized capable of binding IREs (134, 159).

FBXL5's protein levels change as a function of iron availability; however, the mechanism of its iron-dependent regulation is unclear. Elucidation of this regulatory mechanism will help to understand how IRP2 stability is tied to intracellular iron levels. Therefore, our laboratory sought to reveal the mechanisms governing FBXL5 regulation.

FBXL5 is Post-Translationally Regulated in an Iron- and Oxygen-Dependent Manner

In conditions where iron is plentiful, FBXL5 polyubiquitinates IRP2 targeting it for degradation by the proteasome. It has been also demonstrated that oxygen availability regulates IRP2 stability. Low oxygen concentrations such as those at which most tissues are exposed to, promote IRP2 accumulation (72, 107). To understand these regulatory mechanisms, cells expressing FLAG-tagged FBXL5 were treated with either ferric ammonium citrate (FAC) or an iron chelator deferoxamine mesylate (DFO). Immunoblot analysis revealed that, opposite to IRP2, FBXL5 protein levels accumulate under high iron condition but they are considerably reduced when iron is limiting (Fig. 2-1A). In cells treated with DFO, FBXL5 degradation was significantly reduced upon addition of the proteasome inhibitor MG132 (Fig. 2-1A). Likewise, FBXL5 levels were decreased when cells were exposed to hypoxia even in the presence of excess iron (Fig. 2-1B). Thus, the iron- and oxygen-dependent regulation of FBXL5 may reciprocally regulate IRP2 stability.

FBXL5 is Polyubiquitinated and Degraded by the Proteasome Under Low Iron Conditions

Treatment of cells with the proteasome inhibitor MG132 blocks FBXL5 degradation under iron limiting conditions (Fig. 2-1A). This suggested that FBXL5 degradation is proteasome-dependent. To further investigate whether FBXL5 degradation by the proteasome is preceded by polyubiquitination, HEK

293 cells stably expressing FLAG-tagged FBXL5 were treated with FAC or DFO in the presence or absence of MG132. FBXL5-FLAG was immunoprecipitated and immunoblotting analysis was done using an ubiquitin antibody. FBXL5 is polyubiquitanated under iron deficient conditions as depicted by increased laddering distinctive of heterogeneous polyubiquitination but diminished under high iron conditions (Fig. 2-2). Thus, these data suggest that FBXL5 is selectively polyubiquitinated when bioavailable iron is limiting, thereby tagging the protein for proteasomal degradation.

FBXL5 Hr Domain Confers Iron-Dependent Regulation to a Heterologous Protein

Previously, our laboratory reported that the region conferring FBXL5 iron-dependent regulation is located in residues 1 to 161. When this domain is deleted, FBXL5 accumulates under both high and low iron conditions (134). Bioinformatic analysis predicted that FBXL5 residues 1-161 adopt a hemerythrin-like (Hr) structure. Previously characterized hemerythrin domains consist of a bundle of α-helices enveloping a di-iron center that binds oxygen. Biophysical and structural studies confirmed the predictions and reported that FBXL5 hemerythrin (Hr) domain consist of a bundle of 5 α-helices encircling a di-iron center that, unlike previously characterized hemerythrin domains, does not seem to bind oxygen (134). This suggests that FBXL5 oxygen-dependent regulation is

independent of oxygen binding. However, oxygen in the environment may alter the oxidation state of the di-iron center, which could affect FBXL5 Hr domain folding. Interestingly, expression of FBXL5 Hr domain was sufficient to recapitulate iron- and oxygen-dependent regulation (134). Therefore, I sought to determine whether FBXL5 Hr domain was both necessary and sufficient to confer iron- and oxygen-dependent regulation.

To answer this question, I tested whether FBXL5 Hr domain could regulate a heterologous protein. HEK 293T cells were transiently transfected with constructs expressing FBXL5 Hr domain fused to either the N-terminus (Hr-Luc) or C-terminus (Luc-Hr) of firefly luciferase. When both fusion constructs were treated with FAC, luciferase activity was increased at least 2-fold but it was reduced in low iron conditions (Fig. 2-3, upper panel). These results correlated with changes in fusion protein accumulation (Fig. 2-3, lower panel). Incubation at low oxygen conditions also reduced luciferase activity and protein accumulation (Fig. 2-3). Therefore, fusion of FBXL5 Hr domain to a heterologous protein convey iron- and oxygen- dependent regulation suggesting that this domain is both necessary and sufficient to confer iron- and oxygen-dependent regulation.

Iron- and Oxygen-Dependent Degradation of FBXL5 Hr Domain is Preceded by its Polyubiquitination

Expression of FBXL5 Hr domain recapitulates FBXL5 iron- and oxygen-dependent regulation. In the presence of sufficient bioavailable iron and oxygen, FBXL5 Hr domain levels are dramatically increased, but it gets degraded when both iron and oxygen are low (134).

To determine whether FBXL5 Hr domain degradation under low iron and oxygen is proteasome-dependent and preceded by its polyubiquitination, HEK 293 stably expressing N-terminus FLAG-tagged and C-terminus HA-tagged FBXL5 Hr domain were incubated with FAC or DFO and in the presence or absence of the proteasome inhibitor MG132. FBXL5 Hr domain was immunoprecipitated using a FLAG antibody and protein accumulation was determined by immunoblotting. In the presence of MG132, FBXL5 Hr domain degradation was significantly reduced under low iron and oxygen conditions (Fig. 2-4). When iron is limiting, FBXL5 Hr domain becomes polyubiquitinated irrespective of the oxygen concentration (Fig. 2-4). Interestingly, under low oxygen conditions, FBLX5 Hr domain gets polyubiquitinated even in the presence of excess iron (Fig. 2-4). Thus, FBXL5 Hr domain becomes polyubiquitinated under low iron and oxygen conditions prior to being degraded by the proteasome.

FBXL5 does not Promote its own Polyubiquitination

FBXL5 responsiveness to changes in iron bioavailability is dependent on its N-terminal hemerythrin-like domain (134). Under iron deficient conditions, FBXL5 Hr domain gets polyubiquitinated and degraded by the protesome (Fig. 2-4). Deletion of this domain leads to constitutive accumulation of FBXL5 independent of iron concentration. In addition, fusion of FBXL5 Hr domain to a heterologous protein makes the protein responsive to changes in bioavailable iron and oxygen (Fig. 2-3). These data suggested that FBXL5 Hr domain might contain a degron that allows FBXL5 to be recognized and ubiquitinated by an E3 ubiquitin ligase.

Several reports indicate that the F-box subunits of Skp1/Cul1/F-box (SCF) E3 ubiquitin ligase complexes can undergo autoubiquitination (49, 137, 169). To investigate whether FBXL5 promotes its own ubiquitination, endogenous FBXL5 was depleted using a siRNA selectively targeting full length FBXL5 in cells stably expressing N-terminus FLAG-tagged and C-terminus HA tagged FBXL5 Hr domain. Then, cells were treated with FAC or DFO in presence or absence of MG132 and protein accumulation and polyubiquitination was determined by immunoblotting. FBXL5 depletion was sufficient to stabilize IRP2 under high iron conditions; however, it neither reduced FBXL5 Hr domain polyubiquitination nor prevented its degradation under low iron conditions (Fig. 2-5), thus, suggesting that autoubiquitination does not take place. These data indicates that a FBXL5 specific E3 ubiquitin ligase is yet to be identified.

FBXL5 Hr Domain Residues 77-81 are Part of a Regulatory Sequence Required for FBLX5 Iron-Dependent Regulation

To identify the region within FBXL5 Hr domain responsible for targeting the protein for degradation, several FBXL5 N-terminal deletion constructs were generated. Deletion mutants Δ1-33, Δ1-59 and Δ1-76 were constitutively degraded. On the other hand, Δ1-81 and Δ1-100 proteins accumulated under both high and low iron conditions suggesting a regulatory sequence might exist C-terminal of residue 76 (Fig. 2-6A). To narrow this region, constructs containing adjacent 5 amino acids deletions in the region spanning residues 67-91 were generated. Interestingly, deletion mutant Δ77-81 protein constitutively accumulates (Fig. 2-6B) suggesting that these residues are part of regulatory sequence required for FBXL5 proteasomal degradation.

Conclusions

Cellular iron homeostasis is primarily regulated by IRPs, which regulate the post-transcriptional expression of genes involved in iron metabolism. IRP2 stability is regulated in an iron- and oxygen-dependent manner. The protein accumulates under iron and oxygen deficient conditions, but it gets degraded by the proteasome when iron is plentiful.

FBXL5, the substrate recognition subunit of a SCF E3 ubiquitin ligase complex, controls IRP2 stability. Depletion of FBXL5 leads to uncontrolled accumulation of IRP2 with concomitant misregulation of its target genes, thus, underscoring the importance of FBXL5 in the regulation of iron homeostasis (134, 159).

Interestingly, FBXL5 is regulated in a reciprocal manner to IRP2 as the protein is stabilized under iron-replete conditions (Fig. 2-1). However, when iron and oxygen bioavailability is limited, FBXL5 is polyubiquitinated and degraded by the proteasome (Fig. 2-2). These data suggest that the iron- and oxygen-dependent regulation of IRP2 may be coupled to reciprocal effects on FBXL5's stability.

FBXL5 N-terminal residues 1 to 161, which adopt a hemerythrin-like (Hr) structure, confer the protein its iron- and oxygen-dependent regulation. Deletion of FBXL5 Hr domain renders the protein constitutively stable and accumulates under high and low iron conditions. Furthermore, fusion of FBXL5 Hr domain to firefly luciferase confers the protein iron- and oxygen-dependent regulation (Fig. 2-3).

Expression of FBXL5 Hr is sufficient to recapitulate the iron- and oxygen-dependent regulation observed in FBXL5 (134). When iron and oxygen are plentiful, FBXL5 Hr domain accumulates but it gets polyubiquitinated and degraded by the proteasome when iron and oxygen are limiting (Fig. 2-4). These

data suggested that FBXL5 Hr domain may contain a regulatory sequence that is recognized by an E3 ubiquitin ligase that targets it for its degradation.

It is not uncommon that the F-box subunits of SCF E3 ubiquitin ligases promote their own ubiquitination (49, 137, 169). However, depletion of endogenous FBXL5 had no effect on FBXL5 Hr domain polyubiquitination or degradation; thus, arguing against the possibility that FBXL5 could ubiquitinate FBXL5 Hr domain in *trans* (Fig. 2-5). N-terminal deletion constructs of FBXL5 revealed that residues 77-81 might be part of a regulatory sequence mediating FBXL5 proteasomal degradation (Fig. 2-6B). This region may be recognized by a yet to be identified E3 ubiquitin ligase.

Overall, the data presented here suggest that mammalian cells, by means of FBXL5 Hr domain, are capable of sensing intracellular iron and oxygen availability and consequently alter the stability of the IRPs in a mechanism mediated by the SCF^{FBXL5} E3 ubiquitin ligase complex. In addition, structural data revealed some unique features that could contribute to its iron and oxygen sensing ability including a fifth helix, not observed in previously characterized Hr domains, that contributes a residue in the iron coordination, and a truncated helix preceded by a extended loop that contains a regulatory element (134, 152). These data were generated in cell-based assays; therefore, the importance of FBXL5 in the regulation of iron homeostasis *in vivo* must be addressed.

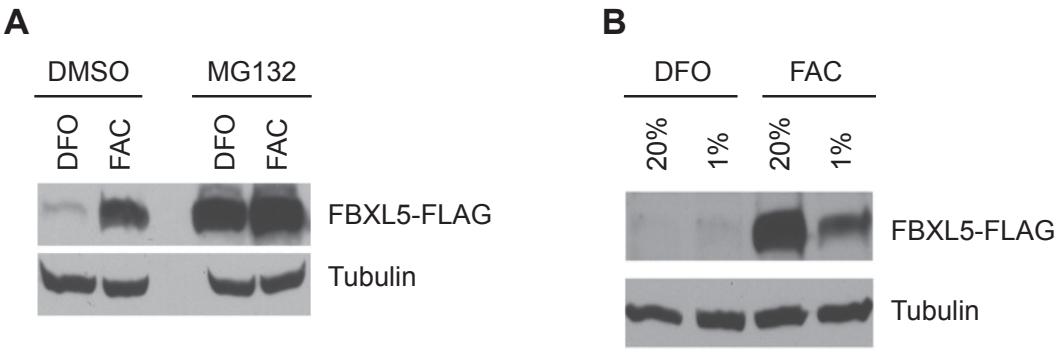

Figure 2-1. FBXL5 is regulated in an iron- and oxygen dependent manner. (A) Immunoblot analysis of stably transfected FBXL5-FLAG protein accumulation under high (FAC) or low (DFO) iron conditions. (B) Immunoblot analysis of FBXL5-FLAG accumulation exposed to normoxia (21% O_2) or hypoxia (1% O_2). Figure courtesy of Joel Thompson.

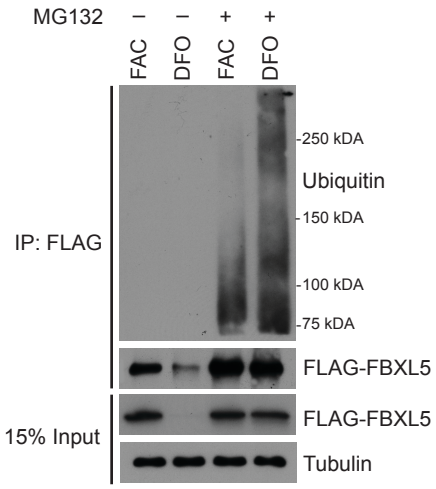

Figure 2-2. FBXL5 degradation under iron-deplete conditions is preceded by its polyubiquitination. Immunoblot analysis of immunoprecipitated FLAG-FBXL5 from cells treated with FAC or DFO in the presence or absence of the proteasome inhibitor MG132.

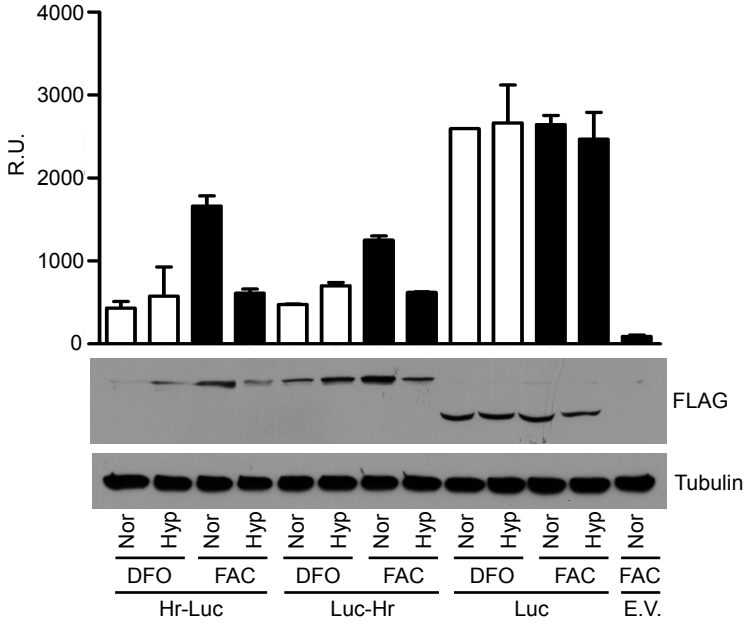

Figure 2-3. FBXL5 hemerythrin domain confers iron- and oxygen-dependent regulation to a heterologous protein. Luciferase activity (upper panel) and protein accumulation levels (lower panel) in HEK 293T cells transiently transfected with fusion proteins. E.V., empty vector.

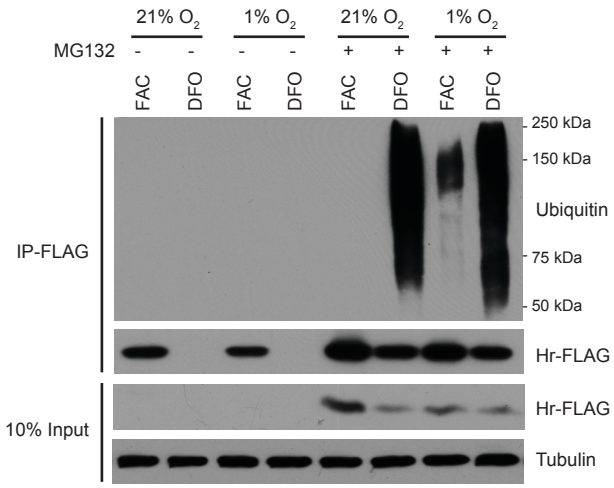

Figure 2-4. FBXL5 Hr domain gets polyuquitinated before being degraded by the proteasome under low iron and oxygen conditions. Immunoblot analysis of immunoprecipitaed N-terminus FLAG-tagged and C-terminus HA-tagged FBXL5 Hr domain from cells treated with FAC or DFO. MG132 was added where indicated to promote accumulation of polyubiquitinated protein.

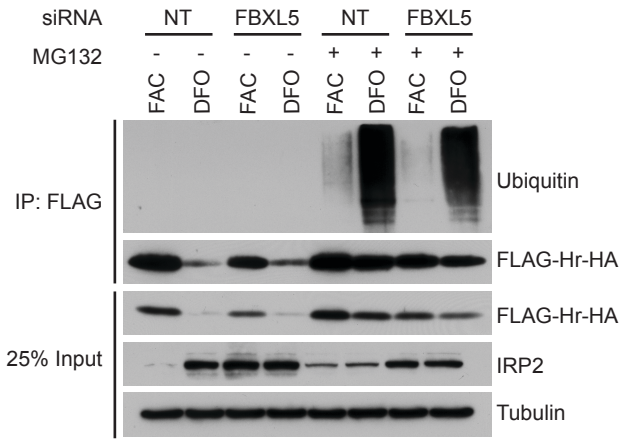

Figure 2-5. Ubiquitination of FBXL5 Hr domain is not dependent on FBXL5. HEK 293 cells stably expressing FLAG- and HA-tagged FBXL5 Hr domain were depleted of endogenous FBXL5 using siRNA prior treatment with FAC or DFO in the presence or absence of MG132. Protein accumulation and polyubiquitination of immunoprecipitaed FBXL5 Hr domain were determined by immunoblotting.

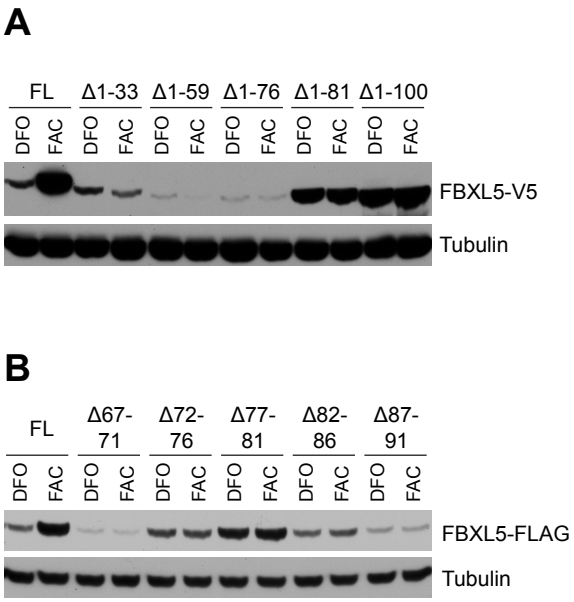

Figure 2-6. FBXL5 Hr domain contains a degron required for targeting the protein for degradation. (A) Immunoblot analysis of FBXL5 N-terminal deletion constructs treated with FAC or DFO. (B) Immunoblot analysis of FBXL5 short internal N-terminal deletion constructs treated with FAC or DFO. Figure courtesy of Joel Thompson.

Chapter 3: FBXL5 is Required for Maintenance of Cellular and Systemic Iron Homeostasis

Introduction

Iron is widely employed as a cofactor throughout biology. Failure to maintain bioavailable iron concentrations within appropriate levels may result in deleterious consequences ranging from iron overload to anemia (17, 64). Iron overload or hemochromatosis is a disease characterized by an increase in the rate of intestinal iron absorption and progressive accumulation of iron in various tissues (119). The most commonly affected tissues include the liver, heart and endocrine glands resulting in cirrhosis, cardiomyopathy and diabetes, respectively. Most types of iron overload disorders are of genetic origin (12, 120). These can be either autosomal recessive or dominant (86). All types of recessive genetic disorders leading to iron overload are the result of a deficit in hepcidin (HAMP) synthesis. Under normal circumstances, in response to high iron serum levels, hepcidin is released from the liver and promotes ferroportin internalization and degradation resulting in decreased iron absorption (57, 58, 166). Pathological reduction of HAMP production results in augmented ferroportin and increased iron absorption. Mutations have been found in HAMP or genes involved in HAMP synthesis. The majority of patients with hemochromatosis have mutation

in HFE or TfR2, which affects 1:500 people of European descent (119). The more severe cases of iron overload are seen in patients with mutations in HAMP or hemojuvelin. Unlike mutations in HFE or TfR2 that severely reduce hepcidin synthesis, mutations in HAMP and hemojuvenil completely abrogate hepcidin production (86, 119, 120). Dominant genetic disorders that lead to hemochromatosis affect ferroportin. Mutations in ferroportin's hepcidin binding site or defective phosphorylation following hepcidin binding render ferroportin resistant to hepcidin (86). To date, all patients identified are heterozygous for mutations in ferroportin as homozygosity would be lethal as suggested by the embryonic lethality of $FPN^{-/-}$ mice (38, 86). Hemochromatosis can also result as a consequence of severe chronic hemolysis, frequent blood transfusions as those needed for patients with Thalassemia or sickle cell disease or excess iron diet (60). Iron overload is treated with regularly scheduled phlebotomies or use of chelating agents such as deferoxamine and deferiprone (119).

Iron deficiency anemia is the most common nutritional disorder in the world (149). More than 30% of the world's population is anemic due to iron deficiency (43). It affects mainly children and pregnant women contributing to 20% of all maternal deaths (87). It is caused by insufficient consumption and absorption of iron or intestinal bleeding. Parasitic worm infections involving hookworms, whipworms and roundworms cause constant, unnoticeable intestinal bleeding leading to iron loss. Parasitic infections including malaria and worms

constitute the main cause of iron- deficiency anemia worldwide (39). Less common types of anemia include Anemia of Inflammation and Iron Resistant Iron Deficiency Anemia (IRIDA). The inability to absorb iron is due to an increase in hepcidin production which results in diminished ferroportin in the cell surface and decreased iron export. In Anemia of Inflammation, hepcidin production is stimulated by inflammatory stimuli such as increased levels of inflammatory cytokines IL-1 and IL-6 (86). Hepcidin transcription persists as long as the inflammatory stimuli are present. IRIDA results as a consequence of mutations to TMPRSS6, a cell surface protease that regulates hemojuvelin levels (17, 40). Loss of TMPRSS6 results in increased hemojuvelin and, therefore, hepcidin up-regulation (86, 145). Clinicopathological features of anemia include low hematocrit, moderate to low hemoglobin and reduced mean cell volume (17, 149). Since both iron excess and deficiency are pathologic, iron homeostasis must be tightly regulated.

Iron Regulatory Proteins 1 and 2 (IRP1 and 2) regulate the post-transcriptional expression of several iron metabolism genes upon binding Iron Responsive Elements (IREs) within the 5′ or 3′ untranslated regions (UTRs) of their mRNAs in iron depleted cells (76, 129). For example, translation of the iron storage protein Ferritin heavy chain 1 (FTH1) is reduced upon binding of IRPs to its 5′ IRE (129, 153). Conversely, iron uptake is promoted by stabilization of the mRNAs encoding the iron import factors TfR1 and DMT-1 upon IRP binding to

IREs within their 3′ UTRs (96). As iron bioavailability increases, IRPs lose their RNA binding capacity, either through conformational changes resulting from the enhanced FeS cluster assembly within IRP1 (70) or enhanced proteasomal degradation of IRP2 (67).

Selective degradation of IRP2 is preceded by its iron-dependent polyubiquitination via a Skp1/Cul1/Rbx1 (SCF) E3 ubiquitin ligase complex containing the F-box and Leucine-rich Repeat Protein 5 (FBXL5) (134, 159). FBXL5 contains an N-terminal hemerythrin-like (Hr) domain characterized by a helical bundle held together by a di-iron center (27, 144, 152). When iron and oxygen are abundant, this domain resides in a compact conformation that masks a degron within the Hr domain itself, promoting FBXL5 accumulation and subsequent IRP2 degradation (27, 134, 152). When low levels of bioavailable iron limit assembly of the di-iron center, the Hr degron becomes accessible and FBXL5 is degraded by the proteasome (27, 151, 152). These properties of the FBXL5 Hr domain suggest that it is a key sensor of bioavailable ferrous iron within cells (27, 133, 152). The importance of FBXL5 to the maintenance of cellular iron homeostasis was initially confirmed through siRNA-mediated knockdown of FBXL5 expression, which resulted in inappropriate stabilization of IRP2 in iron-replete cells (134). Such cells aberrantly repress ferritin expression while promoting continued iron uptake through stabilization of the TfR1 mRNA (134, 159), exacerbating the metabolic stress of excessive iron.

Although the importance of FBXL5 in cellular iron homeostasis has been previously addressed, the physiological role of FBXL5 is unknown. Specifically, FBXL5's roles in iron absorption, storage, erythropoiesis and development remain unanswered. To investigate the *in vivo* role for FBXL5 in the maintenance of iron homeostasis, we generated mice in which the *Fbxl5* gene locus has been disrupted.

FBXL5 is Ubiquitously Expressed

As all mammalian cells have a requirement for iron, yet are susceptible to damage when bioavailable iron accumulates, a *bona fide* cellular iron sensor should be ubiquitously expressed. FBXL5 mRNA levels were measured by quantitative Real-Time PCR (qRT-PCR) across panels of human and murine tissue extracts. As predicted, FBXL5 expression was detected in all samples with the highest relative levels present in the brain, particularly the metal-rich cerebellum (122), eye and testis (Fig. 3-1*A* and *B*). These same FBXL5 mRNA-abundant tissues also tend to express relatively high levels of IRP1 and IRP2 mRNAs (Fig. 3-1*A* and *B* and (107)). In the mouse, FBXL5 expression is high at embryonic day (E) 7.5 (Fig. 3-1*B*), suggesting a role in early embryogenesis, though its expression decreases as the embryo progresses through development (E11 and E15).

Mice Lacking a Functional *Fbxl5* Gene Die During Embryogenesis

To determine the physiological role of the iron sensor FBXL5 in the maintenance of iron homeostasis, we generated mice where FBXL5 expression has been globally ablated using gene trap technology. The trapping vector contains a splicing acceptor (SA) site follow by a promoterless selection marker (Neo) with a polyadenylation (pA) signal. Insertion of this gene-trapping (GT) vector downstream of *FBXL5*'s second exon generated a disrupted allele ($Fbxl5^{GT}$; Fig. 3-2A). Disruption of the FBXL5 locus was confirmed by genotyping PCR (Fig. 3-2B). Progeny from mice containing one copy of this non-functional allele were genotyped at various developmental time points. While wild type ($Fbxl5^{+/+}$), heterozygous ($Fbxl5^{+/GT}$) and homozygous null ($Fbxl5^{GT/GT}$) embryos were initially observed in a Mendelian 1:2:1 ratio, no $Fbxl5^{GT/GT}$ pups were born (Table 1). In the mixed genetic background of our mice, E9.5 $Fbxl5^{GT/GT}$ embryos exhibited growth retardation as compared to wild type and heterozygous littermates (Fig. 3-3). Although developmentally delayed, histopathological analysis revealed that E9.5 $Fbxl5^{GT/GT}$ embryos had undergone normal placentation as demonstrated by the fusion and formation of the chorioallantoic plate (Fig. 3-4A) with subsequent mixing of maternal and fetal blood (Fig. 3-4B). Furthermore, gastrulation and cardiovascular development

(Fig. 3-5) were normal as well. However, at E10.5 these embryos appeared very distorted and were completely absorbed by day E12.5.

Iron Metabolism Genes are Aberrantly Regulated in *Fbxl5*$^{GT/GT}$ Mouse Embryonic Cells

Given FBXL5's proposed role in mediating cellular iron homeostasis *in vivo*, we suspected that *Fbxl5*$^{GT/GT}$ embryos would fail to properly regulate IRE-containing mRNAs. The early embryonic lethality of the *Fbxl5*$^{GT/GT}$ mice prematurely precluded the in-depth analysis of FBXL5's role in iron homeostasis. To circumvent this problem, we generated mouse embryonic cell (MEC) lines from *Fbxl5*$^{+/+}$, *Fbxl5*$^{+/GT}$ and *Fbxl5*$^{GT/GT}$ embryos harvested on day E8 (Fig. 3-6*A*). *Fbxl5*$^{+/+}$ and *Fbxl5*$^{+/GT}$ cells depleted of bioavailable iron with the metal chelator deferoxamine mesylate (DFO) strongly accumulate IRP2 compared to iron-replete cells incubated with ferric ammonium citrate (FAC). However, *Fbxl5*$^{GT/GT}$ cells aberrantly accumulate IRP2 under both conditions (Fig. 3-7A). Total IRP1 protein levels remained constant under all conditions and in all cell types (Fig. 3-7*A*). This inappropriately accumulated IRP2 is competent for IRE binding (Fig. 3-7B) and *Fbxl5*$^{GT/GT}$ cells exhibit increased TfR1 expression and decreased ferritin expression under iron-replete conditions (Fig. 3-7A and 3-6B). An increase in iron uptake, coupled with a decrease in iron storage capacity, could

result in the over-accumulation of iron accompanied by increased oxidative stress in these FBXL5-null cells.

Ablation of IRP2 but not IRP1 Rescues FBXL5 Knockout Early Mortality

To ascertain whether embryonic lethality was due to deregulated IRP2 expression, we crossed *Fbxl5*$^{+/GT}$ mice with IRP2 knockout mice (52). Viable *Irp2*$^{-/-}$*; Fbxl5*$^{GT/GT}$ mice were born from *Irp2*$^{+/-}$*; Fbxl5*$^{+/GT}$ intercrosses, though no *Irp2*$^{+}$*; Fbxl5*$^{GT/GT}$ mice were observed (Table 2). Like their littermates, *Irp2*$^{-/-}$*; Fbxl5*$^{GT/GT}$ mice grow normally and are fertile. This result suggests that the early embryonic mortality of FBXL5-null animals is due to the constitutive accumulation of IRP2 with concomitant misregulation of its target genes. Interestingly, when *Irp1*$^{+/-}$*; Fbxl5*$^{+/GT}$ mice were crossed, no *Irp1*$^{-/-}$*; Fbxl5*$^{GT/GT}$ pups were observed at birth (Table 3), despite the significant redundancy in IRP1 and IRP2 function as assessed in cell culture models(52, 89, 107, 127).

***Fbxl5*$^{+/GT}$ Mice Differ from *Fbxl5*$^{+/+}$ Littermates When Fed a Low Iron Diet**

In contrast to the embryonic lethality of FBXL5-null mice, *Fbxl5* heterozygous (*Fbxl5*$^{+/GT}$) mice are born at expected ratios, grow normally, and are fertile. To determine if *Fbxl5*$^{+/GT}$ mice manifest a non-overt iron related phenotype(s), we challenged wild type and heterozygous mice with a low iron (5

ppm) diet and compared their results to mice weaned onto an iron-sufficient (50 ppm) diet (107, 127). After 3 weeks ingesting the specified diets, blood was collected by cardiac puncture from anesthetized mice and complete blood counts (CBC) and serum iron levels were determined. Wild type mice fed a low iron diet exhibited an expected 77% decrease in serum iron levels despite a compensatory 149% increase in the total iron binding capacity (TIBC) of transferrin (Table 4). Consistent with the low dietary iron availability, wild type animals report significant reductions in hematocrit and hemoglobin levels, and a modest reduction in the number of red blood cells (RBC) (Table 4).

All measurements taken from *Fbxl5*$^{+/GT}$ mice fed an iron sufficient (50 ppm) diet were indistinguishable from control wild type mice. Even *Fbxl5*$^{+/GT}$ mice fed a low iron diet exhibit similar changes in serum iron and TIBC values to those of their wild type counterparts (Table 4). However, this reduced iron availability does not subsequently result in any corresponding reductions in hematocrit, hemoglobin, or erythrocyte levels in the *Fbxl5* heterozygotes (Table 4).

To discard the possibility that this phenotype is due to the mixed background of our mice, *Fbxl5*$^{+/GT}$ mice were backcrossed to 129/SvEv mice to generate syngeneic *Fbxl5*$^{+/GT}$ mice. Similar to mixed background *Fbxl5*$^{+/GT}$ mice, syngeneic *Fbxl5*$^{+/GT}$ mice have normal hematocrit, hemoglobin and red blood cell values when fed a low iron diet (Table 5). These data suggest that *Fbxl5*$^{+/GT}$ mice

have altered systemic iron homeostasis so as to make iron preferentially available to the erythroid compartment irrespective of genetic background.

No Additional Iron is Mobilized from *Fbxl5*$^{+/GT}$ Liver Stores

Unlike wild type mice, *Fbxl5*$^{+/GT}$ mice retain normal hematocrit and hemoglobin values when dietary iron availability is limited. We hypothesized that the requisite iron needed to maintain these levels in the heterozygous could be made available either through depletion of iron stores or through increased intestinal absorption. A major site of iron storage is the liver (76). To examine whether the iron content of livers differed between wild type and heterozygous mice fed the low iron diet, total metal content was determined by inductively coupled plasma mass spectrometry (ICP-MS). As shown in Fig. 3-8, total iron content in the liver was reduced an equivalent amount in all mice fed the low iron diet for three weeks, providing no indication that additional iron was mobilized from *Fbxl5*$^{+/GT}$ liver stores.

Iron Absorption and Systemic Distribution are Altered in *Fbxl5*$^{+/GT}$ Mice Fed a Low Iron Diet

To determine if *Fbxl5*$^{+/GT}$ mice are more efficient than wild type mice at absorbing limiting dietary iron, ^{59}Fe was directly introduced via gastric gavage

into the stomachs of mice that had been fed a low iron diet for three weeks. These mice were sacrificed at various time points and the distribution of ^{59}Fe in various tissues was measured. At the earliest time point (1 hr), almost 80-fold more ^{59}Fe was incorporated within the duodena of *Fbxl5*$^{+/GT}$ mice on low iron diets as compared to wild type animals (Fig. 3-9*A*). This increased efficiency in intestinal uptake was accompanied by a corresponding 3-fold increase in serum ^{59}Fe levels at 1 hr (Fig. 3-9*B*). The whole body distribution of ^{59}Fe is also markedly different in the *Fbxl5*$^{+/GT}$ mice, as this newly absorbed iron is made preferentially available to the bone marrow (Femur; Fig. 3-9*C*) and spleen (Fig. 3-9*D*) for rapid incorporation into red blood cells (Fig. 3-9*E*), rather than sites of storage (liver; Fig. 3-9*F*).

Fbxl5 Haploinsufficiency Specifically Alters the Iron-Responsiveness of the Duodenum

Though *Fbxl5*$^{+/GT}$ mice are indistinguishable from *Fbxl5*$^{+/+}$ mice when fed an iron sufficient diet, the heterozygous mice take up iron more efficiently when dietary availability is limiting. To determine the underlying cause of this difference, immunoblot analysis was used to examine the expression of iron metabolism genes in the intestines of *Fbxl5*$^{+/GT}$ mice. In wild type mice fed a low iron diet, intestinal iron absorption is typically promoted in multiple ways. At the cell autonomous level (45, 54), IRP activity is induced within iron-depleted

intestinal epithelial cells (Fig. 3-10A), stabilizing an IRE-containing DMT1 transcript (Table 5) and subsequently promoting iron uptake through increased DMT1 expression (Fig. 3-10*A*). At the same time, reduced serum iron levels attenuate hepcidin (HAMP) transcription in the liver (Table 5) (57, 58). A reduction in circulating hepcidin levels stabilizes the iron export protein ferroportin (Fig. 3-10*A*) to facilitate iron absorption through the intestine. In the *Fbxl5*$^{+/GT}$ animals, the systemic, ferroportin-dependent, response is identical to *Fbxl5*$^{+/+}$ mice, both at the level of hepcidin expression in the liver (Table 5) and ferroportin accumulation in the duodenum (Fig. 3-10*A*). However, the cell autonomous response to low iron is dramatically altered in the duodena of mice containing only a single functional copy of the *Fbxl5* gene. In these *Fbxl5*$^{+/GT}$ mice fed a low iron diet, IRP2 protein levels are 7-fold higher than in the corresponding wild type mice (Fig. 3-10A and Table 6). The accompanying 2-fold increase in IRP-binding activity (Fig. 3-11) mimics the 2-fold additional increase in the IRE-containing DMT-1 mRNA (but not the IRE-independent DMT-1 mRNA isoform; Table 5) and DMT-1 protein levels (Fig. 3-10A and Table 6) in the *Fbxl5*$^{+/GT}$ duodenum samples. Interestingly, this enhanced IRP responsiveness appears to be primarily limited to the intestine as the expression of iron metabolism genes was identical between wild type and heterozygous livers (Fig. 3-10*B*), spleens, and brains (Tables 5 and 6).

Conclusions

While FBXL5 clearly contributes to the regulation of cellular iron homeostasis by coupling intracellular iron levels to IRP2 degradation (134, 159), the in vivo roles of FBXL5 are only beginning to be delineated.

Disruption of the ubiquitously-expressed (Fig. 3-1) murine *Fbxl5* gene results in a failure to sense changes in cellular iron availability accompanied by constitutive IRP2 accumulation and misexpression of IRP2 target genes under iron replete conditions (Figs. 3-6B and 3-7A). Mice lacking a functional FBXL5 gene die during embryogenesis (Fig.3-2 and table 1), though viability can be restored by simultaneous deletion of the IRP2, but not IRP1, gene (Tables 2 and 3). Mice containing a single functional *Fbxl5* allele behave similar to their wild type littermates when fed an iron-sufficient diet. However, unlike wild type mice that manifest decreased hematocrit and hemoglobin levels when fed a low-iron diet, *Fbxl5* heterozygotes maintain normal serum levels (Table 4). In these mice, the increased iron available to the erythroid lineage does not come at the expense of total liver stores (Fig. 3-8) but is instead due to increased iron absorption (Fig. 3-9). Molecular characterization of various tissues suggests that the iron-sensitivity of the FBXL5 sensor differs in the duodenum, altering the iron-responsiveness of Divalent Metal Transporter-1 (DMT-1) expression (Fig. 3-10 and Tables 5 and 6). Together these results provide new insights into the

relationship between cellular and systemic iron homeostasis and the privileged role of the intestine in their regulation.

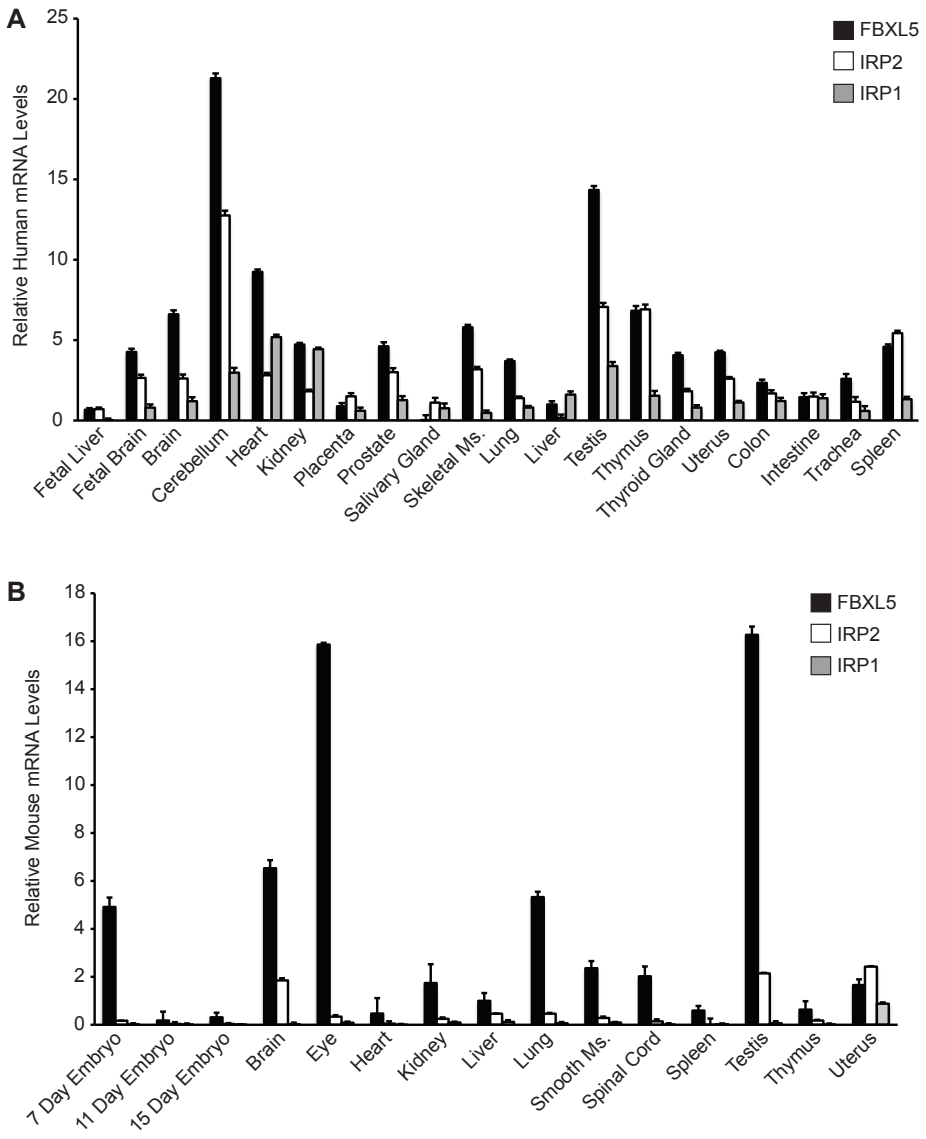

Figure 3-1. FBXL5 is ubiquitously expressed in humans and mice. Relative mRNA levels of FBXL5, IRP1, and IRP2 were quantitated by qPCR from human (*A*) and murine (*B*) tissue samples. Each column represents the average of three experiments ± SD.

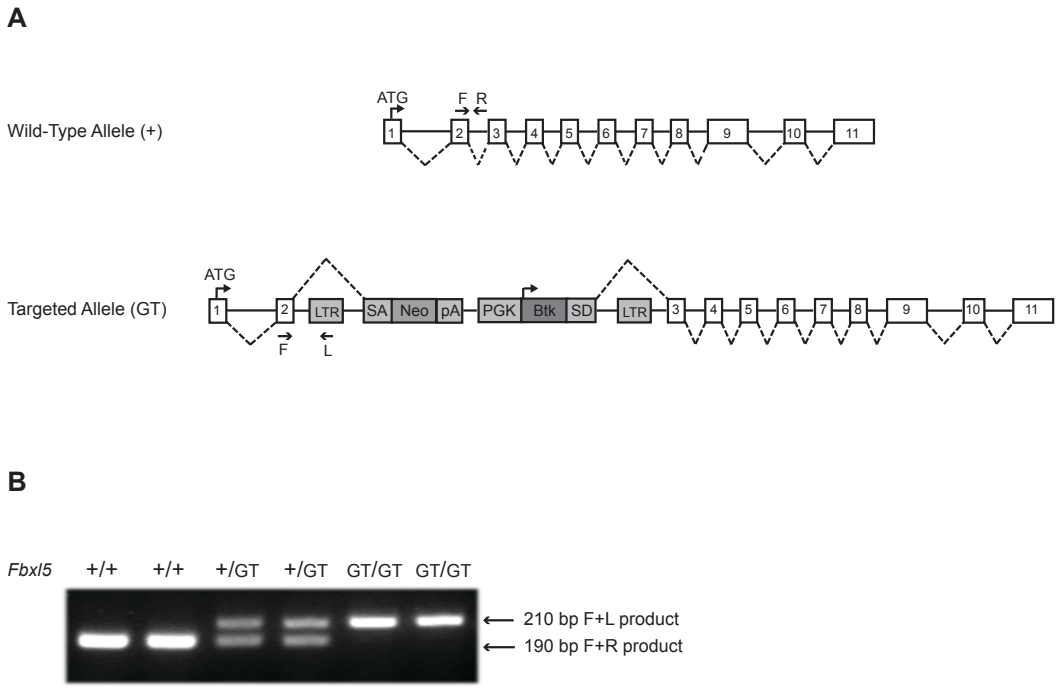

Figure 3-2. Disruption of the murine FBXL5 gene. (*A*) Embryonic stem cells containing a gene-trapped (GT) FBXL5 allele were used to generate FBXL5-null mice. A trapping vector containing a promoter-less neomycin (Neo) resistance cassette flanked by a splicing acceptor (SA) site and a polyadenylation signal sequence (pA) was inserted 3′ of FBXL5 exon 2. Utilization of the SA site generates a truncated FBXL5 mRNA transcript competent for Neo expression. The trapping vector also contains the first exon of the Bruton's tyrosine kinase (Btk) gene flanked by the PGK promoter sequence and a splicing donor site (SD). The resultant chimeric fusion transcript was used to generate a sequence tag of the trapped gene by 3′ RACE. (B) Genotypic analysis by PCR using genomic DNA isolated from wild type mice ($Fbxl5^{+/+}$), heterozygous mice ($Fbxl5^{+/GT}$), or FBXL5-null mice ($Fbxl5^{GT/GT}$).

Table 1. Genotypes of embryos from heterozygous matings

	No. of Progeny			
Stage	+/+	+/GT	GT/GT	Total
E9.5	20	44	18	82
E10.5	11	22	9	42
E11.5	12	28	10*	50
E12.5	10	22	0	32
Postnatal	85	155	0	240

* Partially absorbed Embryos

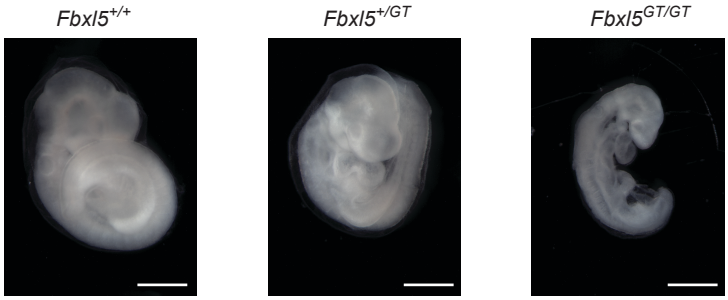

Figure 3-3. *Fbxl5*$^{GT/GT}$ embryos exhibit growth retardation with respect to their wild type (*Fbxl5*$^{+/+}$) and heterozygous (*Fbxl5*$^{+/GT}$) littermates. Embyos were harvested at day E9.5 and fixed in 4% paraformaldehyde. Bar = 1mm.

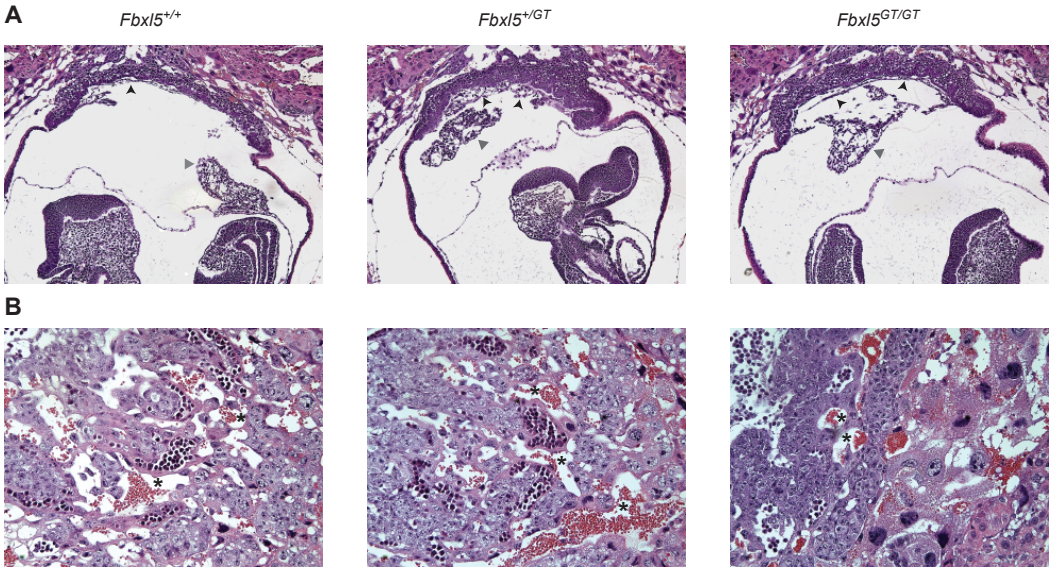

Figure 3-4. *Fbxl*$^{GT/GT}$ embryos undergo normal placentation. Histological analysis (H&E stained) of sagittal section of *Fbxl5*$^{+/+}$, *Fbxl5*$^{+/GT}$ and *Fbxl5*$^{GT/GT}$ embryos (E9.0) reveals (*A*) formation of the chorioallantoic plate (allantois, gray arrows; chorioallantoid plate, black arrows) and (*B*) maternal (*) and fetal blood mixing in the chorioallantoic plate.

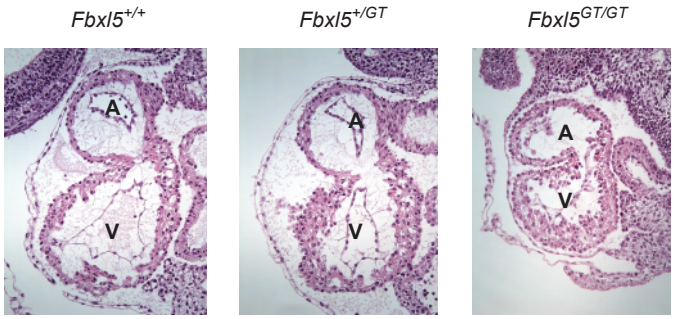

Figure 3-5. *Fbxl5*$^{GT/GT}$ embryos have normal heart development. Histological analysis (H&E stained) of sagittal sections of *Fbxl5*$^{+/+}$, *Fbxl5*$^{+/GT}$ and *Fbxl5*$^{GT/GT}$ embryonic hearts (E9.0). A = atrium; V = ventricle.

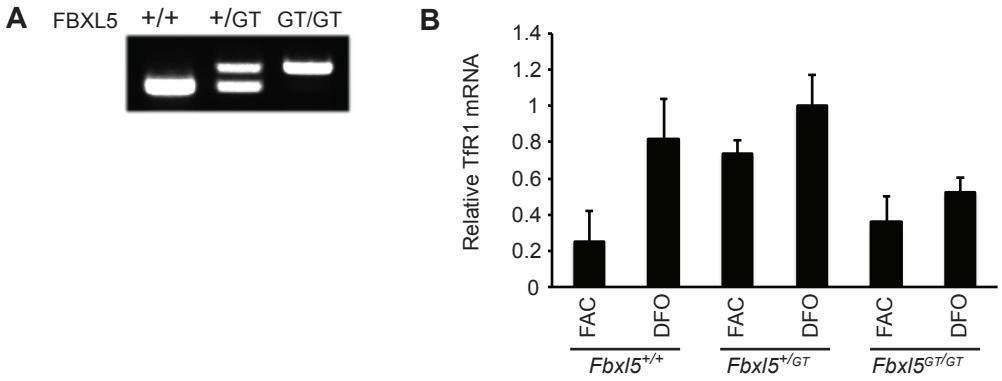

Figure 3-6. Generation of *Fbxl5*$^{+/+}$, *Fbxl5*$^{+/GT}$ and *Fbxl5*$^{GT/GT}$ mouse embryonic cells. (*A*) Mouse embryonic cells genotypes assessed by PCR assay (Fig. S1). (*B*) Relative TfR1 mRNA accumulation measured by qPCR. Each column represents the average of three experiments ± SD.

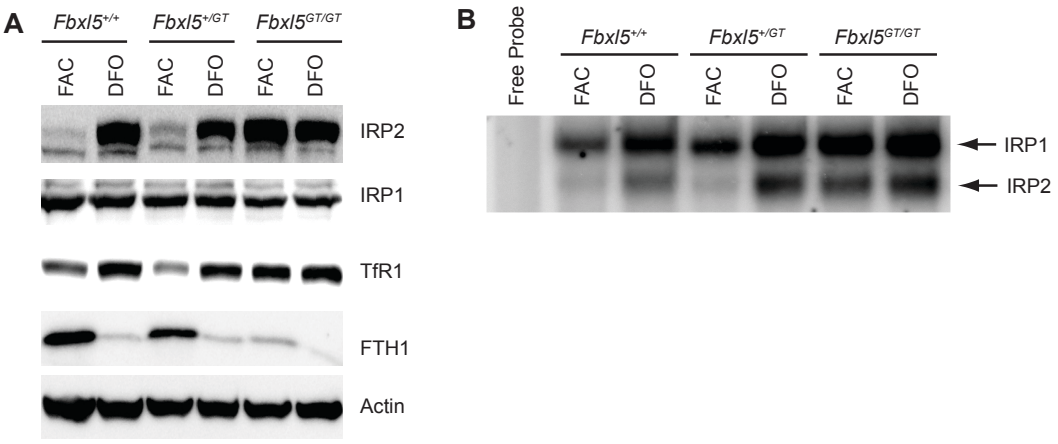

Figure 3-7. Iron metabolism genes are aberrantly regulated in *Fbxl5*$^{GT/GT}$ mouse embryonic cells. (*A*) Immunoblot analysis of IRP1 and IRP2 and their target genes Transferrin Receptor 1 (TfR1) and Ferritin Heavy Chain 1 (FTH1) from mouse embryonic cells treated with FAC and DFO. Actin levels were assessed as a loading control. (*B*) Assessment of RNA binding activity from mouse embryonic cells treated with FAC or DFO.

Table 2. Genotypes of mice produced from *Fbxl5*$^{+/GT}$; *Irp2*$^{+/-}$ intercrosses

	No. of Animals			
	Irp2$^{+/+}$	*Irp2*$^{+/-}$	*Irp2*$^{-/-}$	Total
Fbxl5$^{+/+}$	11	20	7	38
Fbxl5$^{+/GT}$	24	36	7	67
Fbxl5$^{GT/GT}$	0	0	5	5
Total	35	56	19	110

p-value for the Chi-Square test was 0.0698 indicating that the genotype distribution was not significantly different from expected Mendelian ratios.

Table 3. Genotypes of mice produced from *Fbxl5*$^{+/GT}$; *Irp1*$^{+/-}$ intercrosses

	No. of Animals			
	Irp1$^{+/+}$	*Irp1*$^{+/-}$	*Irp1*$^{-/-}$	Total
Fbxl5$^{+/+}$	37	54	21	112
Fbxl5$^{+/GT}$	39	124	37	200
Fbxl5$^{GT/GT}$	0	0	0	0
Total	76	178	58	312

p-value for the Chi-Square test was 0.0042 indicating that the genotype distribution was significantly different from expected Mendelian ratios.

Table 4. Hematological parameters and serum values from *Fbxl5*$^{+/+}$ and *Fbxl5*$^{+/GT}$ mice fed either an iron sufficient or low iron diet

	Fbxl5$^{+/+}$		*Fbxl5*$^{+/GT}$	
	Sufficient Fe	Low Fe	Sufficient Fe	Low Fe
RBC (M/µl)	9.21 ± 0.26	7.62 ± 0.43[a]	9.19 ± 0.23	9.32 ± 0.36[a]
Hematocrit (%)	52.64 ± 2.19	33.53 ± 1.87[b]	51.29 ± 1.73	48.84 ± 2.11[b]
Hemoglobin (g/dL)	13.76 ± 0.33	9.91 ± 0.79[c]	13.72 ± 0.45	13.17 ± 0.51[c]
Iron (µg/dL)	253.3 ± 20.17	58.50 ± 9.71	252.8 ± 5.36	53.25 ± 10.3
TIBC (µg/dL)	337.5 ± 7.8	504.2 ± 9.44	334.5 ± 26.3	556.25 ± 34.8
Saturation (%)	75.25 ± 6.32	12.75 ± 1.41	76.75 ± 4.95	10.00 ± 2.12

Note. Values expressed as mean ± SD of 12 replicates. In the rows, differences between paired values denoted by superscript letters are statistically significant as determined by t-test. [a] $p = 0.0069$; [b] $p < 0.0001$; [c] $p < 0.005$.

Table 5. Hematological parameters and serum values from syngeneic Fbxl5$^{+/+}$ and Fbxl5$^{+/GT}$ mice fed either an iron sufficient or low iron diet

	Fbxl5$^{+/+}$		*Fbxl5*$^{+/GT}$	
	Sufficient Fe	Low Fe	Sufficient Fe	Low Fe
RBC (M/µl)	9.98 ± 0.32	7.01 ± 0.53[a]	8.93 ± 1.12	8.74 ± 0.21[a]
Hematocrit (%)	51.44 ± 1.26	28.55 ± 1.76[b]	48.93 ± 2.41	44.94 ± 2.69[b]
Hemoglobin (g/dL)	15.26 ± 0.33	9.21 ± 0.56[c]	14.96 ± 1.06	12.60 ± 0.33[c]
Iron (µg/dL)	285.2 ± 35.96	57.01 ± 13.1	298.7 ± 48.6	51.03 ± 10.2
TIBC (µg/dL)	343.75 ± 20	576 ± 18.71	333.5 ± 28.1	579 ± 13.78
Saturation (%)	87.25 ± 4.83	10.75 ± 3.86	89.5 ± 11.09	9.75 ± 1.72

Note. Values expressed as mean ± SD of 12 replicates. In the rows, differences between paired values denoted by superscript letters are statistically significant as determined by t-test. [a] $p = 0.0033$; [b] $p < 0.0051$; [c] $p < 0.0006$.

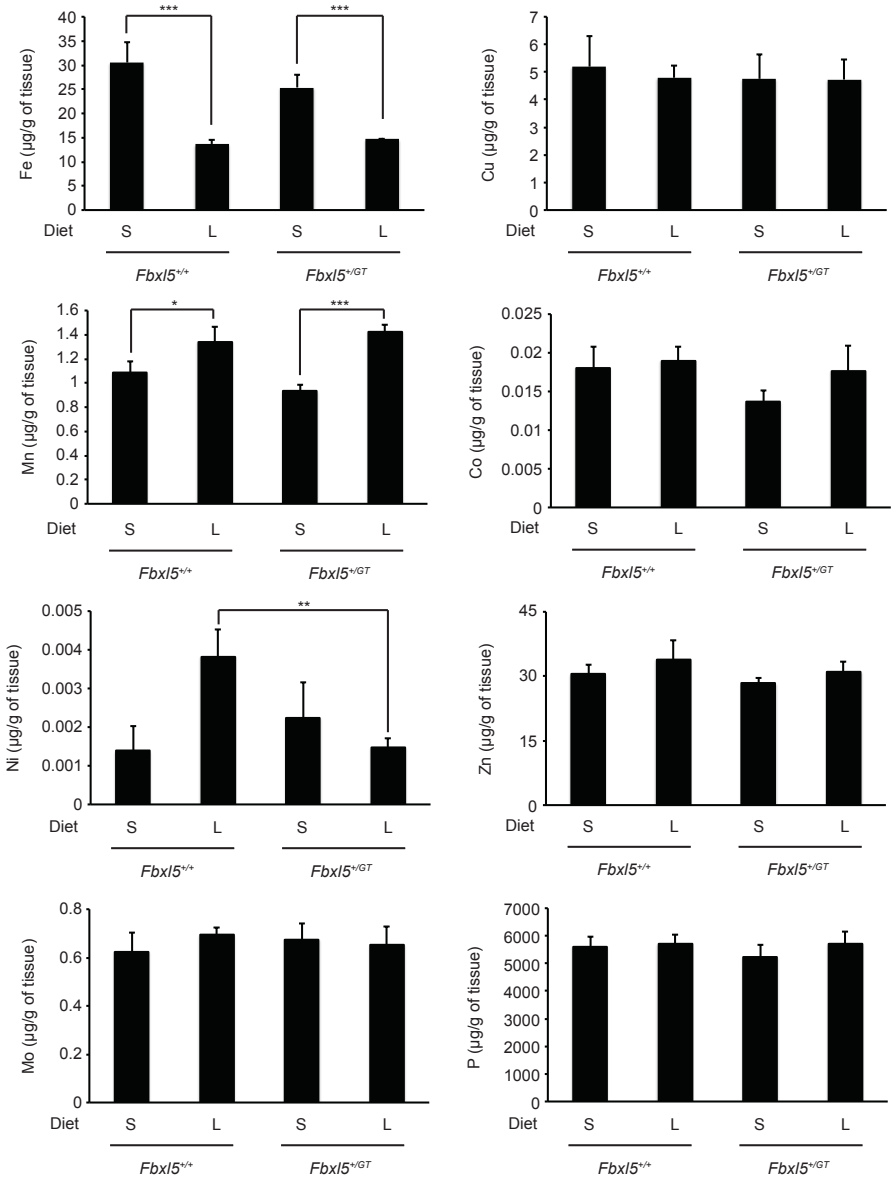

Figure 3-8. Total element concentrations in *Fbxl5*$^{+/+}$ and *Fbxl5*$^{+/GT}$ mice. The iron (Fe), copper (Cu), manganese (Mn), cobalt (Co), nickel (Ni), zinc (Zn), molybdenum (Mo) and phosphorus (P) content in perfused livers from FBXL5$^{+/+}$ and FBXL5$^{+/GT}$ mice fed either an iron sufficient (S; 50 ppm) or a low (L; 5 ppm) iron diet for 3 weeks. Each column represents the average of 4 mice ± SD and statistically-significant differences were determined by t-test: *** $p < 0.0001$, ** $p < 0.003$, * $p < 0.05$.

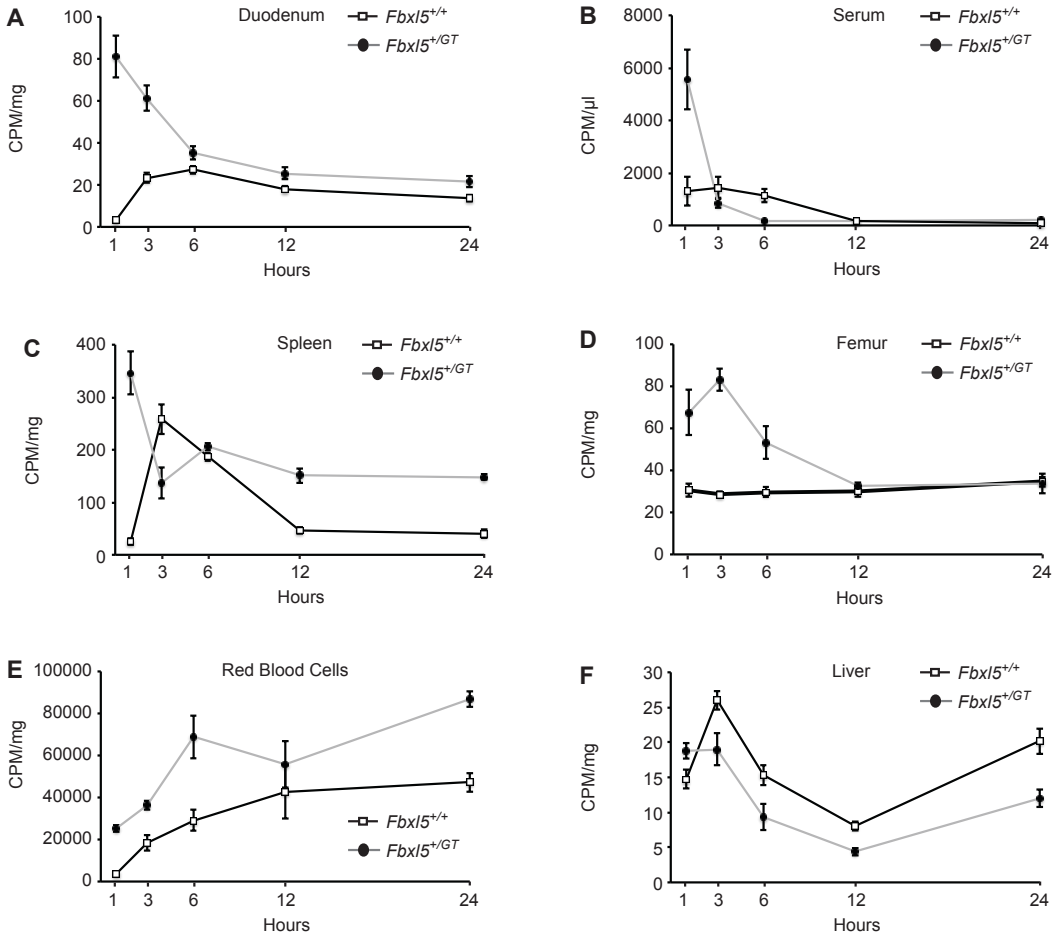

Figure 3-9. *Fbxl5*$^{+/GT}$ mice fed a low iron diet for three weeks have altered ^{59}Fe absorption and distribution profiles compared to wild type littermates. ^{59}Fe levels were measured in the (*A*) duodenum, (*B*) serum, (*C*) femur, (*D*) spleen, (*E*) red blood cells and (*F*) liver at the indicated time points. Each point represents the average values from 4 mice ± SD.

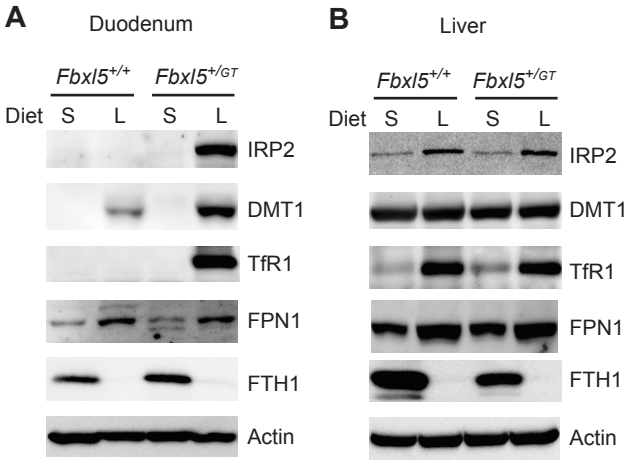

Figure 3-10. The duodena of *Fbxl5*$^{+/GT}$ mice display a heightened responsiveness to a low iron diet. Immunoblot analysis of IRP2 and its targets DMT1, TfR1, ferroportin (FPN1) and FTH1 in the duodenum (*A*) and liver (*B*) of *Fbxl5*$^{+/+}$ and *Fbxl5*$^{+/GT}$ mice fed either an iron sufficient (S; 50 ppm) or low (L; 5 ppm) iron diet for three weeks. Actin levels were assessed as a loading control. Quantitation is provided in Table 6.

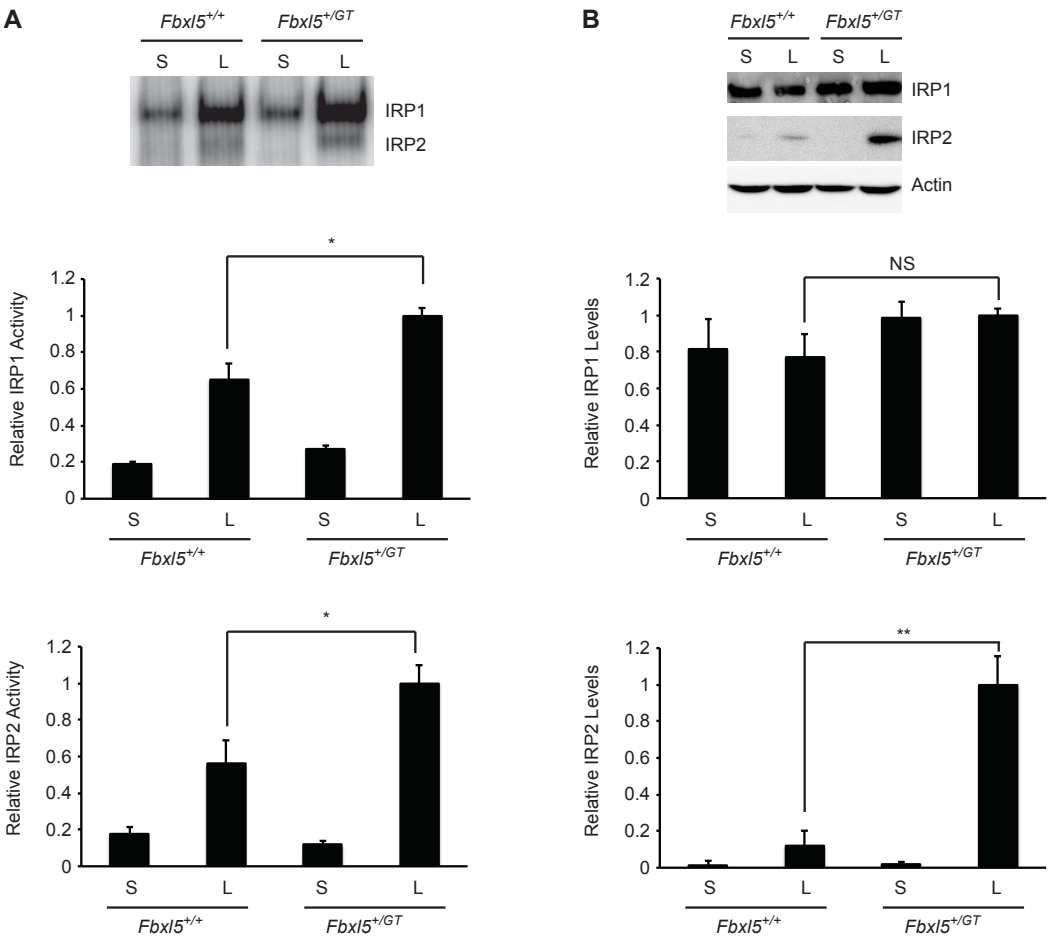

Figure 3-11. The IRE binding activity of IRP1 and IRP2 are increased in *Fbxl5*$^{+/GT}$ mice fed a low iron diet. (*A*) Measurement of IRE binding activity by EMSA from duodenum lysates made from *Fbxl5*$^{+/+}$ and *Fbxl5*$^{+/GT}$ mice fed either a low iron (L; 5 ppm) or iron sufficient (S; 50 ppm) diet for 3 weeks. Quantification of IRE binding activity is indicated below. (B) Immunoblot analysis and quantification of IRP1 and IPR2 protein levels from the same duodenum lysates. Each column represents the average of 4 mice ± SD and statistically-significant differences were determined by t-test: * $p < 0.05$; ** $p < 0.03$.

Chapter 4: Discussion and Future Directions

Iron- and Oxygen-Dependent Regulation of FBXL5

Cellular iron homeostasis is regulated primarily by the IRPs (107), which controls the post-transcriptional expression of genes involved in iron metabolism in a coordinated fashion (76). Under oxygen and iron deplete conditions IRP2 inhibits the translation of the iron storage protein ferritin upon binding to its 5' IRE (41, 90, 101). At the same time, iron uptake is promoted by stabilization of mRNA encoding the iron import factor TfR1 (96, 153, 165). When iron is abundant, IRP2 loses its IRE binding capacity through enhanced proteasomal degradation (67).

Regulation of IRP2 necessitates that cells sense both bioavailable iron and oxygen and couple this information to changes in IRP2 stability. Work from our laboratory and others reported that a Skp1/Cullin/F-box (SCF) E3 ubiquitin complex containing the F-box and Leucine rich repeat protein 5 (FBXL5) regulates IRP2 stability (134, 159). Depletion of FBXL5 leads to aberrant accumulation of IRP2 with concomitant misregulation of its target genes; hence, underscoring FBXL5 importance in iron homeostasis (134, 159). Interestingly, FBXL5 is regulated in an inverse fashion to IRP2. The protein is stabilized under iron-replete conditions but polyubiquitinated and degraded by the proteasome

when iron and oxygen are low (Fig. 2-1A and B, Fig. 2-2). Therefore, the ironand oxygen-dependent regulation of IRP2 is coupled to reciprocal effects on FBXL5's stability.

Deletion mutagenesis mapped the region conferring FBXL5 iron- and oxygen-dependent to the N-terminal 1-161 residues. Deletion of this domain renders the protein constitutively stable and accumulates under both high and low iron conditions (134). Furthermore, expression of this domain is sufficient to recapitulate iron-dependent regulation (134). Biophysical and structural studies revealed that FBXL5 1-161 residues adopt a hemerythrin-like (Hr) folding consisting of a bundle of 5 α-helices held together by a di-iron center and its stability is better increased in presence of iron as compared to other metals (27, 144, 152). These data suggested that FBXL5 Hr domain serves as an iron sensor that regulates FBXL5 stability.

Since deletion of FBLX5 hr domain resulted in constitutive accumulation of FBXL5 and fusion of this domain to firefly luciferase conferred the protein iron- and oxygen-dependent regulation (Fig. 2-3), a regulatory sequence (degron) that directs recognition by an E3 ubiquitin ligase must exist in this domain. A series of deletion constructs revealed that removal of amino acids 77-81 from the hemerythrin domain leads to constitutive accumulation of FBXL5 under both high and low iron conditions (Fig. 2-6A and B).

Identification of a putative degron in the hemerythrin domain, together with the fact that FBXL5 Hr domain is polyubiquitinated and degraded by the proteasome under iron- and oxygen-deplete conditions (Fig. 2-4), suggested that FBXL5 iron- and oxygen-dependent degradation is mediated by an E3 ubiquitin ligase. There are many examples in nature where the F-box subunit of a SCF E3 ligase complex undergoes autoubiquitination. The F-box proteins Grr1, Cdc4p and Met3op are components of different SCF complexes, and they are degraded in an ubiquitin-proteasome dependent manner (49). However, their ubiquitination requires the presence of all SCF components as well as an intact F-box suggesting that these proteins undergo autoubiqutination in a *cis* manner (49). This type of regulation is unlikely to occur in FBXL5 as the hemerythrin domain, unable to assemble into a SCF complex, gets ubiquitinated and degraded (Fig 2-4). Autoubiquitination can also occur in *trans*. The F-box protein Skp2 is has been shown to undergo autoubiquitination in *trans* (169). Unlike Skp2, depletion of endogenous FBXL5, capable of stabilizing IRP2, does not affect neither FBXL5 Hr domain polyubiquitination nor its degradation (Fig. 2-5). Interestingly, a report indicates that overexpression of dominant negative Cul-1 results in increased accumulation of FBXL5 suggesting that a SCF E3 ligase complex not containing FBXL5 may regulate FBXL5's stability (173). Overall, these data argues against FBXL5 promoting its own ubiquitination and, therefore, an E3 ubiquitin ligase responsible for targeting FBXL5 for degradation is yet to be found.

FBXL5 Hr domain compact tertiary structure makes the degron inaccessible for an E3 ubiquitin ligase to promote its ubiquitination. Therefore, in order for FBXL5 to be targeted for degradation, it must undergo a conformational change that exposes this regulatory sequence. Thermal denaturation assays showed that iron removal from the FBXL5 Hr domain results in a significant conformational change that disrupts the compact tertiary structure of the domain (133, 152, 171). This remark was confirmed by limited proteolysis experiments (27, 152). In the presence of iron, FBXL5 hemerythrin (Holo-FBXL5 Hr) domain is resistant to proteolysis but is degraded in cells depleted of iron. These observations suggest that in response to changes in iron bioavailability, FBXL5 undergoes conformational changes that control its stability (27, 152).

Overall, these data propose a model in which in the presence of abundant iron and oxygen, FBXL5 Hr domain resides in a compact conformation that masks a degron within the domain itself, promoting FBXL5 accumulation and subsequent IRP2 degradation. When low levels of bioavailable iron limit assembly of the di-iron center, FBXL5 Hr degron becomes accessible, FBXL5 is degraded and IRP2 is stabilized. These properties of FBXL5 Hr domain suggest that it is a key sensor of bioavailable iron within the cell.

Physiological Role of FBXL5

FBXL5 plays a critical role in the maintenance of cellular iron homeostasis (134, 159). Its Hr domain serves as direct sensor of cellular iron availability and governs the selective accumulation of FBXL5 in iron replete cells. In turn, FBXL5 assembles into an E3 ubiquitin ligase complex that mediates the polyubiquitination of IRP2 (134, 159). Subsequent proteasomal degradation of IRP2 promotes cellular adaptation to elevated iron bioavailability in part by alleviating repression of ferritin translation to promote iron storage while attenuating expression of proteins engaged in iron import.

Here I show that previous *in vitro* findings extend to a required *in vivo* role for FBXL5. Global inactivation of the *Fbxl5* gene results in embryonic lethality, with growth defects readily apparent prior to day E9 despite normal placentation, gastrulation, and cardiovascular development (Figs. 3-3, 3-4 and 3-5). Similarly, Ching et al. performing forward genetic mutagenesis using *N-ethyl-N*-nitrosourea (ENU) in mice identified a mutation where methionine 127 was replaced by lysine, which resulted in midgestation death (26). This mutation, located in FBXL5 hemerythrin domain, may perturb proper folding of the hemerythrin domain rendering the protein constitutively unfolded and, therefore, degraded.

As predicted, cells derived from FBXL5-null embryos are unable to sufficiently degrade IRP2 when incubated in the presence of excess iron and are apt to import iron that cannot be appropriately sequestered within the limiting

amount of ferritin available (Fig. 3-7A). Using an independently generated *Fbxl5* knockout mouse, it was recently shown that FBXL5-null embryos accumulate excess ferrous iron and are exposed to damaging levels of oxidative stress (110). Likewise, mice where ferritin heavy chain expression has been ablated ($Fth^{-/-}$) die at day E3.5 because entering iron cannot be sequestered leading to overproduction of reactive oxygen species, which are detrimental for cell macromolecules (44).

Because many E3 ligases ubiquitinate multiple substrates (80), it remains possible that unregulated accumulation of additional putative FBXL5 substrates, including the dynactin component $p150^{Glued}$(177), could contribute to embryonic death. However, simultaneous inactivation of both the *Fbxl5* and *Irp2* genes is sufficient to reverse the embryonic lethality and produce viable pups despite the absence of a functional copy of the *Fbxl5* gene (Table 2), also consistent with a prior report (110). Though these results do not preclude the possibility of additional FBXL5 substrates, a critical role for the iron-sensing SCF^{FBXL5} E3 ligase in the maintenance of *in vivo* cellular iron homeostasis, through its regulatory effects on IRP2, has been validated.

Despite sharing >70% identity (98), the mechanisms by which the IRE-binding activity of IRP1 and IRP2 are inactivated in iron-replete cells largely differ. Under normal cellular conditions the primary mechanism through which IRP1 RNA binding is inactivated by iron involves insertion of an iron-sulfur cluster, converting IRP1 to the holo- or cytosolic isoform of aconitase that cannot

bind IREs (118, 162). In this holo conformation, IRP1 is refractory to both degradation and IRE recognition. Though the apo form of IRP1 is also a substrate for FBXL5-mediated degradation (29, 134, 164), the contribution of protein degradation to IRP1 regulation is not completely understood. Enhanced IRP1 degradation is important when the Fe-S cluster switch mechanism is not fully operative (29). In extracts from both mouse embryonic cells and duodenum, IRE binding by IRP1 is enhanced upon partial or complete FBXL5 inactivation (Fig. 3-7B), even though total IRP1 protein accumulation remains relatively constant (Fig. 3-7A). However, if only a small percentage of IRP1 protein were competent for RNA-binding, as is the case in liver ad perhaps other tissues (107), significant changes in the accumulation of this apo form directly stemming from a block SCF^{FBXL5}-mediated degradation may be difficult to detect by immunoblot analysis over the background of bulk holo-IRP1. Alternatively, iron-sulfur cluster assembly on IRP1 may be compromised in FBXL5-deficient cells as a result of increased oxidative stress (51, 116) or some other mechanism.

IRP1 and IRP2 are generally thought to bind the same mRNA targets *in vivo* (89) and their physiological roles are also presumed to be largely redundant (107). However, despite FBXL5-dependent effects on IRP1 activity, simultaneous inactivation of the *Irp1* gene product did not rescue the embryonic lethality in FXBL5-null mice (Table 3). This result was somewhat surprising given that in extracts from both mouse embryonic cells and duodenum, IRP1 has a total RNA

binding capacity comparable IRP2's (Fig. 3-7B and Fig. 3-11). If rescue of embryonic lethality upon IRP2 ablation were solely due to a reduction in the total IRE-binding capacity within cells, IRP1 inactivation might be expected to result in similar compensatory changes in total IRE-binding capacity in many iron-replete, FBXL5-null, tissues. Though indicating that IRP1 and IRP2 have distinct physiological roles, these results cannot distinguish between the possible underlying mechanisms including IRP2-selective IRE targets (15), differences in temporal and spatial expression patterns (Fig. 3-1), or differential responsiveness in the context of additional physiological stresses such as hypoxia (71, 72, 108).

In addition to the similar results observed upon global FBXL5 inactivation, Moroishi and colleagues also constructed a mouse model in which FBXL5 was selectively ablated in the liver. Though viable, these mice exhibited both cell-autonomous effects, including hallmarks of liver damage, and systemic effects, consisting of increased serum iron levels likely due to decreased hepcidin expression in the liver. When challenged with a high iron diet, severe iron overload was restricted to the liver and proved fatal within a day (110). In this context, the phenotype we observed with the heterozygous *Fbxl5*$^{+/GT}$ mice was of particular interest in at least two key respects: 1) the phenotype was manifested with a low iron diet and 2) the phenotype suggests that the intestine has distinct iron-sensing characteristics that may underlie a more privileged role in the

maintenance of systemic iron homeostasis in response to iron deficiency than previously appreciated.

Fbxl5 haploinsufficiency had no observed effect on the behavior of most tissues we examined, including the liver, either from animals fed a low iron (5 ppm) or iron-sufficient (50 ppm) diet (Fig. 3-10B and Table 6). We also saw no difference in animals fed standard chow that contains excess iron (250 ppm, data not shown), though it remains possible that new phenotypes could emerge in the $Fbxl5^{+/GT}$ mice when challenged with supraphysiological dietary iron. Nevertheless, $Fbxl5^{+/GT}$ mice fed a low iron diet were more effective than their wild type littermates at absorbing iron to maintain their hematocrit and hemoglobin levels. These systemic adaptations were mirrored by corresponding changes in gene expression within the duodenum, including increased induction of IRP2 protein levels, IRE-binding capacity, and DMT1 expression (Figs. 3-10A, 3-11 and Table 6). TfR1 also contains IREs within its 3′ UTR (91) and likewise accumulates in the intestines of the $Fbxl5^{+/GT}$ mice fed the low iron diet (Fig. 3-10A and Table 6), though the relevance of this observation in iron absorption is unclear as TfR1 is not responsible for iron uptake from the lumen. Because IRP2 levels are normal in the mice fed a high iron diet (Fig. 3-10A), there does not appear to be an overall diminished capacity for IRP degradation. Rather, the intestines of these heterozygotes are responding as though they were further iron-deficient than their wild type counterparts. IRP2 induction is exacerbated under

iron-deficient conditions, perhaps revealing that the iron-sensing "set point" of the duodenum is distinct from most other tissues. Disruption of iron-responsive regulatory proteins in the intestine, including deletion of the IRPs (55) or Hypoxia Inducible Factor 2α genes (102), has been previously shown to compromise iron absorption and initiate systemic responses in the liver. However, hemoglobin and hematocrit levels are maintained in the *Fbxl5*$^{+/GT}$ mice despite no changes from the wild type expression levels of traditional systemic regulators of iron mobilization (liver hepcidin) or erythropoiesis (Renal erythropoietin; EPO) (Table 5).

While the serum values in Table 4 reflect steady-state measurements, the flux measurements in Fig. 2-9 clearly show preferential targeting of serum iron to the erythron. It remains unclear as to whether the liver "refuses" iron or whether the erythron is more effective in its capture. Immature RBC have much higher TfR1 levels than hepatocytes (121), and it remains possible that iron homeostasis is also altered in erythropoietic tissues to further facilitate uptake of absorbed iron, though we detected no comparable changes in gene expression in the spleen (Tables 5 and 6).

Together these results validate an important physiological role for the iron-sensing FBXL5 protein in the regulation of IRPs and the maintenance of both cellular and systemic iron homeostasis. Cells lacking FBXL5 expression fail to recognize their metabolic iron status and continuously accumulate toxic levels of

bioavailable iron in an unregulated fashion. These effects are specifically mediated through IRP2 stabilization and further reaffirm that IRP1 and IRP2 are not fully redundant. FBXL5 also plays a role in establishing IRP responsiveness when iron is limiting, as revealed by the altered behavior of the duodenum in *Fbxl5* heterozygotes.

The damage incurred in iron-replete livers lacking FBXL5 suggests that it may be a genetic modifier of hemochromatosis, perhaps further exacerbated by increased iron absorption. It would be of great interest to cross $Hfe^{-/-}$ mice, a model of hemochromatosis (178), with $Fbxl5^{+/-}$ mice. $Hfe^{-/-}$ mice develop iron overload at 8 weeks of age (178). This is characterized by increased intestinal absorption, elevated serum iron levels and high liver iron concentration regardless of the iron content of the diet (2, 158, 178). Progeny from $Hfe^{-/-}$ and $Fbxl5^{+/-}$ crosses are likely to show an exacerbated iron overload phenotype as $Fbxl5^{+/-}$ mice have augmented iron absorption

Interestingly, that FBXL5 haploinsufficient mice maintain normal hematocrit and hemoglobin levels indicates that a partial inhibition of FBXL5 expression may also have physiological benefits, as iron deficiency is the most common nutritional disorder worldwide (43). Lastly, as revealed upon FBXL5 depletion, the intestine has iron-responsive characteristics distinct from those of other tissues, conferring the capacity to influence systemic iron homeostasis in a previously unappreciated manner. It will be of great interest to investigate those

responsible factors that work in conjunction with the FBXL5 iron sensor to establish the homeostatic iron setpoint.

It is also possible that the increased iron absorption in the intestine of *Fbxl5*$^{+/-}$ mice is secondary to misregulation of iron homeostasis in the erythroid system. As erythropoiesis uses 80% of the bioavailable iron, it is believed that, in addition to the liver, the erythroid system may regulate iron absorption as well. *Hfe*$^{-/-}$ mice, which are hepcidin deficient, are still capable of down regulating, slightly, intestinal iron absorption when fed a high iron diet (5). This suggests that a yet-to-be-found factor controlling iron absorption might be released from the erythroid system to secure iron availability for erythrocyte production. Generation of mice where FBXL5 is selectively deleted in erythrocytes progenitor cells may help to elucidate this question.

Summary

Biochemical and molecular biology assays revealed that FBXL5 features a hemerythrin-like domain that serves as a direct sensor of cellular iron and oxygen availability and subsequently governs FBXL5's own stability. Importantly, *in vivo* deletion of the ubiquitously-expressed murine *Fbxl5* gene results in a failure to sense increased cellular iron availability, accompanied by constitutive IRP2 accumulation and misexpression of IRP2 target genes. FBXL5-null mice die during embryogenesis, though viability is restored by simultaneous

deletion of the *IRP2*, but not *IRP1*, gene. *Fbxl5* heterozygous mice behave like their wild type littermates when fed an iron-sufficient diet. However, unlike wild type mice that manifest decreased hematocrit and hemoglobin levels when fed a low-iron diet, *Fbxl5* heterozygotes maintain normal hematologic values due to increased iron absorption. IRP2's responsiveness to low iron is specifically enhanced in the duodena of the heterozygotes and is accompanied by increased expression of the Divalent Metal Transporter-1. These results confirm FBXL5's role in the *in vivo* maintenance of cellular and systemic iron homeostasis and reveal a privileged role for the intestine in their regulation by virtue of its unique FBXL5 iron sensitivity.

Chapter 5: Materials and Methods

Animals

Murine 129 Sv/Ev embryonic stem (ES) cells heterozygous for the gene-trapped *Fbxl5* allele (clone OST386421) were obtained from Texas A&M Institute for Genomic Medicine. The trapping vector (VICTR 74) contains a promoterless selectable marker Neo flanked by a splicing acceptor (SA) site and a poly A sequence (pA). Insertion of the vector into a gene leads to the splicing of the endogenous upstream exons into this cassette to generate a truncated fusion transcript. The trapping vector also contains the first exon of Bruton's tyrosine kinase (Btk) gene controlled by a promoter that is active in mouse embryonic stem cells, phosphoglycerate kinase (Pgk), upstream of a splicing donor (SD). Splicing from this signal gives rise to a fusion transcript that can be used to generate a sequence tag of the trapped gene by 3' Rapid Amplification of cDNA Ends (RACE). The Btk exon contains termination codons in all reading frames to prevent translation of the fusion transcripts. In clone OST386421, the trapping vector is inserted downstream of FBXL5 second exon as determined by 3' RACE. ES cells were injected into C57Bl/6J blastocysts at the UTSW Transgenic Technology Center and resulting chimeric mice were crossed to C57Bl/6J mice (Jackson Laboratories) to produce heterozygous anima

Genotyping

Mouse genomic DNA was isolated from tail biopsies following overnight digestion at 55°C in buffer containing 50 mM Tris-HCl (pH 8.0), 10 mM EDTA, 100 mM NaCl, 0.1% SDS and 1mg/ml proteinase K, followed by heat inactivation. PCR was performed using the primer pairs to distinguish the FBXL5 wild type (oligo F; 5′-GGGCTGAAGAATGTCAAGGTAAGTCGCA-3′ and oligo R; 5′-CTTGCTATAAGCCTTCACTGTAACCAATCCTC-3′) and gene trap (oligo F; 5′-GGGCTGAAGAATGTCAAGGTAAGTCGCA-3′ and oligo L; 5′-ATAAACCCTCTTGCAGTTGCATC-3′) alleles (Fig. S1*B*). PCR conditions were as follows: 30 cycles at 94°C for 30 s, 57°C for 30 s, and 72°C for 60 s.

Feeding and Determination of Iron Absorption and Distribution

Fbxl5 wild type and *Fbxl5* heterozygous mice were weaned onto ad libitum iron sufficient (50 ppm) or low iron (5 ppm) diet (Harlan-Teklad) for 3 weeks. For the ^{59}Fe feeding experiments, mice fed a low iron diet for three weeks were then fasted for 24 hrs and gavaged with an olive-tipped needle containing 200 μl of PBS supplemented with 2.5 μCi $^{59}FeCl_3$ (PerkinElmer) and 0.5 M ascorbic acid. At the indicated time points, animals were exsanguinated and ^{59}Fe accumulation in tissues was measured in a Packard Cobra Gamma Counter. Blood samples were collected from the tail vein or via cardiac puncture following

intraperitoneal administration of anesthetic rodent cocktail (ketamine/xylazine/acepromazine). Complete Blood Count analysis was performed by the UTSW Diagnostic Lab. Serum iron concentration, iron saturation and total iron binding capacity (TIBC) were measured by Idexx laboratories, Cornell University. The *Irp1*$^{-/-}$ and *Irp2*$^{-/-}$ mice were generously provided by Matthias Hentze. They were bred, mated to *Fbxl5*$^{+/-}$ mice and maintained by Dr. Richard Eisenstein at the University of Wisconsin-Madison. All animal experiments were performed with the approval of the UT Southwestern Medical Center Institutional Animal Care and Use Committee.

Embryo Isolation and Histology

Timed pregnancies were set up by mating *Fbxl5* heterozygous mice. Day E0.5 was determined upon finding of vaginal plugs. Embryos were isolated at days E9.5, E10.5, E11.5 and E12.5 and fixed in 4% paraformaldehyde for 48 hrs at room temperature. Fixed embryos were serially sectioned (5 μm), and stained with hematoxylin and eosin (H&E). Review and photography of all histologic preparations were performed with a Leica DM2000 photomicroscope equipped with brightfield and epifluorescence illumination and an Optronics Microfire digital CCD color camera interfaced with a Macintosh G4 computer. Images were

captured using PictureFrame 2.0 acquisition and software (Optronics,Inc. Goleta, CA, USA) and processed with Adobe Photoshop CS5.

Isolation, Culture and Characterization of Mouse Embryonic Cells

Mouse embryonic cells were prepared as described (95). Briefly, E8 embryos were digested with trypsin at 37°C for 30 min. Cells were cultured on a layer of mitotic inactivated mouse embryonic fibroblast feeder cells in Dulbecco's Modified High Glucose Eagles Medium (Hyclone) supplemented with 20% fetal bovine serum (Atlanta Biological), 1X nonessential amino acids (HyClone), 1X penicillin and streptomycin (HyClone), 2 mM Glutamine (HyClone), 55 μM β-mercaptoethanol (Sigma) and 110 mg/L of pyruvate (Hyclone). After 4 weeks, cells were grown without feeder cells and immortalized upon transfection of the SV40 large T antigen (pSV3-Neo, ATCC) with Lipofectamine 2000 (Invitrogen). Stably transfected cells were selected in the presence of 500 μg/ml G418.

Immunoblot Analysis

Cells and tissues were lysed in buffer containing 150 mM NaCl, 50 mM Tris-HCl pH 7.4, 1% Triton X-100, 1X Protease Inhibitor Cocktail (Sigma) and 250 μM phenylmethylsulfonyl fluoride. Tissue samples were briefly homogenized and cleared through 22G needles. Samples were resolved by SDS-PAGE. Rabbit anti-mouse IRP2 antibodies were kindly provided by Dr. Tracey Ruoualt and Dr.

Rick Eisenstein. Rabbit anti-Ferroportin 1 and rabbit anti-DMT1 antibodies were a gift from Dr. Jerry Kaplan. Additional antibodies are listed in Table 7. Immune complexes were detected by enhanced chemiluminescence, quantified on a Kodak Image Station (4000R Pro), and analyzed using Carestream molecular imaging software (version 5.0.2.30). All values were normalized to actin levels.

RNA Isolation and Quantitative Real Time PCR

Total RNA was isolated from cells and tissues using the RNeasy kit (Qiagen) as per manufacturer's instructions. RNA was DNase I (Roche) treated and reverse transcribed using the superScrip® II kit (Invitrogen). Quantitative Real Time PCR was performed using PowerSYBR green mix (Applied Biosystems) on the 7900HT Fast Real-Time PCR System (Applied Biosystems). Genes and primers sets used are listed in Table 5. mRNA expression levels were normalized against Glyceraldehyde 3 Phosphate Dehydrogenase (GAPDH) or cyclophilin and analyzed using the SDS 2.2 software (Applied Biosystems). The thermal cycle conditions were as follow: 2 minutes at 50°C and 10 minutes at 95°C followed by 40 cycles of 95°C for 15 seconds and 60°C for 1 minute. For determination of FBXL5, IRP1 and IRP2 expression pattern, human and mouse total RNA master panels were obtained from Clonetech.

Electrophoretic Mobility Shift Assay (EMSA)

Cells treated with 100 μM FAC or 100 μM DFO for 16 hours or tissues from animals fed an iron sufficient or a low iron diet for 3 weeks were washed with 1X PBS and incubated with lysis buffer (20 mM HEPES (pH 7.4), 3 mM $MgCl_2$, 40 mM KCl, 5% glycerol, 0.2% Nonidet P-40, 1 mM DTT, 250 μM PMSF, 1X protease inhibitor cocktail (Sigma)). Lysates containing 12 μg of protein were incubated with 100 Kcpm of ^{32}P-labeled rat L-ferritin IRE RNA probe for 30 minutes at room temperature in a reaction containing 1 mM DTT, 0.06 U/μL RNase inhibitor (New England Biolabs), 5% glycerol, 20 mM HEPES (pH 7.4), 40 mM KCl, and 3 mM $MgCl_2$. Heparin (2mg/ml) and RNAse T1 (10U) were added and the samples incubated another 10 minutes. Protein-bound RNA complexes were resolved by electrophoresis in a 5% nondenaturing polyacrylamide gel at 4°C and visualized by phosphorimager analysis.

Inductively Coupled Plasma Mass Spectroscopy (ICP-MS)

Mice were anesthetized with rodent cocktail and blood collected from tail vein. A 25G infusion needle connected to a peristaltic pump was inserted into the left ventricle of exposed hearts and the right atrium was clipped. Mice were perfused with Ringer's buffer (155 mM NaCl, 5 mM KCl, 2 mM $CaCl_2$, 1 mM $MgCl_2$, 2 mM NaH_2PO_4, 10 mM HEPES, 10 mM glucose, and ~10 U heparin/ml)

for 7 minutes. Once pale, livers were harvested and ICP-MS analysis of total metal content was performed.

Cell Culture Based Ubiquitination Assay

HEK 293 cells stably expressing N-terminal 3xFLAG-tagged and C-terminal HA-tagged FBXL5 Hemerythrin (Hr) domain were treated with or without 30 μM MG132 (Boston Biochem) for 1 hour follow by addition of 50 μM Ferric Ammonium Citrate (FAC) or 50 μM Deferoxamine (DFO). Cells were then incubated for 16 hours under atmospheric (~20%) or low (1%) oxygen conditions. Cell extracts were prepared by adding lysis buffer containing 50mM Tris-HCl (pH 8), 150mM NaCl, 1% triton X-100, 250 μM PMSF, 1X protease inhibitor cocktail and 10mM N-ethylmaleimide. Lysates were incubated 20 minutes at 4°C, and cysteine (0.1% final conc.) was added to neutralize the N-ethylmaleimide. Lysates were clarified by centrifugation at 17,000 xg for 20 minutes and protein concentration was determined by the Bradford assay.

Lysates (~1mg) were incubated with 12 μl of FLAG M2 resin (Sigma) overnight to immunoprecipitate Hr. Resin was washed three times with lysis buffer, and immunoprecipitated Hr was eluted using FLAG peptide. Proteins were resolved by SDS-PAGE and analyzed by immunobloting using antibodies against ubiquitin (Santa Cruz), FLAG (Sigma) and tubulin (Sigma).

The ubiquitination assay of full length FBLX5 was carried out using a HEK 293T cell line stably expressing N-terminal 3X FLAG-tagged FBXL5. Cells were treated with or without 30 μM MG132 for 1 hour followed by incubation with 50 μM Ferric Ammonium Citrate (FAC) or 50 μM Deferoxamine (DFO) for 6 hours. The rest of assay was carried out as described above. To suppress endogenous FBXL5 expression, HEK-Hr cells were transfected with a FBXL5 siRNA (Dharmacon, catalog number D-012424-04) and a non-targeting siRNA (Dharmacon, cat. # D-001210-01) for 48 hours.

Luciferase Gene Reporter Assay

1 μg of N-terminal or C-terminal FBXL5 Hr domain fused to firefly luciferase was transfected into HEK 293T cells using lipofectamine 2000 as per manufacturer's intructions. 24 hours following transfection, cells were treated with either 100 μM FAC or 100 μM DFO and incubated an additional 24 hours under atmospheric (~21%) or low (1%) oxygen conditions. Cells were disrupted using lysis buffer containing 30 mM Tricine (pH 7.8), 8 mM magnesium acetate, 0.2 mM EDTA and 1% triton at 4°C. Lysates were then transferred to a 96-well plate and ATP, Coenzyme A, b-mercaptoethanol and D-luceferin (Molecular probes) were added to final concentration of 375 μM, 375 μM, 50 mM and 125

μM respectively. Luminescence was measured in a plate reader (Bio-Tek, Synergy HT). Assays were performed in triplicate.

Degron Mapping

FBXL5 deletion constructs were generated either by standard methods or by the PCR overlap extension method using the oligonucleotides as listed in table 6. For constructs containing a V5 epitope tag, the pcDNA 3.1 vector (Invitrogen) was used, whereas constructs containing a FLAGepitope were generated in the pCI vector (gift from X. Wang). Deletion constructs were transiently transfected into HEK 293T cells using lipofectamine 2000 as per manufacturer's instructions. 24 hours following transfection, cells were treated with 100 μm FAC or 100 μM DFO for 16 hours. Finally, cells were harvested using 1X sample buffer and protein accumulation was measured by immunoblotting.

Table 6. qRT-PCR primers

Mouse Transferrin Receptor 1	Forward	5’-GAGCCCAGAGAGACGCTTTG-3’
	Reverse	5’-GACCTGTTCCCACACTGGACTT-3’
Mouse FBXL5	Forward	5’-TTGCACAAATGGAAAAACGTGTA-3’
	Reverse	5’-GAGGTACCAACATATGGCAGAACA-3’
Mouse IRP2	Forward	5’-GTCATGAGGGAGGCAGTGAAAA-3’
	Reverse	5’-GGACAGGCAGGGTGGACTTT-3’
Mouse IRP1	Forward	5’-CTTCTTCCCGGTTGATGAAGTTA-3’
	Reverse	5’-TTCCTCGCGGCCTGTCT-3’
Mouse Ferritin	Forward	5’-GCTTCTTTTTTGATCGGGATGA-3’
	Reverse	5’-GCCAATTCGCGGAAGAAGT-3’
Mouse GAPDH	Forward	5’-GGTGAAGGTCGGTGTGAACG-3’
	Reverse	5’-CTCGCTCCTGGAAGATGGTG-3’
Mouse DMT1 (IRE)	Forward	5'-AGCTAGGGCATGTGGCACTCT-3'
	Reverse	5'-ATGTTGCCACCGCTGGTATC-3'
Mouse DMT1 (No IRE)	Forward	5'-GTGGTGGCTGCAGTGGTTAGCG-3'
	Reverse	5'-GCGGTCAGTCCCAGGCGGTACG-3'
Mouse Ferroportin	Forward	5’-GCTGCTAGAATCGGTCTTTGGT-3’
	Reverse	5’-CAGCAACTGTGTCACCGTCAA-3’
Mouse Hepcidin	Forward	5’-TCTTCTGCATTGGTATCGCA-3’
	Reverse	5’-GAGCAGCACCACCTATCTCC-3’
Mouse DcytB	Forward	5’-CATCCTCGCCATCATCTC-3’
	Reverse	5’-GGCATTGCCTCCATTTAGCTG-3’
Mouse Erythropoietin	Forward	5’-ATTGATGTCGCCTCCAGATACCAC-3’
	Reverse	5’-TAGACCCGGAAGAGCTTGCAGAAA-3’
Mouse Cyclophilin	Forward	5’-TGGAGAGCACCAAGACAGACA-3’
	Reverse	5’-TGCCGGAGTCGACAATGAT-3’
Human Cyclophilin	Forward	5’-TGCCATCGCCAAGGAGTAG-3’
	Reverse	5’-TGCACAGACGGTCACTCAAA-3’
Human IRP2	Forward	5’-TGAGGGAGGCAGTGAAAACTCT-3’
	Reverse	5’-CTGTAAGATCTGTCGGACAAGCA -3’
Human IRP1	Forward	5’-TGGGTGTGATCCCACTTGAA-3’
	Reverse	5’-GATGGCTTCTACCACAGGTTCAG-3’
Human FBXL5	Forward	5’-CTTACCCAGACTGACATTTCAGATTC-3’

	Reverse	5’-GAAGACTCTGGCAGCAACCAA-3’

Table 7. Deletion constructs PCR primers

FBXL5 F	5′-GGAGGTCGACTCATTCGCCAGAGCGGCAGC-3’
FBXL5 R	5′-GGAGGGATCCACCATGGCGCCCTTTCCTGAAGAAGTGGAC-3’
Δ1-33	5'-GGAGGATCCACCATGGCGTTTTCCAACAACAACGATTTCCG-3’
Δ1-59	5'-GGAGGATCCACCATGGCGATTGAAAATGAATACATTATTGGTTTG-3’
Δ1-76	5'-GGAGGATCCACCATGTATAATGTACATTCTGACAATAAACTCTCC-3’
Δ1-81	5'-GGAGGATCCACCATGGCGGACAATAAACTCTCCGAGATGCT-3’
Δ1-100	5'-GGAGGATCCACCATGGCGAATGAATATGAACAGTTAAATTATGCAA
Δ67-71	5'-GAATACATTATTCGCAGCCAGACCATTTATAATGTACATTCTG-3’ 5'-GGTCTGGCTGCGAATAATGTATTCATTTTCAATCTG-3’
Δ72-76	5'-TTGCTTCAACAATATAATGTACATTCTGACAATAAACTCTCCG-3’ 5'-ATGTACATTATATTGTTGAAGCAAACCAATAATGTATTC-3’
Δ77-81	5'-AGCCAGACCATTGACAATAAACTCTCCGAGATG-3’ 5'-GAGTTTATTGTCAATGGTCTGGCTGCGTTGTTG-3’
Δ82-86	5'-AATGTACATTCTGAGATGCTTAGCCTCTTTGAAAAGG-3’ 5'-GCTAAGCATCTCAGAATGTACATTATAAATGGTCTGGC-3’
Δ87-91	5'-AATAAACTCTCCTTTGAAAAGGGACTGAAGAATGTTAAGAATG-3’ 5'-TCCCTTTTCAAAGGAGAGTTTATTGTCAGAATGTACATTATA-3’
Δ143-161	5'-GAATATTTTACCAAGGATACTGCAGAACTCCTTAGA-3’ 5'-TGCAGTATCCTTAAAATATTCCATTAACATGGGCTG-3’

Table 8. Antibody information

Antibody	**Vendor**	**Catalog #**
Mouse Anti-FLAG M2	Sigma	F3165
Mouse Anti-V5	Invitrogen	R960-25
Mouse Anti-Tubulin	Sigma	T6199
Mouse Anti-Ubiquitin	Santa Cruz	SC-8017
Mouse Anti-Transferrin Receptor 1	Invitrogen	136800
Mouse Anti-Actin	MP Biomedicals	863793
Rabbit Anti-Ferritin	Cell Signaling	3998
Goat Anti-Mouse IgG-HRP	Santa Cruz	SC-2055
Goat Anti-Rabbit IgG-HRP	Santa Cruz	SC-2054

APPENDIX

Table 9. Relative mRNA accumulation as measured by qRT-PCR

		Fbxl5$^{+/+}$		*Fbxl5*$^{+/GT}$	
		Sufficient Fe	Low Fe	Sufficient Fe	Low Fe
Duodenum					
	DMT1	0.28 ± 0.02	0.47 ± 0.01[a]	0.13 ± 0.004	1 ± 0.06[a]
	DMT1 No IRE	1 ± 0.023	0.96 ± 0.02	0.90 ± 0.04	0.78 ± 0.05
	FPN	1 ± 0.09	0.13 ± 0.006	0.60 ± 0.03	0.45 ± 0.06
	TfR1	0.05 ± 0.003	0.52 ± 0.02[b]	0.15 ± 0.01	1 ± 0.02[b]
	DcytB	0.04 ± 0.002	1 ± 0.04	0.03 ± 0.001	0.76 ± 0.18
	FBXL5	1 ± 0.01	0.87 ± 0.02	0.93 ± 0.03	0.94 ± 0.05
	IRP2	0.64± 0.05	0.71± 0.03	0.68± 0.06	1 ± 0.15
	FTH1	1 ± 0.03	0.90 ± 0.01	0.91 ± 0.09	0.88 ± 0.02
Liver					
	DMT1	0.87 ± 0.06	0.99 ± 0.04	0.99 ± 0.05	1 ± 0.04
	FPN	1 ± 0.03	0.64 ± 0.04	0.85 ± 0.03	0.45 ± 0.02
	TfR1	0.15 ± 0.11	0.87 ± 0.1	0.41 ± 0.06	1 ± 0.07
	HAMP	1 ± 0.03[c]	6E-^{04} ± 4E^{-05}	0.5 ± 0.01[c]	4E-^{04} ± 2E^{-05}
	DcytB	0.94 ± 0.08	0.96 ± 0.06	1 ± 0.1	0.91 ± 0.1
	FBXL5	1 ± 0.03	0.89 ± 0.07	0.85 ± 0.02	0.85 ± 0.09
	IRP2	0.85 ± 0.05	0.79 ± 0.02	0.95 ± 0.02	1 ± 0.06
	FTH1	1 ± 0.01	0.99 ± 0.02	0.89 ± 0.03	0.92 ± 0.02
Brain					
	TfR1	0.82 ± 0.12	0.90 ± 0.02	0.86 ± 0.03	1 ± 0.02
	FBXL5	1 ± 0.02	0.93 ± 0.04	0.92 ± 0.03	0.86 ± 0.1
	IRP2	0.95 ± 0.02	0.95 ± 0.07	1 ± 0.05	0.87 ± 0.09
	FTH1	0.94 ± 0.02	1 ± 0.03	0.92 ± 0.03	0.91 ± 0.02
Spleen					
	TfR1	0.68 ± 0.08	0.92 ± 0.02	0.81 ± 0.01	1 ± 0.01
	FBXL5	0.82 ± 0.02	1 ± 0.017	0.80 ± 0.03	0.84 ± 0.04
	IRP2	0.85 ± 0.02	0.98 ± 0.016	0.99 ± 0.01	1 ± 0.07
	FTH1	0.90 ± 0.02	1 ± 0.01	0.94 ± 0.03	0.90 ± 0.03

Jejunun					
	TfR1	0.063 ± 0.007	0.90 ± 0.07	0.075 ± 0.08	1 ± 0.05
	FBXL5	1 ± 0.04	0.83 ± 0.01	0.81 ± 0.1	0.89 ± 0.02
	IRP2	0.76 ± 0.1	0.75 ± 0.05	1 ± 0.08	0.89 ± 0.04
	FTH1	0.96 ± 0.02	0.91 ± 0.02	1 ± 0.01	0.99 ± 0.01
Ileum					
	TfR1	0.37 ± 0.05	0.61 ± 0.03	0.081 ± 0.01	1 ± 0.05
	FBXL5	1 ± 0.03	0.90 ± 0.02	0.91 ± 0.09	0.89 ± 0.02
	IRP2	0.87 ± 0.1	0.89 ± 0.02	1 ± 0.03	0.90 ± 0.09
	FTH1	0.84 ± 0.01	0.90 ± 0.01	1 ± 0.01	0.82 ± 0.02
Kidney					
	EPO	0.02 ± 0.01	1 ± 0.3	0.036 ± 0.01	0.69 ± 0.2

Note. Values expressed as mean ± SD of 12 replicates. In the rows, differences between paired values denoted by superscript letters are statistically significant as determined by t-test. $^{a}p = 0.0073$; $^{b}p = 0.008$; $^{c}p = 0.0027$.

Table 10. Protein accumulation assessed by immunoblot analysis

		Fbxl5$^{+/+}$		*Fbxl5*$^{+/GT}$	
		Sufficient Fe	Low Fe	Sufficient Fe	Low Fe
Duodenum					
	IRP2	0.11 ± 0.006	0.14 ± 0.087[a]	0.10 ± 0.004	1 ± 0.056[a]
	DMT1	0.02 ± 0.002	0.49 ± 0.01[b]	0.023 ± 0.002	1 ± 0.16[b]
	TfR1	0.05 ± 0.003	0.06 ± 0.02[c]	0.64 ± 0.01	1 ± 0.02[c]
	FPN	0.20 ± 0.02	0.81 ± 0.078	0.38 ± 0.01	1 ± 0.086
	FTH1	0.76± 0.04	0.09 ± 0.006	1 ± 0.05	0.19 ± 0.008
Liver					
	IRP2	0.24 ± 0.06	1 ± 0.11	0.19 ± 0.04	0.94± 0.063
	DMT1	0.87 ± 0.06	0.99 ± 0.04	0.99 ± 0.05	1 ± 0.04
	TfR1	0.19 ± 0.01	0.85 ± 0.001	0.36 ± 0.05	1 ± 0.16
	FPN	0.64 ± 0.04	1 ± 0.03	0.45 ± 0.02	0.85 ± 0.03
	FTH1	1 ± 0.01	0.09 ± 0.02	0.79 ± 0.17	0.01 ± 0.002
Spleen					
	IRP2	0.87 ± 0.12	1 ± 0.13	0.82 ± 0.09	0.87± 0.09
	DMT1	0.92 ± 0.04	1 ± 0.093	0.89 ± 0.06	0.92± 0.04
	TfR1	1 ± 0.05	0.93 ± 0.03	0.90 ± 0.13	0.89 ± 0.11
	FPN	0.75 ± 0.15	0.83 ± 0.04	1 ± 0.096	0.86 ± 0.04
	FTH1	1 ± 0.11	0.24 ± 0.001	0.71 ± 0.007	0.22 ± 0.008
Brain					
	IRP2	0.83 ± 0.06	0.89 ± 0.04	0.86 ± 0.08	1 ± 0.11
	TfR1	0.90 ± 0.08	0.89 ± 0.03	0.84 ± 0.02	1 ± 0.07
	FPN	0.93 ± 0.12	0.82 ± 0.07	0.88 ± 0.09	1 ± 0.13
	FTH1	0.91 ± 0.07	1 ± 0.04	0.71 ± 0.21	0.74 ± 0.24
Jejunun					
	IRP2	0.21 ± 0.01	0.38 ± 0.012	0.11 ± 0.01	1 ± 0.05
	TfR1	0.11 ± 0.008	1 ± 0.1	0.54 ± 0.1	0.78 ± 0.07
	FPN	0.42 ± 0.01	1 ± 0.02	0.35 ± 0.01	0.83 ± 0.09
	FTH1	0.84 ± 0.08	0.18 ± 0.09	1 ± 0.1	0.22 ± 0.17
Ileum					
	IRP2	0.18 ± 0.02	1 ± 0.03	0.42 ± 0.01	0.73 ± 0.08
	TfR1	0.80 ± 0.07	0.72 ± 0.06	1 ± 0.02	0.62 ± 0.06

	FPN	0.18 ± 0.01	0.90 ± 0.04	0.63 ± 0.08	1 ± 0.07
	FTH1	1 ± 0.1	0.08 ± 0.02	0.61 ± 0.16	0.13 ± 0.1

Note. Values expressed as mean ± SD of 12 replicates. In the rows, differences between paired values denoted by superscript letters are statistically significant as determined by t-test. [a] $p = 0.0053$; [b] $p = 0.0046$; [c] $p = 0.0061$.

BIBLIOGRAPHY

1. **Abboud, S., and D. J. Haile.** 2000. A novel mammalian iron-regulated protein involved in intracellular iron metabolism. The Journal of biological chemistry **275:**19906-19912.
2. **Ahmad, K. A., J. R. Ahmann, M. C. Migas, A. Waheed, R. S. Britton, B. R. Bacon, W. S. Sly, and R. E. Fleming.** 2002. Decreased liver hepcidin expression in the Hfe knockout mouse. Blood cells, molecules & diseases **29:**361-366.
3. **Aisen, P., C. Enns, and M. Wessling-Resnick.** 2001. Chemistry and biology of eukaryotic iron metabolism. The international journal of biochemistry & cell biology **33:**940-959.
4. **Aisen, P., A. Leibman, and J. Zweier.** 1978. Stoichiometric and site characteristics of the binding of iron to human transferrin. The Journal of biological chemistry **253:**1930-1937.
5. **Ajioka, R. S., J. E. Levy, N. C. Andrews, and J. P. Kushner.** 2002. Regulation of iron absorption in Hfe mutant mice. Blood **100:**1465-1469.
6. **Ajioka, R. S., J. D. Phillips, and J. P. Kushner.** 2006. Biosynthesis of heme in mammals. Biochimica et biophysica acta **1763:**723-736.
7. **Andrews, N. C.** 1999. Disorders of iron metabolism. The New England journal of medicine **341:**1986-1995.
8. **Andrews, N. C., and P. J. Schmidt.** 2007. Iron homeostasis. Annual review of physiology **69:**69-85.
9. **Asada-Senju, M., T. Maeda, T. Sakata, A. Hayashi, and T. Suzuki.** 2002. Molecular analysis of the transferrin gene in a patient with hereditary hypotransferrinemia. Journal of human genetics **47:**355-359.
10. **Aziz, N., and H. N. Munro.** 1986. Both subunits of rat liver ferritin are regulated at a translational level by iron induction. Nucleic acids research **14:**915-927.
11. **Aziz, N., and H. N. Munro.** 1987. Iron regulates ferritin mRNA translation through a segment of its 5' untranslated region. Proceedings of the National Academy of Sciences of the United States of America **84:**8478-8482.
12. **Brandhagen, D. J., V. F. Fairbanks, K. P. Batts, and S. N. Thibodeau.** 1999. Update on hereditary hemochromatosis and the HFE gene. Mayo Clinic proceedings. Mayo Clinic **74:**917-921.

13. **Bruick, R. K.** 2003. Oxygen sensing in the hypoxic response pathway: regulation of the hypoxia-inducible transcription factor. Genes & development **17:**2614-2623.
14. **Brzoska, K., S. Meczynska, and M. Kruszewski.** 2006. Iron-sulfur cluster proteins: electron transfer and beyond. Acta biochimica Polonica **53:**685-691.
15. **Butt, J., H. Y. Kim, J. P. Basilion, S. Cohen, K. Iwai, C. C. Philpott, S. Altschul, R. D. Klausner, and T. A. Rouault.** 1996. Differences in the RNA binding sites of iron regulatory proteins and potential target diversity. Proceedings of the National Academy of Sciences of the United States of America **93:**4345-4349.
16. **Camaschella, C., A. Campanella, L. De Falco, L. Boschetto, R. Merlini, L. Silvestri, S. Levi, and A. Iolascon.** 2007. The human counterpart of zebrafish shiraz shows sideroblastic-like microcytic anemia and iron overload. Blood **110:**1353-1358.
17. **Camaschella, C., and E. Poggiali.** 2011. Inherited disorders of iron metabolism. Current opinion in pediatrics **23:**14-20.
18. **Canonne-Hergaux, F., S. Gruenheid, P. Ponka, and P. Gros.** 1999. Cellular and subcellular localization of the Nramp2 iron transporter in the intestinal brush border and regulation by dietary iron. Blood **93:**4406-4417.
19. **Canonne-Hergaux, F., A. S. Zhang, P. Ponka, and P. Gros.** 2001. Characterization of the iron transporter DMT1 (NRAMP2/DCT1) in red blood cells of normal and anemic mk/mk mice. Blood **98:**3823-3830.
20. **Casey, J. L., M. W. Hentze, D. M. Koeller, S. W. Caughman, T. A. Rouault, R. D. Klausner, and J. B. Harford.** 1988. Iron-responsive elements: regulatory RNA sequences that control mRNA levels and translation. Science **240:**924-928.
21. **Chattipakorn, N., S. Kumfu, S. Fucharoen, and S. Chattipakorn.** 2011. Calcium channels and iron uptake into the heart. World journal of cardiology **3:**215-218.
22. **Chen, H., Z. K. Attieh, T. Su, B. A. Syed, H. Gao, R. M. Alaeddine, T. C. Fox, J. Usta, C. E. Naylor, R. W. Evans, A. T. McKie, G. J. Anderson, and C. D. Vulpe.** 2004. Hephaestin is a ferroxidase that maintains partial activity in sex-linked anemia mice. Blood **103:**3933-3939.
23. **Chen, H., T. Su, Z. K. Attieh, T. C. Fox, A. T. McKie, G. J. Anderson, and C. D. Vulpe.** 2003. Systemic regulation of Hephaestin and Ireg1 revealed in studies of genetic and nutritional iron deficiency. Blood **102:**1893-1899.

24. **Cherukuri, S., R. Potla, J. Sarkar, S. Nurko, Z. L. Harris, and P. L. Fox.** 2005. Unexpected role of ceruloplasmin in intestinal iron absorption. Cell metabolism **2:**309-319.
25. **Chhangani, D., A. P. Joshi, and A. Mishra.** 2012. E3 ubiquitin ligases in protein quality control mechanism. Molecular neurobiology **45:**571-585.
26. **Ching, Y. H., R. J. Munroe, J. L. Moran, A. K. Barker, E. Mauceli, T. Fennell, F. Dipalma, K. Lindblad-Toh, L. M. Abcunas, J. F. Gilmour, T. P. Harris, S. L. Kloet, Y. Luo, J. L. McElwee, W. Mu, H. K. Park, D. L. Rogal, K. J. Schimenti, L. Shen, M. Shindo, J. Y. Shou, E. K. Stenson, P. J. Stover, and J. C. Schimenti.** 2010. High resolution mapping and positional cloning of ENU-induced mutations in the Rw region of mouse chromosome 5. BMC genetics **11:**106.
27. **Chollangi, S., J. W. Thompson, J. C. Ruiz, K. H. Gardner, and R. K. Bruick.** 2012. Hemerythrin-like Domain within F-box and Leucine-rich Repeat Protein 5 (FBXL5) Communicates Cellular Iron and Oxygen Availability by Distinct Mechanisms. The Journal of biological chemistry **287:**23710-23717.
28. **Chung, J., C. Chen, and B. H. Paw.** 2012. Heme metabolism and erythropoiesis. Current opinion in hematology **19:**156-162.
29. **Clarke, S. L., A. Vasanthakumar, S. A. Anderson, C. Pondarre, C. M. Koh, K. M. Deck, J. S. Pitula, C. J. Epstein, M. D. Fleming, and R. S. Eisenstein.** 2006. Iron-responsive degradation of iron-regulatory protein 1 does not require the Fe-S cluster. The EMBO journal **25:**544-553.
30. **Crichton, R. R., and M. Charloteaux-Wauters.** 1987. Iron transport and storage. European journal of biochemistry / FEBS **164:**485-506.
31. **Crichton, R. R., and J. L. Pierre.** 2001. Old iron, young copper: from Mars to Venus. Biometals : an international journal on the role of metal ions in biology, biochemistry, and medicine **14:**99-112.
32. **Curtis, A. R., C. Fey, C. M. Morris, L. A. Bindoff, P. G. Ince, P. F. Chinnery, A. Coulthard, M. J. Jackson, A. P. Jackson, D. P. McHale, D. Hay, W. A. Barker, A. F. Markham, D. Bates, A. Curtis, and J. Burn.** 2001. Mutation in the gene encoding ferritin light polypeptide causes dominant adult-onset basal ganglia disease. Nature genetics **28:**350-354.
33. **De Domenico, I., D. M. Ward, and J. Kaplan.** 2007. Hepcidin regulation: ironing out the details. The Journal of clinical investigation **117:**1755-1758.
34. **De Domenico, I., D. M. Ward, C. Langelier, M. B. Vaughn, E. Nemeth, W. I. Sundquist, T. Ganz, G. Musci, and J. Kaplan.** 2007. The molecular mechanism of hepcidin-mediated ferroportin down-regulation. Molecular biology of the cell **18:**2569-2578.

35. **Del-Castillo-Rueda, A., M. I. Moreno-Carralero, N. Cuadrado-Grande, L. A. Alvarez-Sala-Walther, R. Enriquez-de-Salamanca, M. Mendez, and M. J. Moran-Jimenez.** 2012. Mutations in the HFE, TFR2, and SLC40A1 genes in patients with hemochromatosis. Gene.
36. **Devireddy, L. R., D. O. Hart, D. H. Goetz, and M. R. Green.** 2010. A mammalian siderophore synthesized by an enzyme with a bacterial homolog involved in enterobactin production. Cell **141:**1006-1017.
37. **Donovan, A., A. Brownlie, Y. Zhou, J. Shepard, S. J. Pratt, J. Moynihan, B. H. Paw, A. Drejer, B. Barut, A. Zapata, T. C. Law, C. Brugnara, S. E. Lux, G. S. Pinkus, J. L. Pinkus, P. D. Kingsley, J. Palis, M. D. Fleming, N. C. Andrews, and L. I. Zon.** 2000. Positional cloning of zebrafish ferroportin1 identifies a conserved vertebrate iron exporter. Nature **403:**776-781.
38. **Donovan, A., C. A. Lima, J. L. Pinkus, G. S. Pinkus, L. I. Zon, S. Robine, and N. C. Andrews.** 2005. The iron exporter ferroportin/Slc40a1 is essential for iron homeostasis. Cell metabolism **1:**191-200.
39. **Dreyfuss, M. L., R. J. Stoltzfus, J. B. Shrestha, E. K. Pradhan, S. C. LeClerq, S. K. Khatry, S. R. Shrestha, J. Katz, M. Albonico, and K. P. West, Jr.** 2000. Hookworms, malaria and vitamin A deficiency contribute to anemia and iron deficiency among pregnant women in the plains of Nepal. The Journal of nutrition **130:**2527-2536.
40. **Du, X., E. She, T. Gelbart, J. Truksa, P. Lee, Y. Xia, K. Khovananth, S. Mudd, N. Mann, E. M. Moresco, E. Beutler, and B. Beutler.** 2008. The serine protease TMPRSS6 is required to sense iron deficiency. Science **320:**1088-1092.
41. **Eisenstein, R. S.** 2000. Iron regulatory proteins and the molecular control of mammalian iron metabolism. Annual review of nutrition **20:**627-662.
42. **Eisenstein, R. S., and K. P. Blemings.** 1998. Iron regulatory proteins, iron responsive elements and iron homeostasis. The Journal of nutrition **128:**2295-2298.
43. **Evstatiev, R., and C. Gasche.** 2012. Iron sensing and signalling. Gut **61:**933-952.
44. **Ferreira, C., D. Bucchini, M. E. Martin, S. Levi, P. Arosio, B. Grandchamp, and C. Beaumont.** 2000. Early embryonic lethality of H ferritin gene deletion in mice. The Journal of biological chemistry **275:**3021-3024.
45. **Ferring-Appel, D., M. W. Hentze, and B. Galy.** 2009. Cell-autonomous and systemic context-dependent functions of iron regulatory protein 2 in mammalian iron metabolism. Blood **113:**679-687.
46. **Fleming, M. D., M. A. Romano, M. A. Su, L. M. Garrick, M. D. Garrick, and N. C. Andrews.** 1998. Nramp2 is mutated in the anemic

Belgrade (b) rat: evidence of a role for Nramp2 in endosomal iron transport. Proceedings of the National Academy of Sciences of the United States of America **95:**1148-1153.

47. **Fleming, M. D., C. C. Trenor, 3rd, M. A. Su, D. Foernzler, D. R. Beier, W. F. Dietrich, and N. C. Andrews.** 1997. Microcytic anaemia mice have a mutation in Nramp2, a candidate iron transporter gene. Nature genetics **16:**383-386.
48. **Fleming, R. E., Q. Feng, and R. S. Britton.** 2011. Knockout mouse models of iron homeostasis. Annual review of nutrition **31:**117-137.
49. **Galan, J. M., and M. Peter.** 1999. Ubiquitin-dependent degradation of multiple F-box proteins by an autocatalytic mechanism. Proceedings of the National Academy of Sciences of the United States of America **96:**9124-9129.
50. **Galaris, D., M. Mantzaris, and C. Amorgianiotis.** 2008. Oxidative stress and aging: the potential role of iron. Hormones (Athens) **7:**114-122.
51. **Galaris, D., and K. Pantopoulos.** 2008. Oxidative stress and iron homeostasis: mechanistic and health aspects. Critical reviews in clinical laboratory sciences **45:**1-23.
52. **Galy, B., D. Ferring, M. Benesova, V. Benes, and M. W. Hentze.** 2004. Targeted mutagenesis of the murine IRP1 and IRP2 genes reveals context-dependent RNA processing differences in vivo. RNA **10:**1019-1025.
53. **Galy, B., D. Ferring, and M. W. Hentze.** 2005. Generation of conditional alleles of the murine Iron Regulatory Protein (IRP)-1 and -2 genes. Genesis **43:**181-188.
54. **Galy, B., D. Ferring, B. Minana, O. Bell, H. G. Janser, M. Muckenthaler, K. Schumann, and M. W. Hentze.** 2005. Altered body iron distribution and microcytosis in mice deficient in iron regulatory protein 2 (IRP2). Blood **106:**2580-2589.
55. **Galy, B., D. Ferring-Appel, S. Kaden, H. J. Grone, and M. W. Hentze.** 2008. Iron regulatory proteins are essential for intestinal function and control key iron absorption molecules in the duodenum. Cell metabolism **7:**79-85.
56. **Ganz, T.** 2003. Hepcidin, a key regulator of iron metabolism and mediator of anemia of inflammation. Blood **102:**783-788.
57. **Ganz, T., and E. Nemeth.** 2012. Hepcidin and iron homeostasis. Biochimica et biophysica acta **1823:**1434-1443.
58. **Ganz, T., and E. Nemeth.** 2011. The hepcidin-ferroportin system as a therapeutic target in anemias and iron overload disorders. Hematology / the Education Program of the American Society of Hematology. American Society of Hematology. Education Program **2011:**538-542.

59. **Gatter, K. C., G. Brown, I. S. Trowbridge, R. E. Woolston, and D. Y. Mason.** 1983. Transferrin receptors in human tissues: their distribution and possible clinical relevance. Journal of clinical pathology **36:**539-545.
60. **Gattermann, N.** 2009. The treatment of secondary hemochromatosis. Deutsches Arzteblatt international **106:**499-504, I.
61. **Girelli, D., R. Corrocher, L. Bisceglia, O. Olivieri, L. De Franceschi, L. Zelante, and P. Gasparini.** 1995. Molecular basis for the recently described hereditary hyperferritinemia-cataract syndrome: a mutation in the iron-responsive element of ferritin L-subunit gene (the "Verona mutation"). Blood **86:**4050-4053.
62. **Goetz, D. H., M. A. Holmes, N. Borregaard, M. E. Bluhm, K. N. Raymond, and R. K. Strong.** 2002. The neutrophil lipocalin NGAL is a bacteriostatic agent that interferes with siderophore-mediated iron acquisition. Molecular cell **10:**1033-1043.
63. **Goswami, T., A. Rolfs, and M. A. Hediger.** 2002. Iron transport: emerging roles in health and disease. Biochemistry and cell biology = Biochimie et biologie cellulaire **80:**679-689.
64. **Grosbois, B., O. Decaux, B. Cador, C. Cazalets, and P. Jego.** 2005. [Human iron deficiency]. Bulletin de l'Academie nationale de medecine **189:**1649-1663; discussion 1663-1644.
65. **Gunshin, H., Y. Fujiwara, A. O. Custodio, C. Direnzo, S. Robine, and N. C. Andrews.** 2005. Slc11a2 is required for intestinal iron absorption and erythropoiesis but dispensable in placenta and liver. The Journal of clinical investigation **115:**1258-1266.
66. **Gunshin, H., B. Mackenzie, U. V. Berger, Y. Gunshin, M. F. Romero, W. F. Boron, S. Nussberger, J. L. Gollan, and M. A. Hediger.** 1997. Cloning and characterization of a mammalian proton-coupled metal-ion transporter. Nature **388:**482-488.
67. **Guo, B., J. D. Phillips, Y. Yu, and E. A. Leibold.** 1995. Iron regulates the intracellular degradation of iron regulatory protein 2 by the proteasome. The Journal of biological chemistry **270:**21645-21651.
68. **Guo, B., Y. Yu, and E. A. Leibold.** 1994. Iron regulates cytoplasmic levels of a novel iron-responsive element-binding protein without aconitase activity. The Journal of biological chemistry **269:**24252-24260.
69. **Haile, D. J., M. W. Hentze, T. A. Rouault, J. B. Harford, and R. D. Klausner.** 1989. Regulation of interaction of the iron-responsive element binding protein with iron-responsive RNA elements. Molecular and cellular biology **9:**5055-5061.
70. **Haile, D. J., T. A. Rouault, J. B. Harford, M. C. Kennedy, G. A. Blondin, H. Beinert, and R. D. Klausner.** 1992. Cellular regulation of the iron-responsive element binding protein: disassembly of the cubane

iron-sulfur cluster results in high-affinity RNA binding. Proceedings of the National Academy of Sciences of the United States of America **89:**11735-11739.

71. **Hanson, E. S., and E. A. Leibold.** 1998. Regulation of iron regulatory protein 1 during hypoxia and hypoxia/reoxygenation. The Journal of biological chemistry **273:**7588-7593.
72. **Hanson, E. S., M. L. Rawlins, and E. A. Leibold.** 2003. Oxygen and iron regulation of iron regulatory protein 2. The Journal of biological chemistry **278:**40337-40342.
73. **Harris, Z. L., S. R. Davis-Kaplan, J. D. Gitlin, and J. Kaplan.** 2004. A fungal multicopper oxidase restores iron homeostasis in aceruloplasminemia. Blood **103:**4672-4673.
74. **Harris, Z. L., L. W. Klomp, and J. D. Gitlin.** 1998. Aceruloplasminemia: an inherited neurodegenerative disease with impairment of iron homeostasis. The American journal of clinical nutrition **67:**972S-977S.
75. **Hentze, M. W., and L. C. Kuhn.** 1996. Molecular control of vertebrate iron metabolism: mRNA-based regulatory circuits operated by iron, nitric oxide, and oxidative stress. Proceedings of the National Academy of Sciences of the United States of America **93:**8175-8182.
76. **Hentze, M. W., M. U. Muckenthaler, B. Galy, and C. Camaschella.** 2010. Two to tango: regulation of Mammalian iron metabolism. Cell **142:**24-38.
77. **Hidalgo, C., and M. T. Nunez.** 2007. Calcium, iron and neuronal function. IUBMB life **59:**280-285.
78. **Hintze, K. J., and E. C. Theil.** 2006. Cellular regulation and molecular interactions of the ferritins. Cellular and molecular life sciences : CMLS **63:**591-600.
79. **Hirling, H., B. R. Henderson, and L. C. Kuhn.** 1994. Mutational analysis of the [4Fe-4S]-cluster converting iron regulatory factor from its RNA-binding form to cytoplasmic aconitase. The EMBO journal **13:**453-461.
80. **Ho, M. S., C. Ou, Y. R. Chan, C. T. Chien, and H. Pi.** 2008. The utility F-box for protein destruction. Cellular and molecular life sciences : CMLS **65:**1977-2000.
81. **Ishikawa, H., M. Kato, H. Hori, K. Ishimori, T. Kirisako, F. Tokunaga, and K. Iwai.** 2005. Involvement of heme regulatory motif in heme-mediated ubiquitination and degradation of IRP2. Molecular cell **19:**171-181.
82. **Iwai, K., S. K. Drake, N. B. Wehr, A. M. Weissman, T. LaVaute, N. Minato, R. D. Klausner, R. L. Levine, and T. A. Rouault.** 1998. Iron-

dependent oxidation, ubiquitination, and degradation of iron regulatory protein 2: implications for degradation of oxidized proteins. Proceedings of the National Academy of Sciences of the United States of America **95:**4924-4928.

83. **Iwai, K., R. D. Klausner, and T. A. Rouault.** 1995. Requirements for iron-regulated degradation of the RNA binding protein, iron regulatory protein 2. The EMBO journal **14:**5350-5357.
84. **Jana, N. R.** 2012. Protein homeostasis and aging: role of ubiquitin protein ligases. Neurochemistry international **60:**443-447.
85. **Kang, D. K., J. Jeong, S. K. Drake, N. B. Wehr, T. A. Rouault, and R. L. Levine.** 2003. Iron regulatory protein 2 as iron sensor. Iron-dependent oxidative modification of cysteine. The Journal of biological chemistry **278:**14857-14864.
86. **Kaplan, J., D. M. Ward, and I. De Domenico.** 2011. The molecular basis of iron overload disorders and iron-linked anemias. International journal of hematology **93:**14-20.
87. **Kapur, D., K. N. Agarwal, and S. Sharma.** 2002. Detecting iron deficiency anemia among children (9-36 months of age) by implementing a screening program in an urban slum. Indian pediatrics **39:**671-676.
88. **Kennedy, M. C., L. Mende-Mueller, G. A. Blondin, and H. Beinert.** 1992. Purification and characterization of cytosolic aconitase from beef liver and its relationship to the iron-responsive element binding protein. Proceedings of the National Academy of Sciences of the United States of America **89:**11730-11734.
89. **Kim, H. Y., R. D. Klausner, and T. A. Rouault.** 1995. Translational repressor activity is equivalent and is quantitatively predicted by in vitro RNA binding for two iron-responsive element-binding proteins, IRP1 and IRP2. The Journal of biological chemistry **270:**4983-4986.
90. **Klausner, R. D., T. A. Rouault, and J. B. Harford.** 1993. Regulating the fate of mRNA: the control of cellular iron metabolism. Cell **72:**19-28.
91. **Koeller, D. M., J. L. Casey, M. W. Hentze, E. M. Gerhardt, L. N. Chan, R. D. Klausner, and J. B. Harford.** 1989. A cytosolic protein binds to structural elements within the iron regulatory region of the transferrin receptor mRNA. Proceedings of the National Academy of Sciences of the United States of America **86:**3574-3578.
92. **Koury, M. J., and P. Ponka.** 2004. New insights into erythropoiesis: the roles of folate, vitamin B12, and iron. Annual review of nutrition **24:**105-131.
93. **Laftah, A. H., G. O. Latunde-Dada, S. Fakih, R. C. Hider, R. J. Simpson, and A. T. McKie.** 2009. Haem and folate transport by proton-

coupled folate transporter/haem carrier protein 1 (SLC46A1). The British journal of nutrition **101:**1150-1156.

94. **LaVaute, T., S. Smith, S. Cooperman, K. Iwai, W. Land, E. Meyron-Holtz, S. K. Drake, G. Miller, M. Abu-Asab, M. Tsokos, R. Switzer, 3rd, A. Grinberg, P. Love, N. Tresser, and T. A. Rouault.** 2001. Targeted deletion of the gene encoding iron regulatory protein-2 causes misregulation of iron metabolism and neurodegenerative disease in mice. Nature genetics **27:**209-214.
95. **Lee, J., M. J. Petris, and D. J. Thiele.** 2002. Characterization of mouse embryonic cells deficient in the ctr1 high affinity copper transporter. Identification of a Ctr1-independent copper transport system. The Journal of biological chemistry **277:**40253-40259.
96. **Leibold, E. A., and B. Guo.** 1992. Iron-dependent regulation of ferritin and transferrin receptor expression by the iron-responsive element binding protein. Annual review of nutrition **12:**345-368.
97. **Leibold, E. A., and H. N. Munro.** 1988. Cytoplasmic protein binds in vitro to a highly conserved sequence in the 5' untranslated region of ferritin heavy- and light-subunit mRNAs. Proceedings of the National Academy of Sciences of the United States of America **85:**2171-2175.
98. **Leipuviene, R., and E. C. Theil.** 2007. The family of iron responsive RNA structures regulated by changes in cellular iron and oxygen. Cellular and molecular life sciences : CMLS **64:**2945-2955.
99. **Liu, K., and A. J. Kaffes.** 2012. Iron deficiency anaemia: a review of diagnosis, investigation and management. European journal of gastroenterology & hepatology **24:**109-116.
100. **Liu, T. B., and C. Xue.** 2011. The Ubiquitin-Proteasome System and F-box Proteins in Pathogenic Fungi. Mycobiology **39:**243-248.
101. **Liu, X., and E. C. Theil.** 2005. Ferritins: dynamic management of biological iron and oxygen chemistry. Accounts of chemical research **38:**167-175.
102. **Mastrogiannaki, M., P. Matak, B. Keith, M. C. Simon, S. Vaulont, and C. Peyssonnaux.** 2009. HIF-2alpha, but not HIF-1alpha, promotes iron absorption in mice. The Journal of clinical investigation **119:**1159-1166.
103. **McGregor, J. A., M. Shayeghi, C. D. Vulpe, G. J. Anderson, A. Pietrangelo, R. J. Simpson, and A. T. McKie.** 2005. Impaired iron transport activity of ferroportin 1 in hereditary iron overload. The Journal of membrane biology **206:**3-7.
104. **McKie, A. T.** 2008. The role of Dcytb in iron metabolism: an update. Biochemical Society transactions **36:**1239-1241.

105. **McKie, A. T., D. Barrow, G. O. Latunde-Dada, A. Rolfs, G. Sager, E. Mudaly, M. Mudaly, C. Richardson, D. Barlow, A. Bomford, T. J. Peters, K. B. Raja, S. Shirali, M. A. Hediger, F. Farzaneh, and R. J. Simpson.** 2001. An iron-regulated ferric reductase associated with the absorption of dietary iron. Science **291:**1755-1759.

106. **McKie, A. T., P. Marciani, A. Rolfs, K. Brennan, K. Wehr, D. Barrow, S. Miret, A. Bomford, T. J. Peters, F. Farzaneh, M. A. Hediger, M. W. Hentze, and R. J. Simpson.** 2000. A novel duodenal iron-regulated transporter, IREG1, implicated in the basolateral transfer of iron to the circulation. Molecular cell **5:**299-309.

107. **Meyron-Holtz, E. G., M. C. Ghosh, K. Iwai, T. LaVaute, X. Brazzolotto, U. V. Berger, W. Land, H. Ollivierre-Wilson, A. Grinberg, P. Love, and T. A. Rouault.** 2004. Genetic ablations of iron regulatory proteins 1 and 2 reveal why iron regulatory protein 2 dominates iron homeostasis. The EMBO journal **23:**386-395.

108. **Meyron-Holtz, E. G., M. C. Ghosh, and T. A. Rouault.** 2004. Mammalian tissue oxygen levels modulate iron-regulatory protein activities in vivo. Science **306:**2087-2090.

109. **Millett, E. S., I. Efimov, J. Basran, S. Handa, C. G. Mowat, and E. L. Raven.** 2012. Heme-containing dioxygenases involved in tryptophan oxidation. Current opinion in chemical biology **16:**60-66.

110. **Moroishi, T., M. Nishiyama, Y. Takeda, K. Iwai, and K. I. Nakayama.** 2011. The FBXL5-IRP2 axis is integral to control of iron metabolism in vivo. Cell metabolism **14:**339-351.

111. **Mullner, E. W., S. Rothenberger, A. M. Muller, and L. C. Kuhn.** 1992. In vivo and in vitro modulation of the mRNA-binding activity of iron-regulatory factor. Tissue distribution and effects of cell proliferation, iron levels and redox state. European journal of biochemistry / FEBS **208:**597-605.

112. **Munoz, M., J. A. Garcia-Erce, and A. F. Remacha.** 2011. Disorders of iron metabolism. Part 1: molecular basis of iron homoeostasis. Journal of clinical pathology **64:**281-286.

113. **Olivares, M., T. Walter, E. Hertrampf, and F. Pizarro.** 1999. Anaemia and iron deficiency disease in children. British medical bulletin **55:**534-543.

114. **Oudit, G. Y., H. Sun, M. G. Trivieri, S. E. Koch, F. Dawood, C. Ackerley, M. Yazdanpanah, G. J. Wilson, A. Schwartz, P. P. Liu, and P. H. Backx.** 2003. L-type Ca2+ channels provide a major pathway for iron entry into cardiomyocytes in iron-overload cardiomyopathy. Nature medicine **9:**1187-1194.

115. **Outten, F. W., and E. C. Theil.** 2009. Iron-based redox switches in biology. Antioxidants & redox signaling **11:**1029-1046.
116. **Pantopoulos, K., and M. W. Hentze.** 1998. Activation of iron regulatory protein-1 by oxidative stress in vitro. Proceedings of the National Academy of Sciences of the United States of America **95:**10559-10563.
117. **Perutz, M. F.** 1969. Structure and function of hemoglobin. Harvey lectures **63:**213-261.
118. **Philpott, C. C., D. Haile, T. A. Rouault, and R. D. Klausner.** 1993. Modification of a free Fe-S cluster cysteine residue in the active iron-responsive element-binding protein prevents RNA binding. The Journal of biological chemistry **268:**17655-17658.
119. **Pietrangelo, A.** 2010. Hereditary hemochromatosis: pathogenesis, diagnosis, and treatment. Gastroenterology **139:**393-408, 408 e391-392.
120. **Pietrangelo, A.** 2005. Non-HFE hemochromatosis. Seminars in liver disease **25:**450-460.
121. **Ponka, P., and C. N. Lok.** 1999. The transferrin receptor: role in health and disease. The international journal of biochemistry & cell biology **31:**1111-1137.
122. **Popescu, B. F., C. A. Robinson, A. Rajput, A. H. Rajput, S. L. Harder, and H. Nichol.** 2009. Iron, copper, and zinc distribution of the cerebellum. Cerebellum **8:**74-79.
123. **Rajagopal, A., A. U. Rao, J. Amigo, M. Tian, S. K. Upadhyay, C. Hall, S. Uhm, M. K. Mathew, M. D. Fleming, B. H. Paw, M. Krause, and I. Hamza.** 2008. Haem homeostasis is regulated by the conserved and concerted functions of HRG-1 proteins. Nature **453:**1127-1131.
124. **Rao, A. U., L. K. Carta, E. Lesuisse, and I. Hamza.** 2005. Lack of heme synthesis in a free-living eukaryote. Proceedings of the National Academy of Sciences of the United States of America **102:**4270-4275.
125. **Richards, M. P.** 2012. Redox Reactions of Myoglobin. Antioxidants & redox signaling.
126. **Richardson, D. R., D. J. Lane, E. M. Becker, M. L. Huang, M. Whitnall, Y. Suryo Rahmanto, A. D. Sheftel, and P. Ponka.** 2010. Mitochondrial iron trafficking and the integration of iron metabolism between the mitochondrion and cytosol. Proceedings of the National Academy of Sciences of the United States of America **107:**10775-10782.
127. **Ross, K. L., and R. S. Eisenstein.** 2002. Iron deficiency decreases mitochondrial aconitase abundance and citrate concentration without affecting tricarboxylic acid cycle capacity in rat liver. The Journal of nutrition **132:**643-651.

128. **Rouault, T. A.** 2012. Biogenesis of iron-sulfur clusters in mammalian cells: new insights and relevance to human disease. Disease models & mechanisms **5:**155-164.
129. **Rouault, T. A.** 2006. The role of iron regulatory proteins in mammalian iron homeostasis and disease. Nature chemical biology **2:**406-414.
130. **Rouault, T. A., M. W. Hentze, S. W. Caughman, J. B. Harford, and R. D. Klausner.** 1988. Binding of a cytosolic protein to the iron-responsive element of human ferritin messenger RNA. Science **241:**1207-1210.
131. **Roughead, Z. K., C. A. Zito, and J. R. Hunt.** 2002. Initial uptake and absorption of nonheme iron and absorption of heme iron in humans are unaffected by the addition of calcium as cheese to a meal with high iron bioavailability. The American journal of clinical nutrition **76:**419-425.
132. **Saeki, Y., and K. Tanaka.** 2012. Assembly and function of the proteasome. Methods Mol Biol **832:**315-337.
133. **Salahudeen, A. A., and R. K. Bruick.** 2009. Maintaining Mammalian iron and oxygen homeostasis: sensors, regulation, and cross-talk. Annals of the New York Academy of Sciences **1177:**30-38.
134. **Salahudeen, A. A., J. W. Thompson, J. C. Ruiz, H. W. Ma, L. N. Kinch, Q. Li, N. V. Grishin, and R. K. Bruick.** 2009. An E3 ligase possessing an iron-responsive hemerythrin domain is a regulator of iron homeostasis. Science **326:**722-726.
135. **Salojin, K. V., R. M. Cabrera, W. Sun, W. C. Chang, C. Lin, L. Duncan, K. A. Platt, R. Read, P. Vogel, Q. Liu, R. H. Finnell, and T. Oravecz.** 2011. A mouse model of hereditary folate malabsorption: deletion of the PCFT gene leads to systemic folate deficiency. Blood **117:**4895-4904.
136. **Samaniego, F., J. Chin, K. Iwai, T. A. Rouault, and R. D. Klausner.** 1994. Molecular characterization of a second iron-responsive element binding protein, iron regulatory protein 2. Structure, function, and post-translational regulation. The Journal of biological chemistry **269:**30904-30910.
137. **Scaglione, K. M., P. K. Bansal, A. E. Deffenbaugh, A. Kiss, J. M. Moore, S. Korolev, R. Cocklin, M. Goebl, K. Kitagawa, and D. Skowyra.** 2007. SCF E3-mediated autoubiquitination negatively regulates activity of Cdc34 E2 but plays a nonessential role in the catalytic cycle in vitro and in vivo. Molecular and cellular biology **27:**5860-5870.
138. **Schade, A. L., and L. Caroline.** 1946. An iron-binding component in human blood plasma. Science **104:**340.
139. **Schade, A. L., R. W. Reinhart, and H. Levy.** 1949. Carbon dioxide and oxygen in complex formation with iron and siderophilin, the iron-binding component of human plasma. Archives of biochemistry **20:**170-172.

140. **Schranzhofer, M., M. Schifrer, J. A. Cabrera, S. Kopp, P. Chiba, H. Beug, and E. W. Mullner.** 2006. Remodeling the regulation of iron metabolism during erythroid differentiation to ensure efficient heme biosynthesis. Blood **107:**4159-4167.
141. **Schultz, I. J., C. Chen, B. H. Paw, and I. Hamza.** 2010. Iron and porphyrin trafficking in heme biogenesis. The Journal of biological chemistry **285:**26753-26759.
142. **Shayeghi, M., G. O. Latunde-Dada, J. S. Oakhill, A. H. Laftah, K. Takeuchi, N. Halliday, Y. Khan, A. Warley, F. E. McCann, R. C. Hider, D. M. Frazer, G. J. Anderson, C. D. Vulpe, R. J. Simpson, and A. T. McKie.** 2005. Identification of an intestinal heme transporter. Cell **122:**789-801.
143. **Sheftel, A. D., S. F. Kim, and P. Ponka.** 2007. Non-heme induction of heme oxygenase-1 does not alter cellular iron metabolism. The Journal of biological chemistry **282:**10480-10486.
144. **Shu, C., M. W. Sung, M. D. Stewart, T. I. Igumenova, X. Tan, and P. Li.** 2012. The structural basis of iron sensing by the human F-box protein FBXL5. Chembiochem : a European journal of chemical biology **13:**788-791.
145. **Silvestri, L., A. Pagani, A. Nai, I. De Domenico, J. Kaplan, and C. Camaschella.** 2008. The serine protease matriptase-2 (TMPRSS6) inhibits hepcidin activation by cleaving membrane hemojuvelin. Cell metabolism **8:**502-511.
146. **Smith, S. R., S. Cooperman, T. Lavaute, N. Tresser, M. Ghosh, E. Meyron-Holtz, W. Land, H. Ollivierre, B. Jortner, R. Switzer, 3rd, A. Messing, and T. A. Rouault.** 2004. Severity of neurodegeneration correlates with compromise of iron metabolism in mice with iron regulatory protein deficiencies. Annals of the New York Academy of Sciences **1012:**65-83.
147. **Smith, S. R., M. C. Ghosh, H. Ollivierre-Wilson, W. Hang Tong, and T. A. Rouault.** 2006. Complete loss of iron regulatory proteins 1 and 2 prevents viability of murine zygotes beyond the blastocyst stage of embryonic development. Blood cells, molecules & diseases **36:**283-287.
148. **Soe-Lin, S., S. S. Apte, B. Andriopoulos, Jr., M. C. Andrews, M. Schranzhofer, T. Kahawita, D. Garcia-Santos, and P. Ponka.** 2009. Nramp1 promotes efficient macrophage recycling of iron following erythrophagocytosis in vivo. Proceedings of the National Academy of Sciences of the United States of America **106:**5960-5965.
149. **Stoltzfus, R.** 2001. Defining iron-deficiency anemia in public health terms: a time for reflection. The Journal of nutrition **131:**565S-567S.

150. **Su, M. A., C. C. Trenor, J. C. Fleming, M. D. Fleming, and N. C. Andrews.** 1998. The G185R mutation disrupts function of the iron transporter Nramp2. Blood **92:**2157-2163.
151. **Thompson, J. W., and R. K. Bruick.** 2012. Protein degradation and iron homeostasis. Biochimica et biophysica acta **1823:**1484-1490.
152. **Thompson, J. W., A. A. Salahudeen, S. Chollangi, J. C. Ruiz, C. A. Brautigam, T. M. Makris, J. D. Lipscomb, D. R. Tomchick, and R. K. Bruick.** 2012. Structural and molecular characterization of iron-sensing hemerythrin-like domain within F-box and leucine-rich repeat protein 5 (FBXL5). The Journal of biological chemistry **287:**7357-7365.
153. **Thomson, A. M., J. T. Rogers, and P. J. Leedman.** 1999. Iron-regulatory proteins, iron-responsive elements and ferritin mRNA translation. The international journal of biochemistry & cell biology **31:**1139-1152.
154. **Tokunaga, F., S. Sakata, Y. Saeki, Y. Satomi, T. Kirisako, K. Kamei, T. Nakagawa, M. Kato, S. Murata, S. Yamaoka, M. Yamamoto, S. Akira, T. Takao, K. Tanaka, and K. Iwai.** 2009. Involvement of linear polyubiquitylation of NEMO in NF-kappaB activation. Nature cell biology **11:**123-132.
155. **Torti, F. M., and S. V. Torti.** 2002. Regulation of ferritin genes and protein. Blood **99:**3505-3516.
156. **Trenor, C. C., 3rd, D. R. Campagna, V. M. Sellers, N. C. Andrews, and M. D. Fleming.** 2000. The molecular defect in hypotransferrinemic mice. Blood **96:**1113-1118.
157. **Trinder, D., P. S. Oates, C. Thomas, J. Sadleir, and E. H. Morgan.** 2000. Localisation of divalent metal transporter 1 (DMT1) to the microvillus membrane of rat duodenal enterocytes in iron deficiency, but to hepatocytes in iron overload. Gut **46:**270-276.
158. **Trinder, D., J. K. Olynyk, W. S. Sly, and E. H. Morgan.** 2002. Iron uptake from plasma transferrin by the duodenum is impaired in the Hfe knockout mouse. Proceedings of the National Academy of Sciences of the United States of America **99:**5622-5626.
159. **Vashisht, A. A., K. B. Zumbrennen, X. Huang, D. N. Powers, A. Durazo, D. Sun, N. Bhaskaran, A. Persson, M. Uhlen, O. Sangfelt, C. Spruck, E. A. Leibold, and J. A. Wohlschlegel.** 2009. Control of iron homeostasis by an iron-regulated ubiquitin ligase. Science **326:**718-721.
160. **Vulpe, C. D., Y. M. Kuo, T. L. Murphy, L. Cowley, C. Askwith, N. Libina, J. Gitschier, and G. J. Anderson.** 1999. Hephaestin, a ceruloplasmin homologue implicated in intestinal iron transport, is defective in the sla mouse. Nature genetics **21:**195-199.

161. **Wachtershauser, G.** 1992. Groundworks for an evolutionary biochemistry: the iron-sulphur world. Progress in biophysics and molecular biology **58:**85-201.
162. **Walden, W. E., A. I. Selezneva, J. Dupuy, A. Volbeda, J. C. Fontecilla-Camps, E. C. Theil, and K. Volz.** 2006. Structure of dual function iron regulatory protein 1 complexed with ferritin IRE-RNA. Science **314:**1903-1908.
163. **Wang, J., G. Chen, M. Muckenthaler, B. Galy, M. W. Hentze, and K. Pantopoulos.** 2004. Iron-mediated degradation of IRP2, an unexpected pathway involving a 2-oxoglutarate-dependent oxygenase activity. Molecular and cellular biology **24:**954-965.
164. **Wang, J., C. Fillebeen, G. Chen, A. Biederbick, R. Lill, and K. Pantopoulos.** 2007. Iron-dependent degradation of apo-IRP1 by the ubiquitin-proteasome pathway. Molecular and cellular biology **27:**2423-2430.
165. **Wang, J., and K. Pantopoulos.** 2011. Regulation of cellular iron metabolism. The Biochemical journal **434:**365-381.
166. **Ward, D. M., and J. Kaplan.** 2012. Ferroportin-mediated iron transport: Expression and regulation. Biochimica et biophysica acta **1823:**1426-1433.
167. **West, A. R., and P. S. Oates.** 2008. Mechanisms of heme iron absorption: current questions and controversies. World journal of gastroenterology : WJG **14:**4101-4110.
168. **Wingert, R. A., J. L. Galloway, B. Barut, H. Foott, P. Fraenkel, J. L. Axe, G. J. Weber, K. Dooley, A. J. Davidson, B. Schmid, B. H. Paw, G. C. Shaw, P. Kingsley, J. Palis, H. Schubert, O. Chen, J. Kaplan, and L. I. Zon.** 2005. Deficiency of glutaredoxin 5 reveals Fe-S clusters are required for vertebrate haem synthesis. Nature **436:**1035-1039.
169. **Wirbelauer, C., H. Sutterluty, M. Blondel, M. Gstaiger, M. Peter, F. Reymond, and W. Krek.** 2000. The F-box protein Skp2 is a ubiquitylation target of a Cul1-based core ubiquitin ligase complex: evidence for a role of Cul1 in the suppression of Skp2 expression in quiescent fibroblasts. The EMBO journal **19:**5362-5375.
170. **Wolf, G.** 2007. Identification of proton-coupled high-affinity human intestinal folate transporter mutated in human hereditary familial folate malabsorption. Nutrition reviews **65:**554-557.
171. **Yamanaka, K., H. Ishikawa, Y. Megumi, F. Tokunaga, M. Kanie, T. A. Rouault, I. Morishima, N. Minato, K. Ishimori, and K. Iwai.** 2003. Identification of the ubiquitin-protein ligase that recognizes oxidized IRP2. Nature cell biology **5:**336-340.

172. **Yang, J., D. Goetz, J. Y. Li, W. Wang, K. Mori, D. Setlik, T. Du, H. Erdjument-Bromage, P. Tempst, R. Strong, and J. Barasch.** 2002. An iron delivery pathway mediated by a lipocalin. Molecular cell **10:**1045-1056.
173. **Yen, H. C., and S. J. Elledge.** 2008. Identification of SCF ubiquitin ligase substrates by global protein stability profiling. Science **322:**923-929.
174. **Yoshikawa, S., K. Muramoto, K. Shinzawa-Itoh, and M. Mochizuki.** 2012. Structural studies on bovine heart cytochrome c oxidase. Biochimica et biophysica acta **1817:**579-589.
175. **Zakin, M. M.** 1992. Regulation of transferrin gene expression. FASEB journal : official publication of the Federation of American Societies for Experimental Biology **6:**3253-3258.
176. **Zhang, A. S., and C. A. Enns.** 2009. Iron homeostasis: recently identified proteins provide insight into novel control mechanisms. The Journal of biological chemistry **284:**711-715.
177. **Zhang, N., J. Liu, X. Ding, F. Aikhionbare, C. Jin, and X. Yao.** 2007. FBXL5 interacts with p150Glued and regulates its ubiquitination. Biochemical and biophysical research communications **359:**34-39.
178. **Zhou, X. Y., S. Tomatsu, R. E. Fleming, S. Parkkila, A. Waheed, J. Jiang, Y. Fei, E. M. Brunt, D. A. Ruddy, C. E. Prass, R. C. Schatzman, R. O'Neill, R. S. Britton, B. R. Bacon, and W. S. Sly.** 1998. HFE gene knockout produces mouse model of hereditary hemochromatosis. Proceedings of the National Academy of Sciences of the United States of America **95:**2492-2497.
179. **Zumbrennen, K. B., E. S. Hanson, and E. A. Leibold.** 2008. HOIL-1 is not required for iron-mediated IRP2 degradation in HEK293 cells. Biochimica et biophysica acta **1783:**246-252.